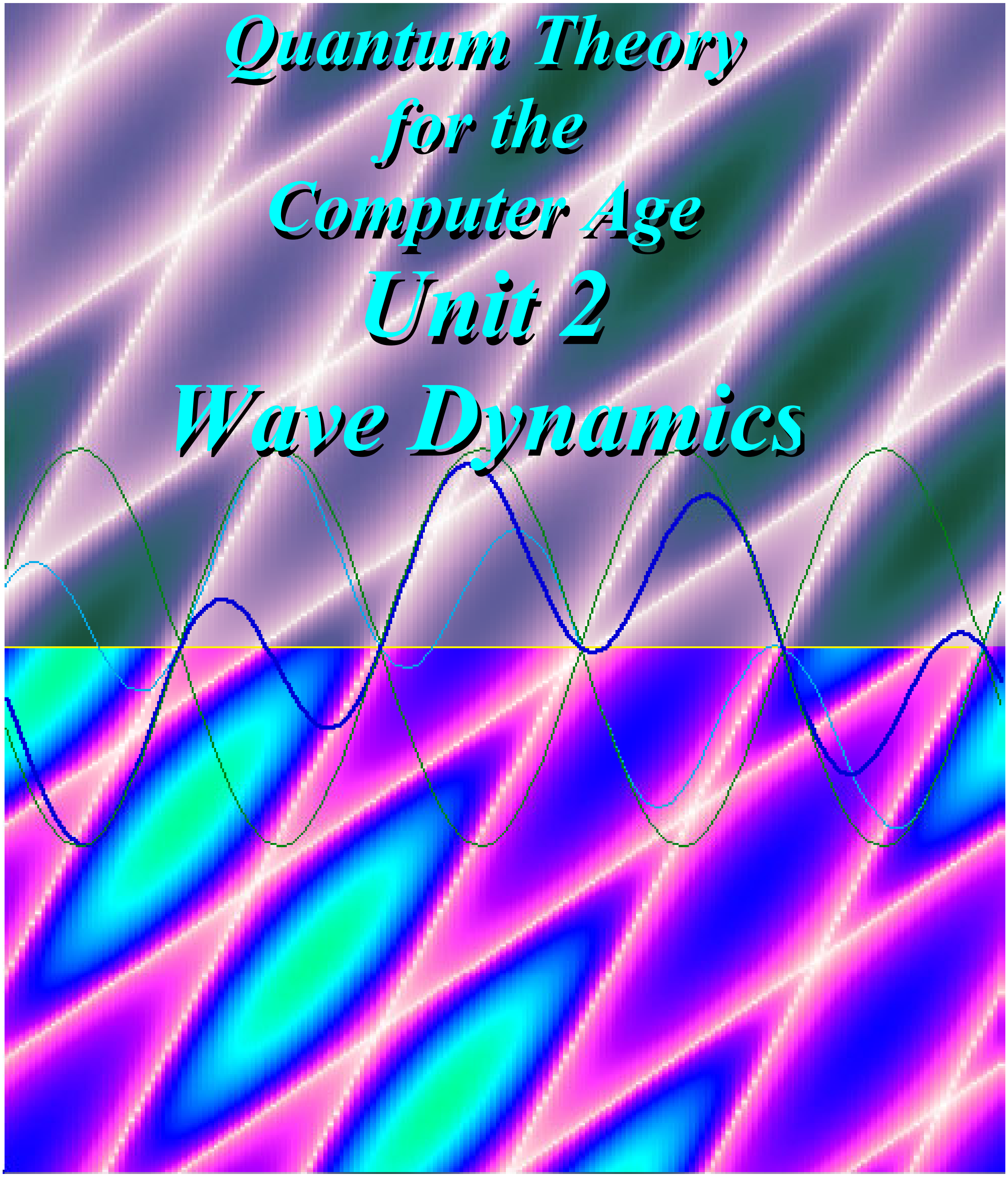
Quantum Theory
for the
Computer Age
Unit 2
Wave Dynamics

Unit 2 Wave Dynamics

Unit 1 used the two states of electromagnetic wave polarization as an introduction to quantum theory but did not consider the propagation of such a wave through space. In Unit 2, wave phase properties in space and time (spacetime) are examined by combining spacetime with wavevector and frequency (per-spacetime) pictures.
A clear understanding of interference properties of light (or γ-waves) leads to simple geometric and algebraic derivations of the special theory of relativity for spacetime and per-spacetime in Chapter 4. In Chapter 5, the per-spacetime theory leads to similar derivations of the dispersion properties of “matter waves” (or μ-waves) and to fundamental ideas of relativistic and non-relativistic quantum theory. Concepts of energy, momentum, mass, acceleration and inertia are seen to arise from quite simple quantum wave interference effects. Wave propagation and modes in two or three dimensions are examined in Chapter 6.

W. G. Harter
Department of Physics
University of Arkansas
Fayetteville

Hardware and Software by

HARTER-*Soft*

Elegant Educational Tools Since 2001

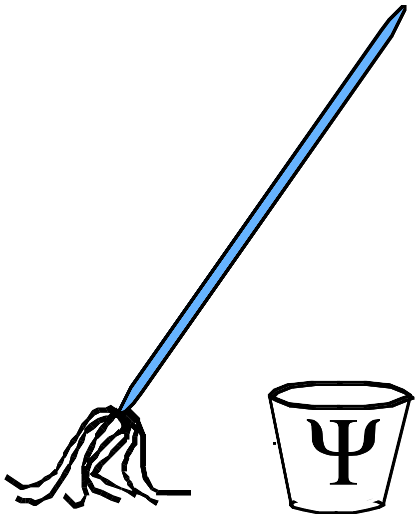

QM for AMOP

Chapter 4
Waves in Space and Time

W. G. Harter

Wave propagation along a line is analyzed using complex functions, phasors, and space-time diagrams for waves having only one or two frequency components and a single dimension of amplitude. (For em-waves: only a single polarization plane.) Ch. 4 includes a derivation of phase velocity, group velocity, standing-wave-ratio, Doppler shift (for em-waves) and the Lorentz transformation theory of special relativity as a result of wave interference. With only two frequency components, a waves-on-line-system is effectively a two-state system and analogous to the 2-state systems introduced in Unit 1. A further analogy, which will be exploited many times in this book, is introduced between optical polarization and waves-on-a-ring

.

Unit 2 Wave Dynamics
Chapter 4. Waves in Space and Time

Having introduced quantum amplitudes in Unit 1 using mostly two-state systems, we now introduce infinite-state wave systems. Quite a jump! It would be nice if we could just take our *(n=2)*-state quantum mechanics and gradually increase n to infinity ($n \to \infty$) and hope to see the limiting case. What makes this particularly difficult is that mathematics has two kinds of infinities; there is the comparatively tame *discrete or denumerable infinity* and then there is the much wilder *continuous or non-denumerable infinity*.

It is the latter that has been used by physicists since the development of differential and integral calculus. It provides us with the tools of real analysis, complex variables, and modern functional analysis. The idea of a real variable x or complex variable z that can assume arbitrary floating-point values (as opposed to only integer values) is so ingrained in our mathematical physics that few can carry on an intelligent conversation without using these continuum concepts.

The object of the next two units is to show how infinite-state quantum systems, even the continuously infinite state systems can be managed using the same sort of Dirac bra-ket and operator mathematics introduced in Unit 1. This accomplishes two things. First, it allows the vast literature base of quantum mechanics to be more easily read and understood. Second, it points out several approaches to numerical simulations of quantum systems on digital computers.

Before beginning this discussion, a word of caution is offered. It is entirely possible that two or three hundred years of continuum mathematics is, for the physicist, like a kind of drug that has hampered us from seeing nature as it really is. The idea that space-time is continuous without limit down to arbitrarily small sizes is being seriously challenged by various grand-unification schemes. The notion of the "point-particle" is also questioned. It is proposed that "elementary" particles are tiny vibrating "strings." Such speculation still lack evidence but the questioning is by itself encouraging.

Also, on a more practical note, no digital computer is capable of truly simulating a continuum, or, for that matter, any kind of infinity. Even floating point numbers are stored as discrete binary integers whose size of mantissa and exponent is limited by size of registers. Also, time simulations and space-time plots are series of discrete steps and pixels that only appear to be continuous because the machinery has become so fast and fine. It might be hoped that analog computers are better realizations of a continuum (forgetting for a moment that their currents and voltages are quantized) but, unfortunately, analog accuracy is far less than digital precision because of thermal noise. So called "quantum computers" have been imagined, but it remains to be seen what form and function these will take.

It helps to approach any comparison of continuous functional analysis and discrete vector analysis by imagining that we need to simulate and store the various mathematical objects as realistically as possible on a standard digital computer. Continuum calculus and analysis have been and will probably always continue to be wonderful tools for discovering certain model approximations, but an increasing number of problems require computer synthesis in order to make consistently accurate predictions.

A Time and Frequency Hero – Ken Evenson (1932-2002)

When US soldiers punch up their GPS coordinates they may owe their lives to an under sung hero and his students who toiled 18-hour days deep inside labs lit only by the purest light in the universe.

Let me introduce an "Indiana Jones" of modern physics. While he may never have been called "Montana Ken," such a name would describe a real life hero from Boseman, MT, whose accomplishments far surpass, in many ways, the fictional character in *Raiders of the Lost Arc* and other cinematic thrillers.

Indeed, I know of a real life moment shared by his wife Vera, when Ken was in a canoe literally inches from the hundred-foot drop-off of Brazil's largest waterfall. But, such outdoor exploits, of which Ken had many, pale in the light of an in-the-lab brilliance and courage that profoundly enriched the world.

Ken is one of few, if not the only physicist to be listed twice in the *Guinness Book of Records*. It was not for jungle exploits but for the highest frequency measurements and speed of light determination that made quantum optics many times more precise.

The meter-kilogram-second (mks) system of units underwent a redefinition largely because of Ken's efforts. Thereafter c was defined as *299,792,458* and the meter was defined in terms of c, instead of the other way around. Time and frequency precision trumped that of distance. Without such resonance precision, the Global Positioning System (GPS) would be impossible.

Ken's courage and persistence at the Time and Frequency Division of the Boulder Laboratories in the National Bureau of Standards (now the National Institute of Standards and Technology or NIST) are legendary as are his railings against boneheaded administrators trying to thwart his efforts. By painstakingly exploiting the resonance properties of metal-insulator diodes, Ken's lab succeeded in literally counting the waves of 200 THz near-infrared radiation and eventually, visible light itself.

4.1 Discrete vs. Continuous: Function Space

Let us first compare a finite *discrete* and *bounded* n-state system (the easiest of all possible mathematical worlds!) to an ∞-state system of the worst kind, which is a *continuous* and *unbounded* system. The discrete and bounded system is indexed by state *index* numbers $a = 1, 2, 3, \ldots, n,$ which are discrete ("quantized") and bounded by a lowest number (1) and a highest number (n). Meanwhile, the continuous (shall we say "indiscreet") and unbounded system is indexed by a real variable x which ranges from $x = -\infty$ to $x = +\infty$,and isn't bounded at all as sketched in the upper part of Fig. 4.1.1.

Imagine that the real variable x stands for a "particle" position coordinate on the x-axis. (The ubiquitous quantum "particle" concept arises again. You are free to substitute the words "electron" or "photon" if that helps any.) The idea is that you could install particle counters at arbitrary x-positions and wait for counts. Clearly, we cannot afford an infinite number of counters, much less an unbounded continuum of them; we're probably lucky just to have one or two left over from our 2-state experiments. So it appears this theory is already in hot water before we even get started. But, let's proceed anyway.

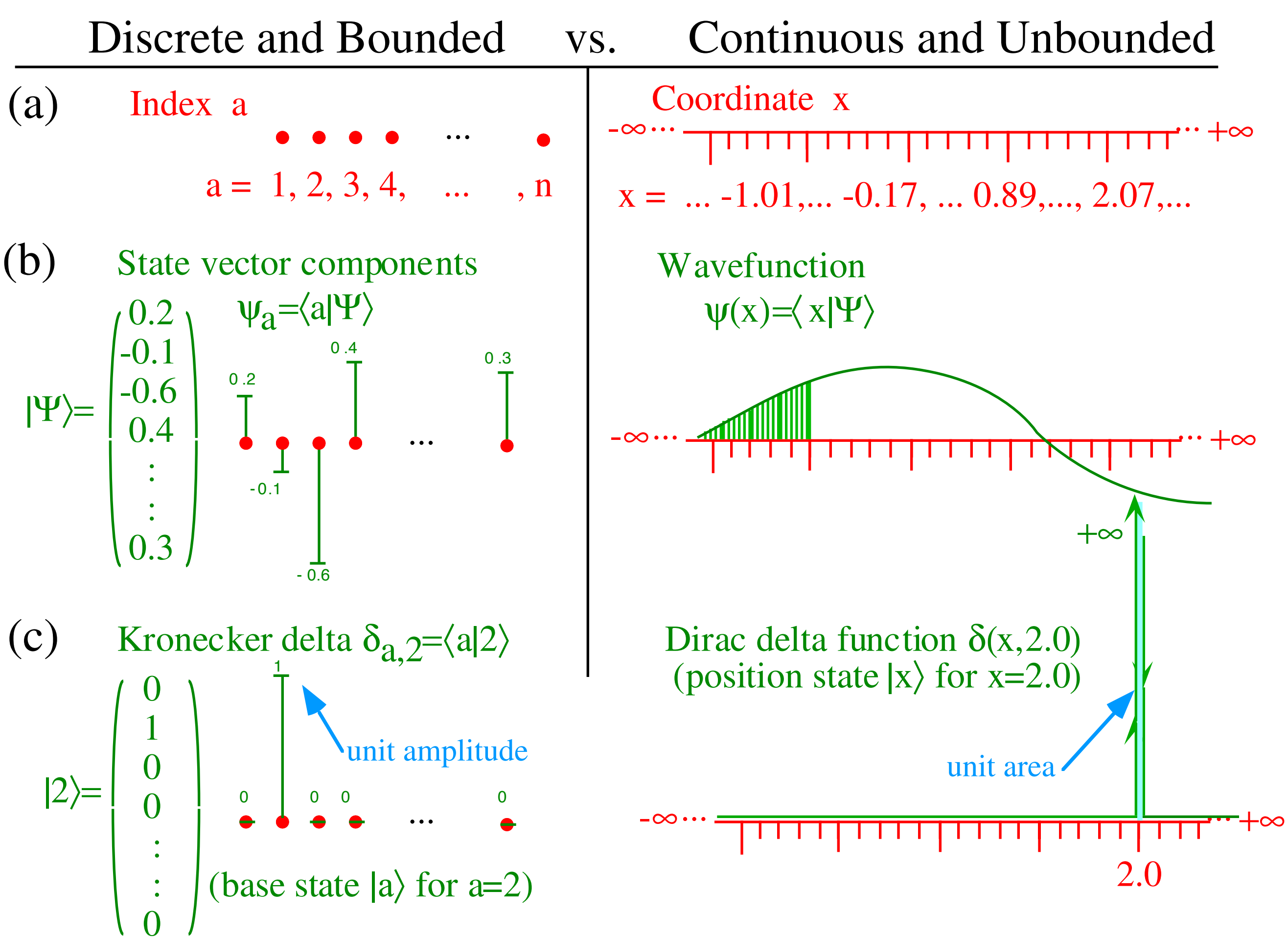

Fig. 4.1.1 Comparison of discrete state space versus continuum wavefunction

(a) State vectors vs. wavefunctions: Dirac delta functions

Fig. 4.1.1 sketches the relation between state vectors in discrete n-state systems and wavefunctions in continuous ∞-state systems. A discrete state $|\Psi\rangle$ is defined by a list of n-numbers $\langle a|\Psi\rangle$ called *amplitudes*, one for each value $a = 1, 2, ..., n$ of an *index*. A continuous state $|\Psi\rangle$ is defined by an infinite list of numbers $\langle x|\Psi\rangle$ called a *wavefunction* $\psi(x)= \langle x|\Psi\rangle$, one for each value $-\infty< x <\infty$ of a *coordinate* x. Of course, if you plot a wavefunction on a computer (as is done in Fig. 4.2.1(b-right)) it will also be a finite list of points; at whatever *resolution* you choose.

As shown in Chapter 1 (Sec. 1.4(b)) each amplitude $\langle a|\Psi\rangle$ is written as a scalar product of the state $|\Psi\rangle$ vector with base bra $\langle a|$. By axiom-2 and 4 we may write

$$\langle a|\Psi\rangle = \sum_{b=1}^{n} \langle a|b\rangle\langle b|\Psi\rangle = \sum_{b=1}^{n} \delta_{ab}\langle b|\Psi\rangle. \tag{4.1.1a}$$

This is a sum involving the *Kronecker delta symbol* $\delta_{a,b}$.

$$\langle a|b\rangle = \delta_{ab} = \begin{Bmatrix} 1 \text{ if: } a=b \\ 0 \text{ if: } a\neq b \end{Bmatrix} \tag{4.1.1b}$$

A common shorthand notation for the sum is the following.

$$\Psi_a = \sum_{b=1}^{n} \delta_{ab}\Psi_b \tag{4.1.1c}$$

Now a similar construction is defined for continuous systems, only each sum is replaced by an integral so (4.1.1a) becomes

$$\langle x|\Psi\rangle = \int_{-\infty}^{\infty} dy\langle x|y\rangle\langle y|\Psi\rangle = \int_{-\infty}^{\infty} dy\,\delta(x,y)\langle y|\Psi\rangle \tag{4.1.2a}$$

This integral involves the *Dirac delta function* $\delta(x,y)=\delta(x-y)$.

$$\langle x|y\rangle = \delta(x,y) = \begin{Bmatrix} \infty \text{ if: } x=y \\ 0 \text{ if: } x\neq y \end{Bmatrix} = \delta(x-y) = \delta(y-x) \tag{4.1.2b}$$

A common shorthand notation for the integral is the following.

$$\Psi(x) = \int_{-\infty}^{\infty} dy\,\delta(x-y)\Psi(y) \tag{4.1.2c}$$

An attempt to plot the Dirac delta function is shown in Fig. 4.1.1(c-right) by showing a "spike" function with unit area, zero base and infinite height. This is a tall order, indeed. It is based upon the requirement that expansion (4.1.2c) be valid for a unit function $\Psi(x) = 1$.

$$1 = \int_{-\infty}^{\infty} dy\,\delta(x-y)\cdot 1 = \int_{-\infty}^{\infty} dx\,\delta(x-y)\cdot 1 \tag{4.1.3}$$

The comparable discrete version is much easier to picture.

$$1 = \sum_{b=1}^{n} \delta_{ab}\cdot 1 = \sum_{a=1}^{n} \delta_{ab}\cdot 1 \tag{4.1.4}$$

A Kronecker delta, like $\delta_{a,2}$ represents a particular base state, in this case, the state $|2\rangle$ for which the probability is 100% certain that the system will be found in state-2 if forced to choose from its basis of n-states $\{|1\rangle,|2\rangle,...,|n\rangle\}$. By analogy, a Dirac delta, such as $\delta(x-2.0)$ represent a coordinate base state $|x\rangle=|2.0\rangle$ for which the probability is 100% certain that the particle is <u>exactly</u> $x=2.0$.

(b) Probability and count rates for continuum states

Does a $|x\rangle$-position state exist? Only in theory. (Here is one more case where "theory" gets a bad name!) In fact, we shall see that it would cost more than all the energy in the universe to put a single electron at *exactly* $x=2$. Such precision is hardly worth the price. For less than $15\ eV$ ($1eV = 1.6E\text{-}19\ J$.) you can locate an electron with a precision of one-tenth of a billionth of a meter. (A tenth of a nanometer or one *Angstrom* $(= 10^{-10}\ m)$ is roughly the diameter of the hydrogen atom.)

A coordinate base state $|x\rangle$ with its Dirac delta representation (4.1.2b) is not a physically realizable state. This is unlike the discrete states of electron or optical polarization which achieve 100% occupation of a $|\uparrow\rangle$ or $|y'\rangle$ base state by just passing through a filter. There is a price of doing calculus with wavefunctions $\Psi(x)$ defined on a continuum. First, you have to deal with infinitesimals and limits and infinite or *unbounded norms* such as the $\langle x|y\rangle = \delta(x\text{-}y)$ in (4.1.2b).

Also, probability definitions must be made more flexible with continuum states. For discrete states, the norm of a state never exceeds $\langle\Psi|\Psi\rangle = 1$ which corresponds to 100% probability. Norms like $\langle x|x\rangle = \infty$ of continuum states are unbounded. Probability $\langle\Psi|\Psi\rangle$ easily exceeds 100% unless the definition of axiom-1 is rescaled to avoid this unphysical situation. A common solution to this problem is to let $|\Psi(x)|^2$ be the probability of finding a particle in a given unit of length, area, or volume so that the measured count rate R is given by a definite integral over the length, area, or volume of a counter.

$$R_{Line\,L} = \int_L dx\left|\Psi(x)\right|^2,\quad R_{Area\,A} = \oiint_A dxdy\left|\Psi(x.y)\right|^2,\quad R_{Volume\,V} = \oiiint_V dxdydz\left|\Psi(x,y,z)\right|^2. \tag{4.1.5}$$

Recall that time is regarded as a continuum, too. Even the simple 2-state experiments we mentioned in Ch. 1 have implicit time limits. (We can't wait forever for those counts!) The implicit per-unit-time is always part of any probability calculation for a quantum system, be it discrete or continuous. So the probability for getting one count or the expected number of counts in a piece of laboratory apparatus will be proportional to a space-time integral such as

$$P = \int_T dt \oiiint_V dxdydz\left|\Psi\right|^2. \tag{4.1.6}$$

When calculus fails to produce analytic integrals we resort to computational approximations. For numerical calculations we must *coursegrain* or *discretize* the entire space (or space-time) occupied by a wavefunction. We imagine the space filled with hundreds, or thousands, or even millions of "bins" or "eyelets" each behaving as a discrete section of a very complex but perfect "do-nothing" analyzer. Then the simulated experiments begin. Each experiment corresponds to replacing one or more of the "eyelets" with counters or more subtle apparatus that responds to (and affects) the phase or amplitude in each bin. In this way, any system is reduced to one that is discrete and bounded, as infinite integrals become finite sums. Part of the artistry of quantum theory and experiment involves relating apparently infinite continua to finite and discrete lattices that may serve as practical approximations to the world.

4.2 Wavefunctions, Wave Velocity, and Wave Visualization

Complex numbers and functions are indispensable computational tools and visualization aids for the physics of waves and particularly for quantum wavefunctions. Some of these ideas are introduced.

(a) Complex amplitudes and phasor clocks

As we mentioned in Ch. 1 (Sec. 1.2(b)), an amplitude is a complex number in modern quantum theory. In the very simplest cases, which involve systems with a single (monochromatic) energy ε or frequency ω, these complex amplitudes have a Planck phase factor.

$$e^{-i\omega t} = \cos\omega t - i\sin\omega t \tag{4.2.1}$$

The angular frequency $\omega=2\pi\nu$ or frequency ν is related by *Planck's constant* $h=2\pi\hbar=6.63E\text{-}34Js$

$$\varepsilon = h\nu = \hbar\omega\,, \tag{4.2.2}$$

to the energy ε of a quantum state. Here, we will view these amplitudes as *phasors* or *quantum clocks* sketched in Fig. 4.2.1-4.2.2. Each of these quantum clocks rotates clockwise as time advances.

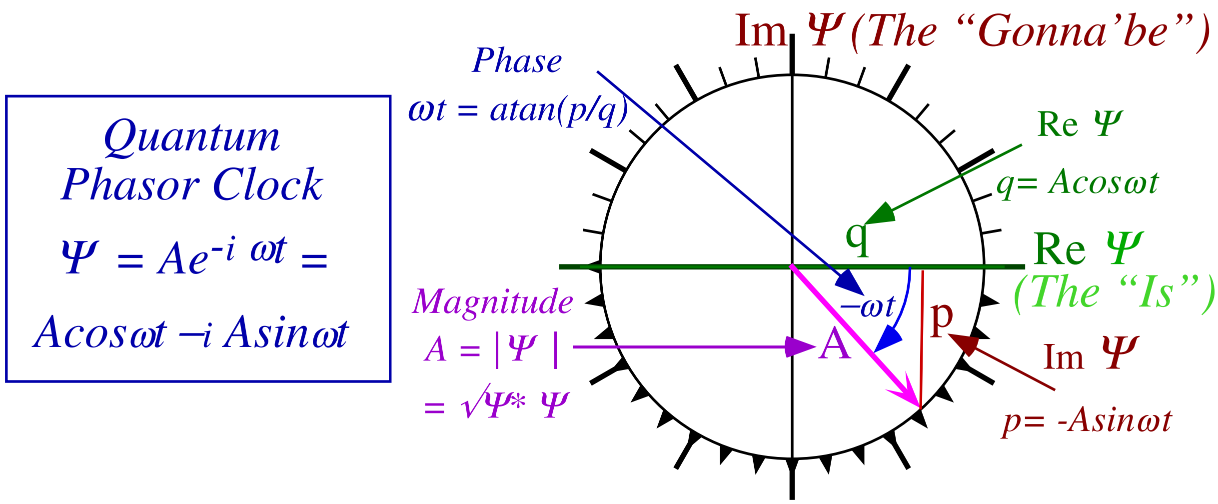

Fig. 4.2.1 Geometry of quantum phasor clock $\Psi=q+ip=Ae^{-i\omega t}=A\cos\omega t - i\,A\sin\omega t$

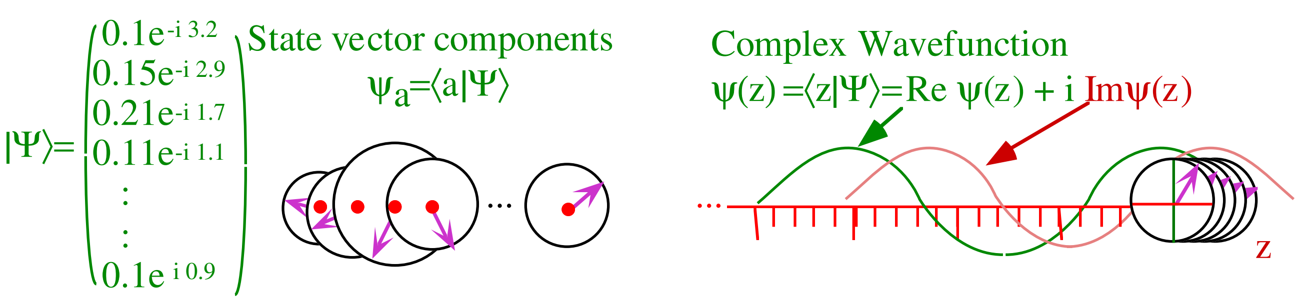

Fig. 4.2.2 Discrete set of complex amplitudes versus complex wavefunction

Complex numbers help to visualize one-dimensional oscillation as a two-dimensional process with an *amplitude* (A) and a *phase* ($-\omega t$) or else *real* ($q=Re\,\Psi$) and *imaginary* ($p=Im\Psi$) parts, which are like oscillator *phase variables* of coordinate (q) and momentum (p). The $e^{-i\omega t}$ amplitude in Fig. 4.2.1 has a negative ($-\omega t$) time-phase so the q-axis and p-axis make right-handed phase space with clockwise circulation. We shall name q and p the *"is"* and *"gonna' be"* variables since $q=Re\,\Psi(z)$ is where the wave *is* and $p=Im\ \Psi(z)$ is where the wave is gonna' be in *1/4*-cycle. (See Fig. 4.2.2.)A mnemonic helps: "Imagination precedes reality." The imaginary wave always precedes the real wave in examples below.

> Please Note: Never NEVER imagine that the phasor "velocity" or "momentum" $p = \text{Im}\Psi$ has any *direct* connection with an actual classical particle velocity, or that the phasor "coordinate" $q = \text{Re}\Psi$ has any direct connection with a particle's location in space or time. The quantum phasors (or wavefunctions they represent) seem to be *behind-the-scenes* objects. (Some will say they're mere theoretical constructions!) In fact, the phasors are so far behind the scene that generally they're not directly observable! Only probability $|\Psi|^2$ is readily observable (but needs millions of irreversible counts to be very useful.)

A complex wavefunction $\psi(z)$ defined over a continuum can be viewed as two overlapping real functions $Re\ \psi(z)$ and $Im\ \psi(z)$ or as a continuous set of phasor clocks as shown in Fig. 4.2.2 (right). Obviously, a continuum of clocks is impossible. So once again, we will settle for a coursegrained picture as indicated in the figure. Only enough clocks to resolve a quarter wavelength, or so, are actually needed.

This Sec. 4.2 has examples of complex wavefunctions and phasor clocks to help analyze quantum waves and wave dynamics in general. These are powerful visual aids as well as computational tools. Note, that the beams we used to begin quantum analysis in Ch. 1 are actually composed of waves of the kind we are introducing here. Every *n*-state beam is described at every point in the *z*-continuum along the beam by a discrete set of *n*-phasors, or equivalently, *n* complex wavefunctions $\{\psi_1(z), \psi_2(z),...,\psi_n(z)\}$.

The 2-state systems such as the optical polarization states of lightbeams, require two phasors to describe the light at any point *z* on a beam. This involves a bit of a notation hassle. In Ch. 1 the letters x and y were used as state indices; they denoted directions of polarization. In this chapter the same letters *x*, *y*, and also *z* are used to designate a continuum coordinate, usually along a beam direction. Be careful to distinguish this nomenclature. Perhaps, *z* should replace *x* everywhere in this chapter.

If x and y-polarization is normal to the beam propagation direction *z*, the notation is not so confusing. An x-phasor describes the x-polarization amplitude $\psi_x(z)=\langle x|\Psi(z)\rangle$ while another y-phasor describes the y-polarization amplitude $\psi_y(z)=\langle y|\Psi(z)\rangle$ at each *z*-point. When a beam gets split by a sorter or analyzer, then each sub-beam also has two phasors (An *n*-state beam has *n*-phasors).

What are we in for? (We really don't know waves at all.)

A word of caution about this unit: It is hoped that you are going to learn things about waves and spacetime that are quite astounding. Most courses that introduce waves do not prepare for this. There is so much to learn about waves. A refrain from a song *Clouds* by Joni Mitchell comes to mind. Here we put "waves" in place of "clouds" in her song in an attempt to describe what is to follow.

Fig. 4.2.3

(b) Wave anatomy: Expo-trig identities

Two key identities, the *expo-cosine* and *expo-sine* relations, let us easily combine two complex waves.

$$\psi_+ = e^{ia} + e^{ib} \quad (expo-cos)$$
$$= e^{i\frac{a+b}{2}}\left(e^{i\frac{a-b}{2}} + e^{-i\frac{a-b}{2}}\right)$$
$$= 2e^{i\frac{a+b}{2}}\cos\frac{a-b}{2} \quad (4.2.3a)$$

$$\psi_- = e^{ia} - e^{ib} \quad (expo-sin)$$
$$= e^{i\frac{a+b}{2}}\left(e^{i\frac{a-b}{2}} - e^{-i\frac{a-b}{2}}\right)$$
$$= 2ie^{i\frac{a+b}{2}}\sin\frac{a-b}{2} \quad (4.2.3b)$$

Each of these identities extracts a wave's *modulus MOD* or *group envelope* embodied by the cosine or sine MOD factor that defines the wave's outside "skin" as sketched in Fig. 4.2.4(a).

$$MOD(\psi_\pm) = |\psi_\pm| = \sqrt{\psi_\pm^{\,*}\psi_\pm} = \begin{cases} \cos\left(\frac{a-b}{2}\right) & \text{for } \psi_+ \\ \sin\left(\frac{a-b}{2}\right) & \text{for } \psi_- \end{cases} \quad (4.2.4a)$$

The wave's *argument ARG* or *overall phase* in the exponential factor $e^{i(a+b)/2}$ define its "insides" or "guts" including its real part Reψ and its imaginary part Reψ sketched in Fig. 4.2.4(b).

$$ARG(\psi_\pm) = ATN\frac{\mathrm{Im}\psi_\pm}{\mathrm{Re}\psi_\pm} = \begin{cases} \left(\frac{a+b}{2}\right) & \text{for } \psi_+ \\ \left(\frac{a+b}{2} + \frac{\pi}{2}\right) & \text{for } \psi_- \end{cases} \quad (4.2.4b)$$

(To some the wave looks like a boa constrictor that has swallowed some very live prey.)

The speed of the outside $MOD(\psi_\pm)$ wave factor is called *group velocity*. The external "skin" of the wave is the only part visible to probability or intensity measurements of $\psi^*\psi$. The speed of exponential phase factor inside the envelope is called *mean phase velocity* or just plain *phase velocity*. The internal phase "guts" of the wave is the part measured by (difficult) phase-sensitive detection schemes. One may think of such "intra-gut" observation as "surgery" for which patient survival is not always possible!

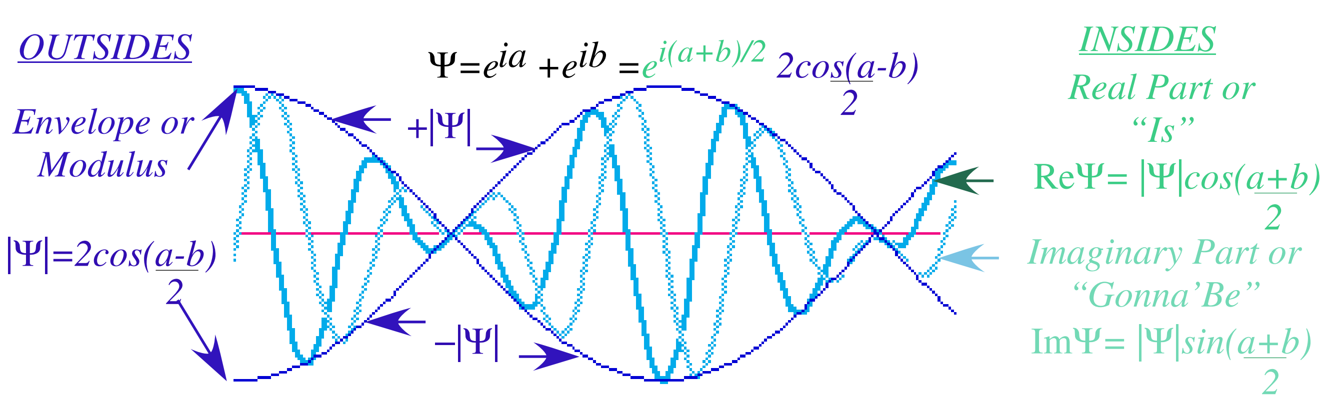

Fig. 4.2.4 Anatomy of a wave combination of two wave components e^{ia} and e^{ib}.
Visualizing Complex Wave Amplitudes and Phasors by WaveIt

Visualization of complex wavefunctions is an important part of being able to work with them. Complex analysis provides powerful techniques, but it is difficult to apply it to physical problems without some intuition. An ability to run fast is of dubious value if you can't see where you're going. Phasor clocks provide a visual representation of complex wavefunctions Ψ. Few 20th century EM and QM texts mention this visual aid in spite of the fact that some 19th century ones did do so. 21st century cyber-animation (Here it's *WaveIt.*) makes phasor animation revealing as well as practical.

The two axes or components of a phasor are the real (x=ReΨ) and the imaginary (y=ImΨ) as in Fig. 4.2.5. When plotting *transverse* waves it helps to rotate the phasor xy-axes *90°* so the real part or x-axis points up in the transverse (+)-direction of the wave amplitude as shown in the figure below.

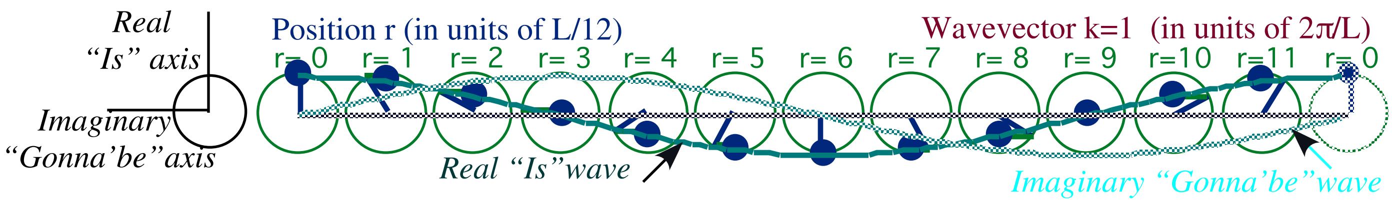

Fig. 4.2.5 Right-moving (Positive k=1) transverse wave $\Psi_{\rightarrow} = e^{i(kr - \omega t)}$ *at time t=0.*

The phasor at position r=0, 1, 2,..., 10, 11 is set to 12, 11, 10, 9,..., 2, 1 o'clock, respectively. As the clocks turn clockwise at angular frequency ω, the transverse "high-noon" peak moves from r=0 to r=1 to r=2 ...in much the same way as solar time settings of global clocks (or temperature above mean T) advance around the world. The real part ReΨ tells what the amplitude "is" while the ImΨ or imaginary part gives its rate of change in ω-units and so tells what it is "gonna' be" 1/4-hour later

When plotting *longitudinal* or *density* waves we place the phasor xy-axes so the real part or x-axis points rightward in the longitudinal direction of (+)-wave amplitude as shown in the figure below. Now the real part "is" the density ρ while the imaginary part gives velocity flow or current ι and thereby predicts what the density (above mean ρ_0) is "gonna' be" 1/4-hour later

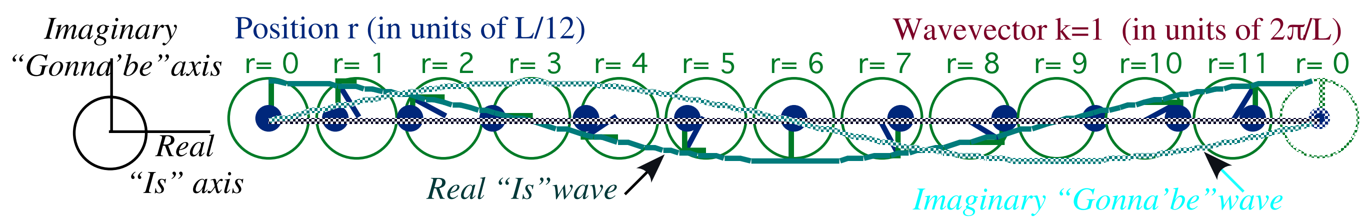

Fig. 4.2.6 Right-moving (Positive k=1) longitudinal $\rho_{\rightarrow} = e^{i(kr - \omega t)}$ *at time t=0.*

An East-to-West or left-moving transverse wave is shown in Fig. 4.2.7. (Here North is up.) The phasors at r=0, 1, 2,..., 10, 11 are set to 1, 2, 3, 4,..., 10, 11 o'clock, respectively. A phasor that is ahead of a neighbor pushes or pulls that neighbor while being pulled or pushed by the neighbor on the other side that is behind in phase. Here the effects of push and pull are equal so no phasor ever changes size.

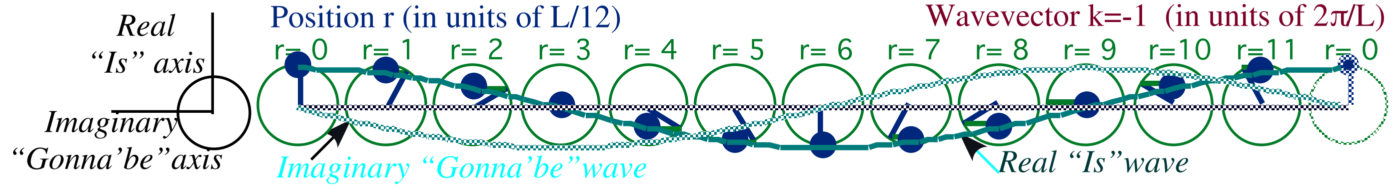

Fig. 4.2.7 Left-moving (Negative k=-1) transverse $\Psi_{\leftarrow} = e^{i(-|k|r\,-\,\omega t)}$ at time t=0. (.)

Vector addition of phasors in Fig. 4.2.5 and Fig. 4.2.7 gives a *standing wave* shown in Fig. 4.2.8-9. Each phasor rotates clockwise synchronously so relative phase difference is constant in time. Position r=6 adds in-phase to give an *anti-node*. Other places like r=10 near *nodes* do not match in phase and cancel.

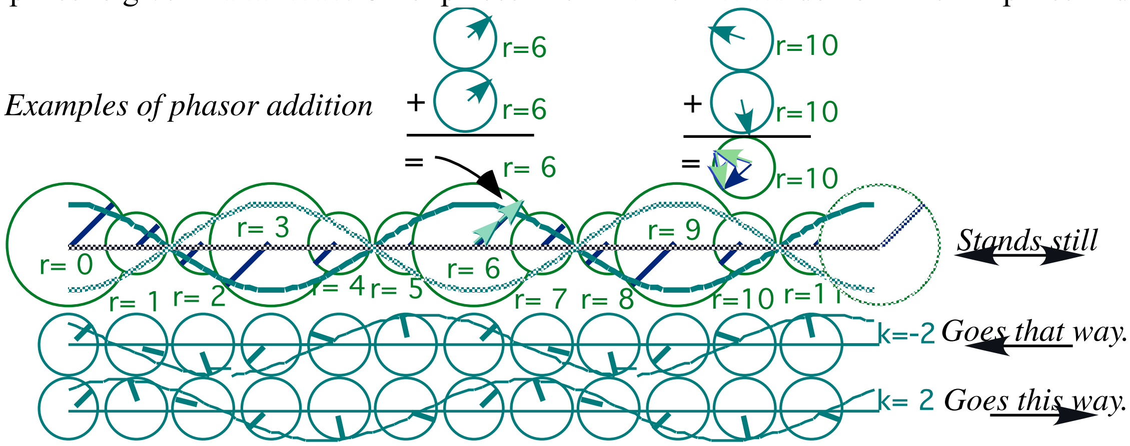

Fig. 4.2.8 Standing wave made by summing phasors of left-and-right moving waves.

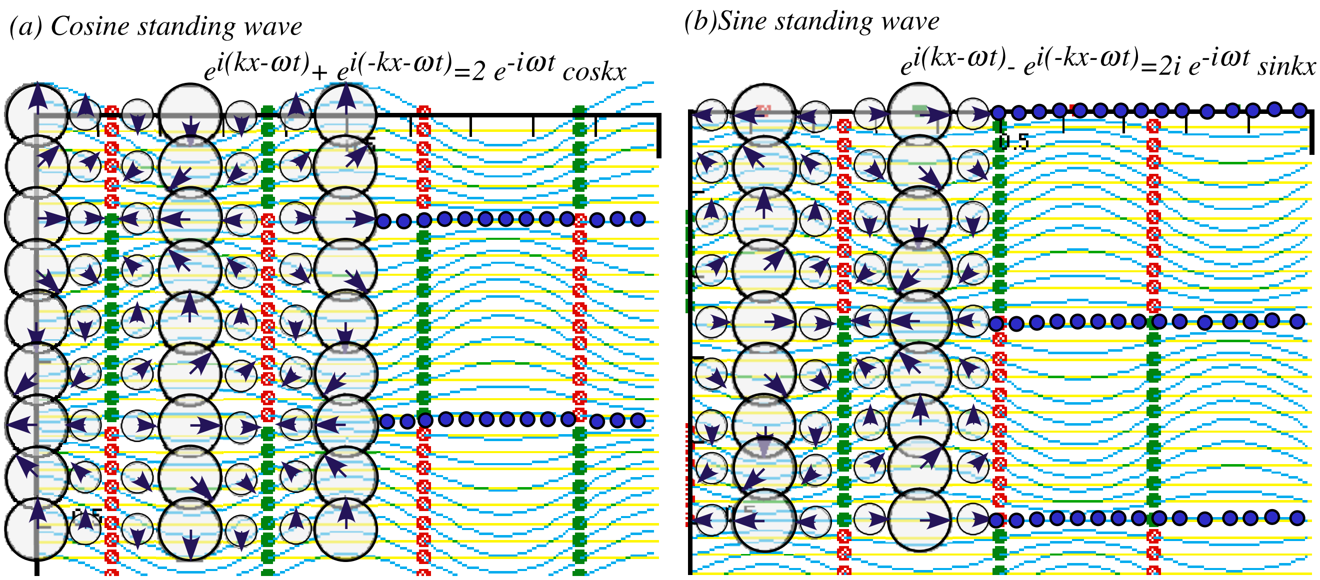

Fig. 4.2.9 Space-time phasor plots. (a) Standing cosine wave Ψ_c and (b) i-sine wave Ψ_s ($\omega = 2c = k\,c$)

Note that each time, all standing-wave phasors are either in phase or else *180°* (π) out of phase with all the others. Also, the size of the phasor dials, while constant in time, varies sinusoidally with the spatial coordinate *x*. That size is determined by the envelope or *MOD* function of (4.2.4).

(c) When Lightwaves Interfere: Phase and Group Velocity

The standard units of time t and space x are *seconds* and *meters*. Pure waves are labeled by inverse units that count waves *per-time* or *frequency* ν, which is *per-second* or *Hertz* ($1Hz=1\ s^{-1}$) and waves *per-meter* that is called *wavenumber* κ whose units are *Kaiser* ($1\ K=1\ cm^{-1}=100\ m^{-1}$). Inverting back gives the *period* $\tau=1/\nu$ or *time for one wave* and *wavelength* $\lambda=1/\kappa$ or the *space occupied by one wave*.

Physicists prefer angular or radian quantities of *radian-per-second* or *angular frequency* $\omega=2\pi\nu$ and *radian-per-meter* or *wavevector* $k=2\pi\kappa$ as used, for example, in a plane wavefunction.

$$\langle k,\omega | x,t\rangle = \psi_{k,\omega}(x,t) = e^{i(kx-\omega t)} = \cos(kx-\omega t) + i\sin(kx-\omega t), \tag{4.2.5}$$

The sine and cosine are functions of wave *phase* $(kx-\omega t)$ given in radians. An extra 2π is needed.

$$\tau = \frac{2\pi}{\omega} = \frac{1}{\nu} \quad (4.2.6a) \qquad\qquad \lambda = \frac{2\pi}{k} = \frac{1}{\kappa} \quad (4.2.6b)$$

Theses are the relations between time and space and *per*-time and *per*-space wave parameters.

Phase velocity

Spacetime plots of the real field $\mathrm{Re}\,\psi_{k,\omega}(x,t)$ for moving laser light waves are shown in Fig. 4.2.10. The left-to-right moving wave $e^{i(kx-\omega t)}$ in Fig. 4.2.10(a) has a positive wavevector k while k is negative for right-to-left moving wave $e^{i(-|k|x-\omega t)}$ in Fig. 4.2.10(b). Light and dark lines mark time paths of crests, zeros, and troughs of $\mathrm{Re}\,\psi_{k,\omega}(x,t)$. A peak for the zero-phase line is where $kx-\omega t$ is zero, that is,

$$kx-\omega t = 0\ , \qquad \text{or:}\quad \frac{x}{t} = V_{phase} = \frac{\omega}{k} = \nu\lambda \tag{4.2.7}$$

Each white line in Fig. 4.2.10 has a phase is an odd multiple $(N=1,3,\ldots)$ of $\pi/2$ and marks a $\lambda/2$-interval.

$$kx-\omega t = \pm N\frac{\pi}{2}\ , \qquad \text{or:}\quad x = V_{phase}t \pm N\frac{\pi}{2k} = V_{phase}t \pm N\frac{\lambda}{4} \tag{4.2.8}$$

The slope or *phase velocity* V_{phase} of optical phase line is a universal constant $c=299{,}792{,}548ms^{-1}$ for light waves. (Recall tribute to Ken Evenson earlier.) Velocity is a ratio of space to time (x/t) or a ratio of per-time to per-space (ν/κ) or (ω/k), or a product of per-time and space $(\nu\lambda)$. The concept of light speed is a deep one and it will be introduced in the *Colorful Relativity* axiom at the beginning of Sec. 4.3.

The standard wave quantities of (4.2.6) are labeled for a long wavelength example (infrared light) in the lower part of Fig. 4.2.10. Note that the $\mathrm{Im}\,\psi_{k,\omega}(x,t)$ wave precedes the $\mathrm{Re}\,\psi_{k,\omega}(x,t)$ wave. Recall the mnemonic, "Imagination precedes reality." It also applies to combined waves treated in the following sections and later chapters.

Fig. 4.2.10 Phasor and spacetime (BohrIt) plots of moving laser waves. (a) Left-to-right. (b) Right-to-left.

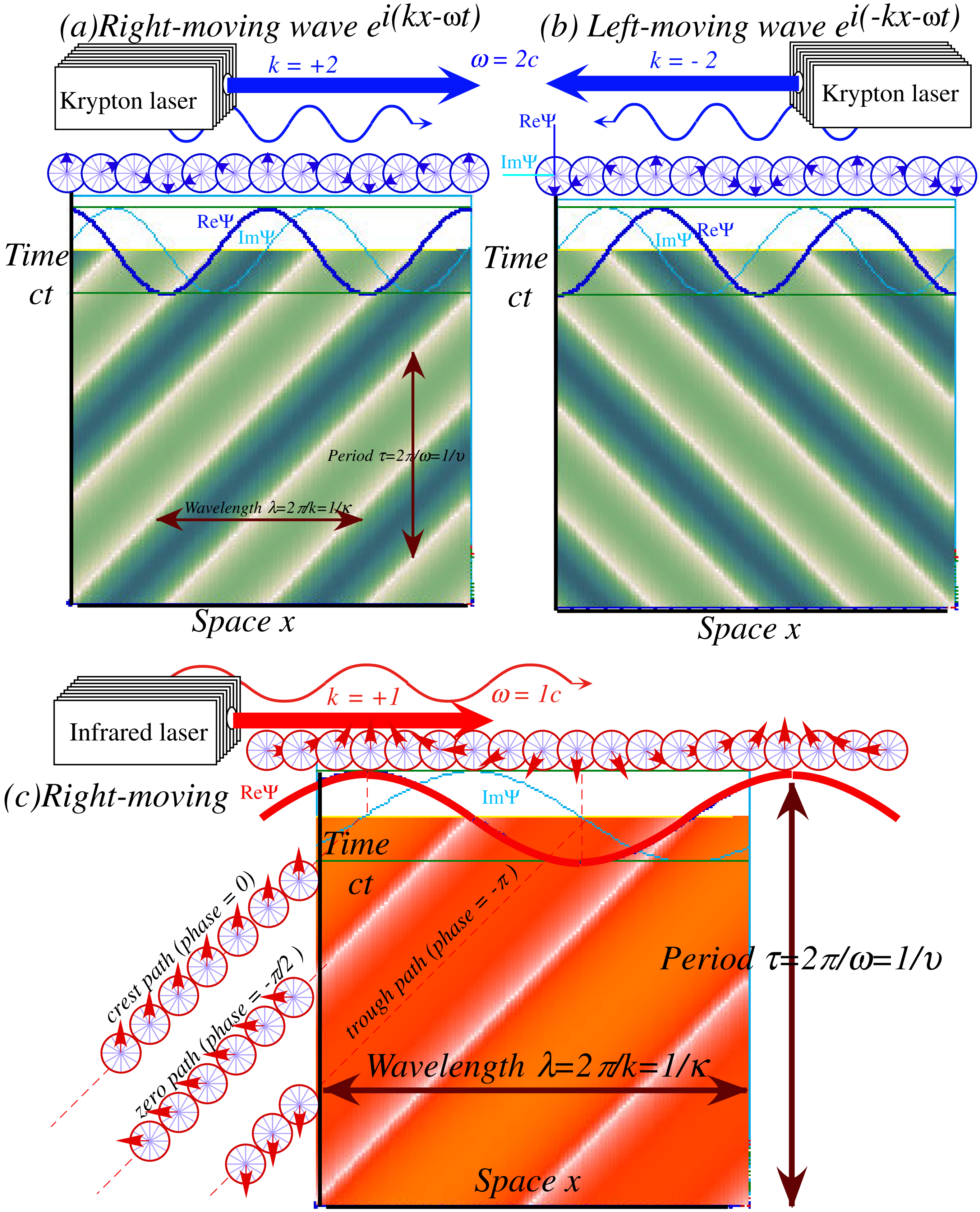

Group velocity

Group velocity is not seen unless at least two different moving waves are combined, and to define it we need waves quite unlike light. Fig. 4.2.11 shows a pair of "non-light" wave sources. The first *source-2* puts out a "red" wave of wavevector-frequency $(k_2,\omega_2)=(1,2)$ while the other *source-4* puts out a "blue" wave of wavevector-frequency $(k_4,\omega_4)=(4,4)$. The "non-light" waves are *Bohr-Schrodinger matter waves* or *μ-waves* (derived later) for an atom of rest mass $(M=2)$ in natural (k,ω) units. But, the following applies to a general wave. You may pick four random numbers for *source-2* (k_2,ω_2) and *source-4* (k_4,ω_4) and the formulas (4.2.9) and (4.2.10) below will still apply.

Given any wavevector-frequencies $\mathbf{K}_2=(k_2,\omega_2)$ and $\mathbf{K}_4=(k_4,\omega_4)$ the *e-cos* relation (4.2.3a) applies.

$$\Psi_{4+2}=e^{i(k_2x-\omega_2t)}+e^{i(k_4x-\omega_4t)}=2e^{i\left(\frac{k_4+k_2}{2}x-\frac{\omega_4+\omega_2}{2}t\right)}\cos\left(\frac{k_4-k_2}{2}x-\frac{\omega_4-\omega_2}{2}t\right)\qquad(4.2.9)$$

In *phase factor* $e^{i()}$ and *group factor* $cos()$ is a sum $\mathbf{K}_{phase}=(\mathbf{K}_4+\mathbf{K}_2)/2$ or difference $\mathbf{K}_{group}=(\mathbf{K}_4-\mathbf{K}_2)/2$.

$$\mathbf{K}_{phase}=\frac{\mathbf{K}_4+\mathbf{K}_2}{2}=\frac{1}{2}\begin{pmatrix}\omega_4+\omega_2\\k_4+k_2\end{pmatrix}==\frac{1}{2}\begin{pmatrix}4+1\\4+2\end{pmatrix}=\begin{pmatrix}2.5\\3.0\end{pmatrix}\qquad(4.2.10a)$$

$$\mathbf{K}_{group}=\frac{\mathbf{K}_4-\mathbf{K}_2}{2}=\frac{1}{2}\begin{pmatrix}\omega_4-\omega_2\\k_4-k_2\end{pmatrix}==\frac{1}{2}\begin{pmatrix}4-1\\4-2\end{pmatrix}=\begin{pmatrix}1.5\\1.0\end{pmatrix}\qquad(4.2.10b)$$

The vectors $\mathbf{K}_2$, $\mathbf{K}_4$, $\mathbf{K}_{phase}$ and $\mathbf{K}_{group}$ are drawn in Fig. 4.2.11(b). Each slope is a *wave velocity*.

$$V_4=\frac{\omega_4}{k_4}=\frac{4}{4}=1\quad(4.2.10c)\qquad V_2=\frac{\omega_2}{k_2}=\frac{1}{2}=0.5\quad(4.2.10d)\qquad V_{phase}=\frac{\omega_4+\omega_2}{k_4+k_2}=\frac{5}{6}=0.83\quad(4.2.10e)\qquad V_{group}=\frac{\omega_4-\omega_2}{k_4-k_2}=\frac{3}{2}=1.5\quad(4.2.10f)$$

The spacetime plot of wave zeros of $\mathrm{Re}\Psi$ in Fig. 4.2.11(a) shows a *group velocity* nearly twice the *mean phase velocity* as given by (4.2.10e-f). This is a peculiarity of Bohr matter waves that is explained later.

Wave lattice paths in space and time

Fig. 4.2.11 is actually a single plot that combines *spacetime (x,t)* with Fourier space or *per-spacetime* (ω,k). It relates localized pulses ("particle-like" waves) to continuous "coherent" waves by a latticework of $\mathrm{Re}\Psi$ wave-zero paths in Fig. 4.2.11(a). On wave *phase-zero paths* the real part of phase factor $e^{i(k_px-\omega_pt)}$ in (4.1.5a) is zero: $k_px-\omega_pt=n_p=N_p\pi/2\ (N_p=\pm1,\pm3...)$. *Group-zero paths* have zero group factor $\cos(k_gx-\omega_gt)$ or: $k_gx-\omega_gt=n_g=N_g\pi/2$. At *wave lattice points (x,t) both* factors are zero.

$$\begin{pmatrix}k_p&-\omega_p\\k_g&-\omega_g\end{pmatrix}\begin{pmatrix}x\\t\end{pmatrix}=\begin{pmatrix}n_p\\n_g\end{pmatrix}\text{ where: }\mathbf{K}_{phase}=\begin{pmatrix}\omega_p\\k_p\end{pmatrix}=\frac{1}{2}\begin{pmatrix}\omega_4+\omega_2\\k_4+k_2\end{pmatrix},\ \mathbf{K}_{group}=\begin{pmatrix}\omega_g\\k_g\end{pmatrix}=\frac{1}{2}\begin{pmatrix}\omega_4-\omega_2\\k_4-k_2\end{pmatrix}\qquad(4.2.11a)$$

Solving this shows that the *wavevector*-vectors $\mathbf{K}_{phase}$ and $\mathbf{K}_{group}$ define *spacetime (x,t)* zero-paths.

$$\begin{pmatrix}x\\t\end{pmatrix}=\frac{\begin{pmatrix}-\omega_g&\omega_p\\-k_g&k_p\end{pmatrix}\begin{pmatrix}n_p\\n_g\end{pmatrix}}{\omega_pk_g-\omega_gk_p}=\frac{-n_p\begin{pmatrix}\omega_g\\k_g\end{pmatrix}+n_g\begin{pmatrix}\omega_p\\k_p\end{pmatrix}}{\omega_pk_g-\omega_gk_p}=-\frac{n_p}{D}\mathbf{K}_{group}+\frac{n_g}{D}\mathbf{K}_{phase}\text{ where: }\begin{pmatrix}n_p\\n_g\end{pmatrix}=\begin{pmatrix}N_p\\N_g\end{pmatrix}\frac{\pi}{2}\qquad(4.2.11b)$$

The phase zeros follow $\mathbf{K}_{phase}$ at V_{phase} while the envelope zeros go along $\mathbf{K}_{group}$ at a higher speed V_{group}. Anti-nodes occupy an "in-between" lattice with even integer $(N_p,N_g=0,\pm2,\pm4...)$.

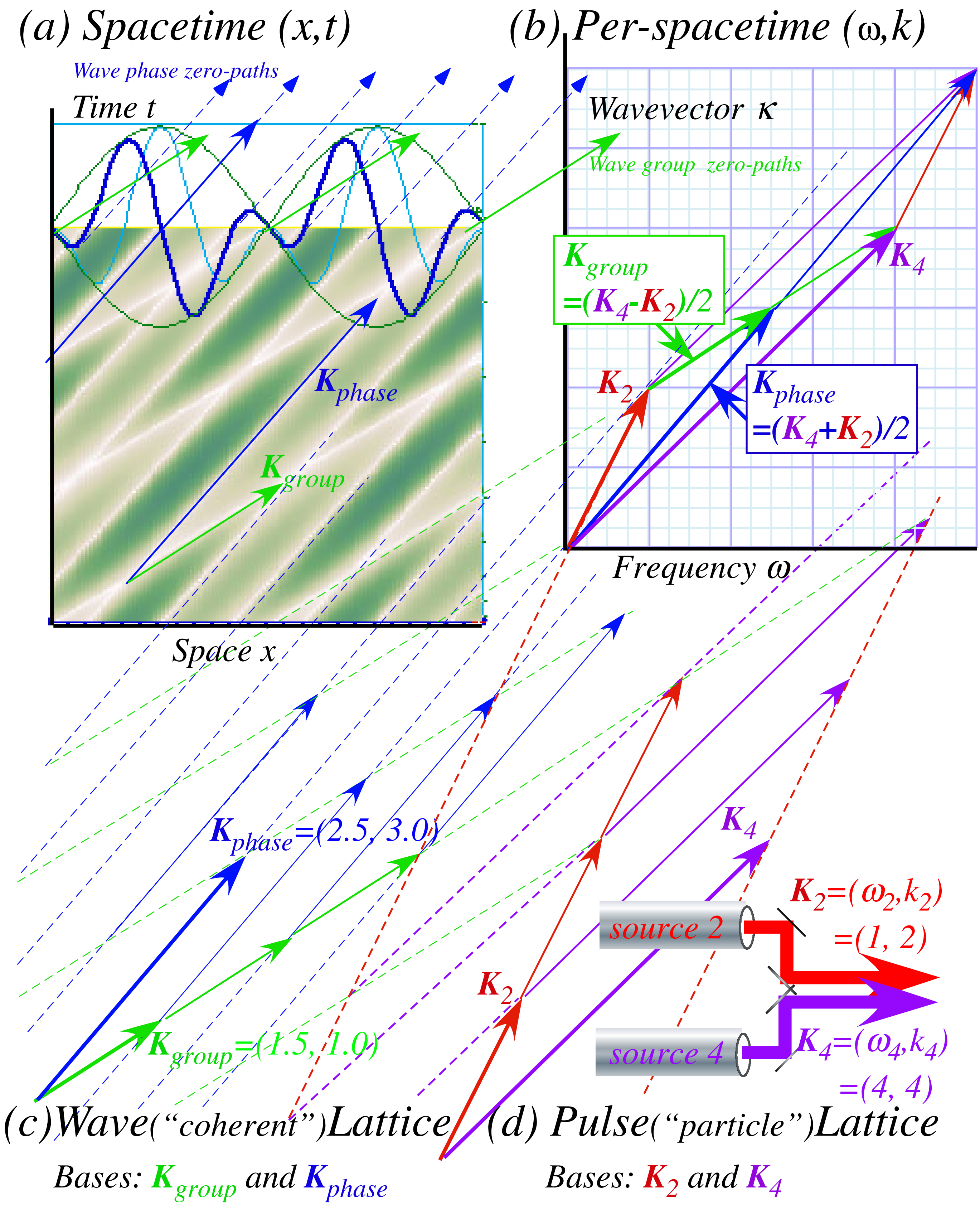

Fig. 4.2.11 Wave paths in spacetime (x,t) and Fourier per-spacetime (ω,k). (a-b) Wave zero paths along group and phase wavevectors. (c-d) Wave lattices with and without coherence.

It should be noted that the joining of a per-spacetime Fourier plot with a spacetime plot is unusual, and requires some care. First, if t is plotted versus x then (4.2.11b) requires that we plot the wavevector k versus the frequency ω instead of the other way around. (The usual dispersion functions $\omega(k)$ are plotted ω against k as will be done in later figures.) Also, we rescale the k-*versus*-ω plot by the determinant $D=\omega_p k_g - \omega_g k_p$ in (4.2.11b) so its lattice in Fig. 4.2.11(b,d) matches the x-*versus*-t wave-zero lattice in Fig. 4.2.11(a).

When that is done, the two plots may use exactly the same lattice vectors $\mathbf{K}_2$, $\mathbf{K}_4$, $\mathbf{K}_{phase}$ and $\mathbf{K}_{group}$ to define unit cells in either plot. While the $\mathbf{K}_2$ and $\mathbf{K}_4$ vectors define a primitive cell in the pulse plot of Fig. 4.2.11(d) discussed below, they also define the diagonals of the phase and group wave-zero cells spanned by $\mathbf{K}_{phase}$ and $\mathbf{K}_{group}$ in Fig. 4.2.11 (a-c). Also, the vectors $\mathbf{K}_{phase}$ and $\mathbf{K}_{group}$ define the diagonals of the primitive $\mathbf{K}_2$ and $\mathbf{K}_4$ cells as required by the vector sum relations in (4.2.10) and Fig. 4.2.11(b).

Particle or pulse lattice paths in space and time

A discussion of the paths of wave packet or pulses for the individual sources completes the picture. Suppose the output of the two sources could not interfere and behaved like Newtonian corpuscles or particles emitted each at their assigned frequency $\omega_2=1$ or $\omega_4=4$ to go along vectors $\mathbf{K}_2$ and $\mathbf{K}_4$ at their assigned phase velocities $V_2 = 0.5$ for *source-2* particles or $V_4 =1.0$ for *source-4* particles as given by (4.2.10c) and (4.2.10d). That is, four times as many $\mathbf{K}_4$ lattice lines as $\mathbf{K}_2$ lines cross the t-axis (or k-axis) but only twice as many $\mathbf{K}_4$ lines as $\mathbf{K}_2$ lines ($k_4/k_2=2$) are found at one time along the x-axis (or ω-axis). In other words, *source-4* goes *"patooey, patooey, patooey, patooey,…"* while *source-2* only spits half as fast, *"patooey,……………, patooey,…"*.

If a pulse-counter at origin $x=0$ could distinguish the "red" $\mathbf{K}_2$ from the "blue" $\mathbf{K}_4$ then it would register four times as many "blue" counts as "red" ones. All this assumes that the pulses or particles have non-dispersing Fourier components with the same phase velocity c, that is, linear dispersion $\omega=ck$, as does light. But, $\mathbf{K}_2$ and $\mathbf{K}_4$ are not on a line through origin in Fig. 4.2.11. Their dispersion is *not* linear, and as will be shown later, extraordinary interference effects arise from non-linear dispersion.

Spacetime lattices collapse for co-propagating optical waves

Fig. 4.2.12 shows the same vectors as Fig. 4.2.11 but for the combination (4.2.9) of optical or laser waves. Both V_2 for *source-2* photons and V_4 for *source-4* photons as given by (4.2.10c-d) now equal c as required by the *Colorful Relativity* axiom that starts the following Sec. 4.3. Then, the phase and group velocities are c by (4.2.10e-f), as well, and scale denominator $D=\omega_p k_g - \omega_g k_p$ in (4.2.11b) is zero. So all the vectors $\mathbf{K}_2$, $\mathbf{K}_4$, $\mathbf{K}_{phase}$ and $\mathbf{K}_{group}$ collapse onto the $45°$ line that holds both phase velocities and group velocities since they all have the speed of light only.

So, the optical co-propagation lattice collapses. To make a spacetime lattice with light requires *counter*-propagating waves. This leads to a simple derivation of the theory of relativity in the following Sec. 4.3 and the basic theory of relativistic quantum mechanics in Chapter 5.

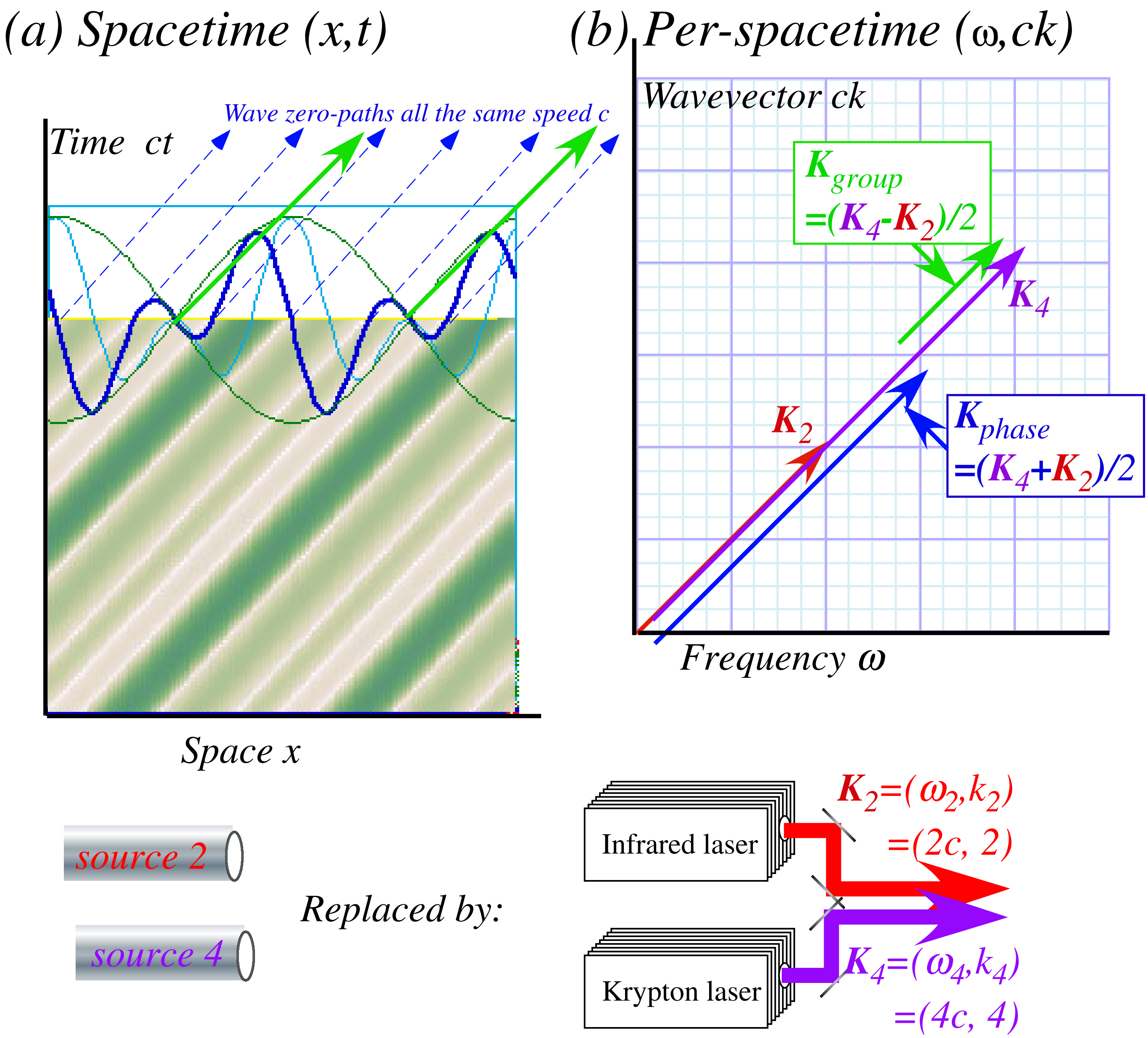

Fig. 4.2.12 Simplified wave dynamics for co-propagating optical sources.

The preceding constructions have managed to put Fourier or wave-like (per-spacetime) properties on the same page, so to speak, with Newtonian or particle-like (spacetime) ones. This is analogous to what is done in X-ray crystallographic analysis in which a real atomic position vector lattice is described using an inverse or reciprocal wavevector lattice.

In either case, the scaling in one is the inverse of the other. A larger wavevector means smaller spacing between waves in position space and *vice-versa*. The scale denominator $D=\omega_p k_g - \omega_g k_p$ in (4.2.11b) takes care of the connection of spacetime and per-spacetime plots *for that particular pair of waves only*. Another pair will generally have a different scale, but you're only allowed one scale factor per plot. Use caution when plotting *three* (or more) waves!

4.3 When Lightwaves Collide: Relativity of Spacetime

The waves combined in Fig. 4.2.12 have positive "kink-vectors" k_m so they both had positive phase velocity $V_{phase}(m)=\omega_m/k_m$. Such waves are *co-propagating* waves. Angular frequency ω_m or "wiggle rate" is positive by a convention so that phasors $e^{-i\omega t}$ always turn clockwise but k_m may have either sign. Now we look at *counter-propagating* waves, in particular, counter propagating green laser beams whose k-vectors and phase velocities have opposite sign as shown in Fig. 4.3.1(a).

If these were water waves going at ±*3 meters per second (mps)*, a boat going *-4 mps* adds *4* to each wave velocity. It goes against the *+3mps*-waves at *3+4=7mps* while catching and passing *-3mps*-waves at *–3+4=+1 mps*, and so, relative to the boat, those waves become co-propagating at *+7* and *+1*.

Can the same trick be done with light? Apparently not, as Fig. 4.3.1(b) shows what is seen by an atom "boat" attempting, by going left relative to lasers, to catch and pass a *–3 Hundred Million meter per second* light wave having k-vector $k_{\leftarrow}=-2$ and frequency $\omega_{\leftarrow}=2c$. (The atom sees lasers going right.)

The atom can never catch the green light from the right hand laser, but it does see a Doppler-red-shift down to a lesser k-vector $k'_{\leftarrow}=-1$ and frequency $\omega'_{\leftarrow}=1c$ for *infrared* light from a laser receding at *180 Million meter per second* or *3c/5*. This is derived easily below in (4.3.5b) as is the perceived *blue*-shifted output of the left hand laser coming *toward* the atom at *3c/5*. Its green light of k-vector $k_{\rightarrow}=+2$ and frequency $\omega_{\rightarrow}=2c$ is Doppler blue-shifted up to *ultraviolet* light of k-vector $k'_{\rightarrow}=+4$ and frequency $\omega'_{\rightarrow}=4c$. (Green wavelength is λ=0.5μm. Its k-vector is $k_{\rightarrow}=2\pi/\lambda$ so the length unit for Fig. 4.3.1 is 2π *microns*. Lightspeed is now *exactly c=2.99792458E8m/s* following ultra-accurate time and frequency determination by Ken Evenson's group that gave rise to the 1980 meter redefinition.)

Atoms will always fail to catch light waves and profoundly so. Even if they go fast enough to Doppler shift a green *600 THz* laser beam to below *1 Hz*, they still face a fundamental axiom or postulate that precludes ever catching a light wave. According to this, we never see light speed slow down *at all*!

(a) The colorful relativity axiom: Using Occam's razor

The Colorful Relativity Axiom: En vacuo, all colors go the same speed $c=\omega/k$ (4.3.1)

Light has *linear dispersion* $\omega=ck$. Otherwise stellar images would arrive color dispersed as if viewed through cheap binoculars, and each color would come in infinite variety. There would be green light from a stationary laser, green light made by an approaching red laser, and green light made by a receding blue laser, all presumably the same frequency but differing somehow in wavelength and speed. An invariant dispersion function wouldn't exist. Such fickle light would interfere itself to **blackness**. The colorful coherent continuous wave (CCCW) axiom is an Occam razor cut of the usual pulse wave (PW) axiom.

Examining the night sky or, better, a Hubble space telescope image, shows that all colors do indeed arrive in step even after billions of years of unimaginably perilous travel. To have even a tiny deviation from linear dispersion would make our night sky into a kaleidoscope of smeared color. Larger deviations would leave us wandering virtually blind in a colorful fog. (See discussion at the end of this section.)

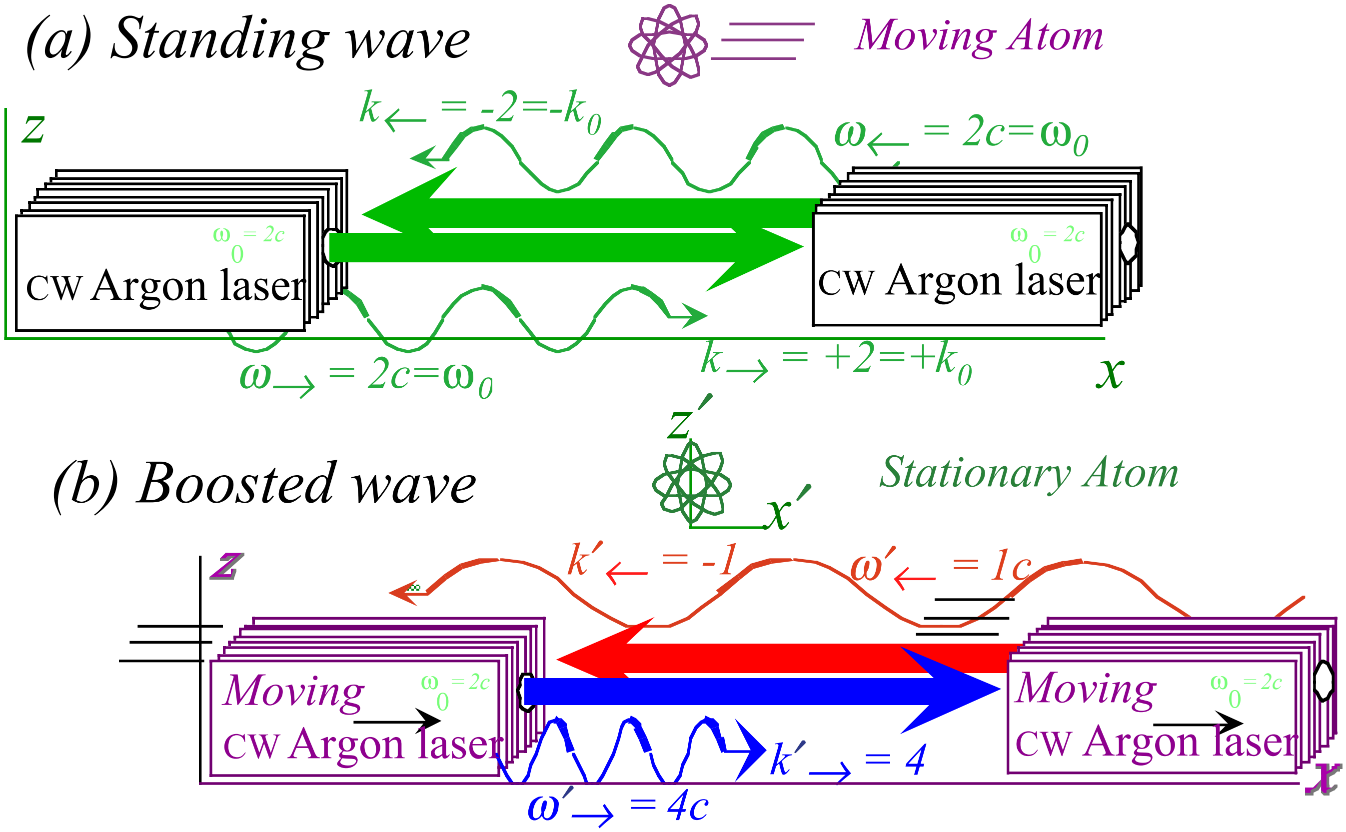

Fig. 4.3.1 Atom in Lasers. (a) Laser frame sees left-moving atom. (b) Atom sees right moving lasers.

Relativity by interfering counter-propagating laser waves

The wave in the laser frame of Fig. 4.3.1(a) is a *standing cosine wave* like Fig. 4.2.9(a).

$$e^{i(k_\rightarrow x-\omega_\rightarrow t)}+e^{i(k_\leftarrow x-\omega_\leftarrow t)}=2e^{i\left(\frac{k_\rightarrow+k_\leftarrow}{2}x-\frac{\omega_\rightarrow+\omega_\leftarrow}{2}t\right)}\cos\left(\frac{k_\rightarrow-k_\leftarrow}{2}x-\frac{\omega_\rightarrow-\omega_\leftarrow}{2}t\right)$$

$$=2e^{i(0x-\omega_0 t)}\cos\left(k_0 x-\frac{0}{2}t\right)=2e^{-i\omega_0 t}\cos k_0 x \quad \text{where: } \begin{cases} k_\rightarrow=k_0=-k_\leftarrow \\ \omega_\rightarrow=\omega_0=\omega_\leftarrow \end{cases} \tag{4.3.2a}$$

Its group or envelope velocity is zero by (4.2.10f), but by (4.2.10e) its mean phase velocity is *infinite*.

$$V_{group}=\frac{\omega_\rightarrow-\omega_\leftarrow}{k_\rightarrow-k_\leftarrow}=0 \quad (4.3.2b) \qquad V_{mean\ phase}=\frac{\omega_\rightarrow+\omega_\leftarrow}{k_\rightarrow+k_\leftarrow}=\infty\ ,\ \text{where: } \begin{cases} k_\rightarrow=k_0=-k_\leftarrow \\ \omega_\rightarrow=\omega_0=\omega_\leftarrow \end{cases} \quad (4.3.2c)$$

V_{group} is represented by a zero slope arrow connecting the ($k_\rightarrow,\omega_\rightarrow$) and ($k_\leftarrow,\omega_\leftarrow$) vectors in Fig. 4.3.2(a) and $V_{mean\ phase}$ is represented by a ∞-slope vector sum of the ($k_\rightarrow,\omega_\rightarrow$) and ($k_\leftarrow,\omega_\leftarrow$). V_{group} is zero since standing wave zeros don't move in the laser frame except when the wave is zero everywhere. (Then they jump at infinite $V_{mean\ phase}$ as seen later!) Now consider what the atom going velocity $-u$ sees in Fig. 4.3.2(b).

The atom sees a laser and attached zeros go by at velocity $+u$ in Fig. 4.3.2(b). What wave does the atom see? Frequency $\omega'_\rightarrow=b\omega_0$ is blue-shifted by factor b and $\omega'_\leftarrow=(1/b)\,\omega_0$ is red shifted by a factor $1/b$ that is *inverse* by time-reversal symmetry. (A receiver tuned to $\omega'_\rightarrow=b\,\omega_0$, to hear an ω_0-tuned transmitter approaching at speed u, keeps the same frequency $\omega'_\rightarrow$ to *transmit* to an $\omega_0=(1/b)\,\omega'_\rightarrow$ tuned receiver *departing* at speed $-u$. Speedy spacemen must listen and talk on different channels. "Roger and over!")

Now the power of Occam's razor is seen. The colorful axiom (4.3.1) demands that all light waves, regardless of color shifts or direction, have the same phase speed c.

$$\omega'_{\rightarrow} / k'_{\rightarrow} = \omega_0 / k_0 = \omega'_{\leftarrow} / k'_{\leftarrow} = \pm c \qquad (4.3.3)$$

So k-vectors use the <u>same</u> Doppler factors b or $1/b$ as frequency (but with a (-)-sign if headed left).

$$\omega'_{\rightarrow} = b\omega_0 \quad (4.3.4a) \qquad \omega'_{\leftarrow} = (1/b)\omega_0 \quad (4.3.4b)$$

$$k'_{\rightarrow} = b\, k_0 \quad (4.3.4c) \qquad k'_{\leftarrow} = -(1/b)\, k_0 \quad (4.3.4d)$$

Now the standing wave (4.3.2a) in the laser frame *(x, y,..)* is a *boosted wave* in the atom frame *(x′, y′,..)*.

$$\begin{aligned} e^{i\left(k'_{\rightarrow}x'-\omega'_{\rightarrow}t'\right)} + e^{i\left(k'_{\leftarrow}x'-\omega'_{\leftarrow}t'\right)} &= 2e^{i\left(\frac{k'_{\rightarrow}+k'_{\leftarrow}}{2}x'-\frac{\omega'_{\rightarrow}+\omega'_{\leftarrow}}{2}t'\right)}\cos\left(\frac{k'_{\rightarrow}-k'_{\leftarrow}}{2}x'-\frac{\omega'_{\rightarrow}-\omega'_{\leftarrow}}{2}t'\right) \\ &= 2e^{i\left(\frac{b-1/b}{2}k_0x'-\frac{b+1/b}{2}\omega_0t'\right)}\cos\left(\frac{b+1/b}{2}k_0x'-\frac{b-1/b}{2}\omega_0t'\right) \end{aligned} \qquad (4.3.4e)$$

Implicit is Einstein's idea: an atom has its own space*time (x′, t′)* frame. So, it sees different group velocity $V'_{group} = \frac{x'}{t'}$ where the new V'_{group} <u>must be velocity u of wave envelope fixed to the laser frame by</u> (4.3.2).

$$V'_{group} = \frac{\omega'_{\rightarrow}-\omega'_{\leftarrow}}{k'_{\rightarrow}-k'_{\leftarrow}} = \frac{b-1/b}{b+1/b}\frac{\omega_0}{k_0} = u\,, \qquad V'_{mean\ phase} = \frac{\omega_{\rightarrow}+\omega_{\leftarrow}}{k_{\rightarrow}+k_{\leftarrow}} = \frac{b+1/b}{b-1/b}\frac{\omega_0}{k_0},$$

$$\frac{V'_{group}}{c} = \frac{b^2-1}{b^2+1} = \frac{u}{c}\,, \qquad \frac{V'_{mean\ phase}}{c} = \frac{b^2+1}{b^2-1} = \frac{c}{u}\,. \qquad (4.3.5a)$$

Then the new $V'_{mean\ phase}$(in c units*)* is *inverse c/u*. We solve for *relativistic Doppler blue shift* or b-factor.

$$b^2 - 1 = \frac{u}{c}b^2 + \frac{u}{c}, \quad \text{or: } b^2 = \frac{1+\frac{u}{c}}{1-\frac{u}{c}}, \quad \text{or: } b = \sqrt{\frac{1+\frac{u}{c}}{1-\frac{u}{c}}}\,(Blue\ shift), \quad \frac{1}{b} = \sqrt{\frac{1-\frac{u}{c}}{1+\frac{u}{c}}}\,(Red\ shift), \qquad (4.3.5b)$$

The wave function (4.3.4e) has *Lorentz factors* $\left(b \pm \frac{1}{b}\right)/2$ that depend on the *relativity speed ratio*: $\beta = \frac{u}{c}$.

$$\frac{b+\frac{1}{b}}{2} = \frac{1}{\sqrt{1-\frac{u^2}{c^2}}} = \frac{1}{\sqrt{1-\beta^2}}, \qquad \frac{b-\frac{1}{b}}{2} = \frac{\frac{u}{c}}{\sqrt{1-\frac{u^2}{c^2}}} = \frac{\beta}{\sqrt{1-\beta^2}}, \quad \text{where: } \beta = \frac{u}{c}. \qquad (4.3.5c)$$

Finally, we equate the wave phases of (4.3.4e) to those of (4.3.2a). (This step needs further discussion!)

$$e^{i\left(\frac{b-1/b}{2}k_0x'-\frac{b+1/b}{2}\omega_0t'\right)}\cos\left(\frac{b+1/b}{2}k_0x'-\frac{b-1/b}{2}\omega_0t'\right) = e^{i\left(\frac{\beta}{\sqrt{1-\beta^2}}k_0x'-\frac{1}{\sqrt{1-\beta^2}}\omega_0t'\right)}\cos\left(\frac{1}{\sqrt{1-\beta^2}}k_0x'-\frac{\beta}{\sqrt{1-\beta^2}}\omega_0t'\right)$$

(Equate mean phases, and equate group phases) :: $\quad e^{-i\omega_0 t} \qquad\qquad \cos k_0 x \qquad (4.3.5d)$

The result is the entire *Lorentz-Einstein transformation* of *special relativity* derived in so few steps!

$$\begin{aligned} k_0x &= \frac{1}{\sqrt{1-\beta^2}}k_0x' - \frac{\beta}{\sqrt{1-\beta^2}}\omega_0t'\,, &\quad \text{or: } x &= \frac{1}{\sqrt{1-\beta^2}}x' - \frac{\beta}{\sqrt{1-\beta^2}}ct'\,, \\ -\omega_0t &= \frac{\beta}{\sqrt{1-\beta^2}}k_0x' - \frac{1}{\sqrt{1-\beta^2}}\omega_0t', &\quad \text{or: } ct &= \frac{-\beta}{\sqrt{1-\beta^2}}x' + \frac{1}{\sqrt{1-\beta^2}}ct'\,. \end{aligned} \qquad (4.3.5e)$$

The atom's spacetime *(x′,ct′)*-axes are based, as in Fig. 4.2.11, on per-spacetime vectors $\mathbf{K}'_{group}$ and $\mathbf{K}'_{phase}$.

$$\mathbf{K}'_{phase} = (k'_p, \omega'_p) = ((k'_{\rightarrow}+k'_{\leftarrow})/2,\ (\omega'_{\rightarrow}+\omega'_{\leftarrow})/2) \qquad \mathbf{K}'_{group} = ((k'_{\rightarrow}-k'_{\leftarrow})/2,\ (\omega'_{\rightarrow}-\omega'_{\leftarrow})/2))$$

(See Fig. 4.3.2(b).) So, relativity is a natural consequence of very basic wave interference phenomena.

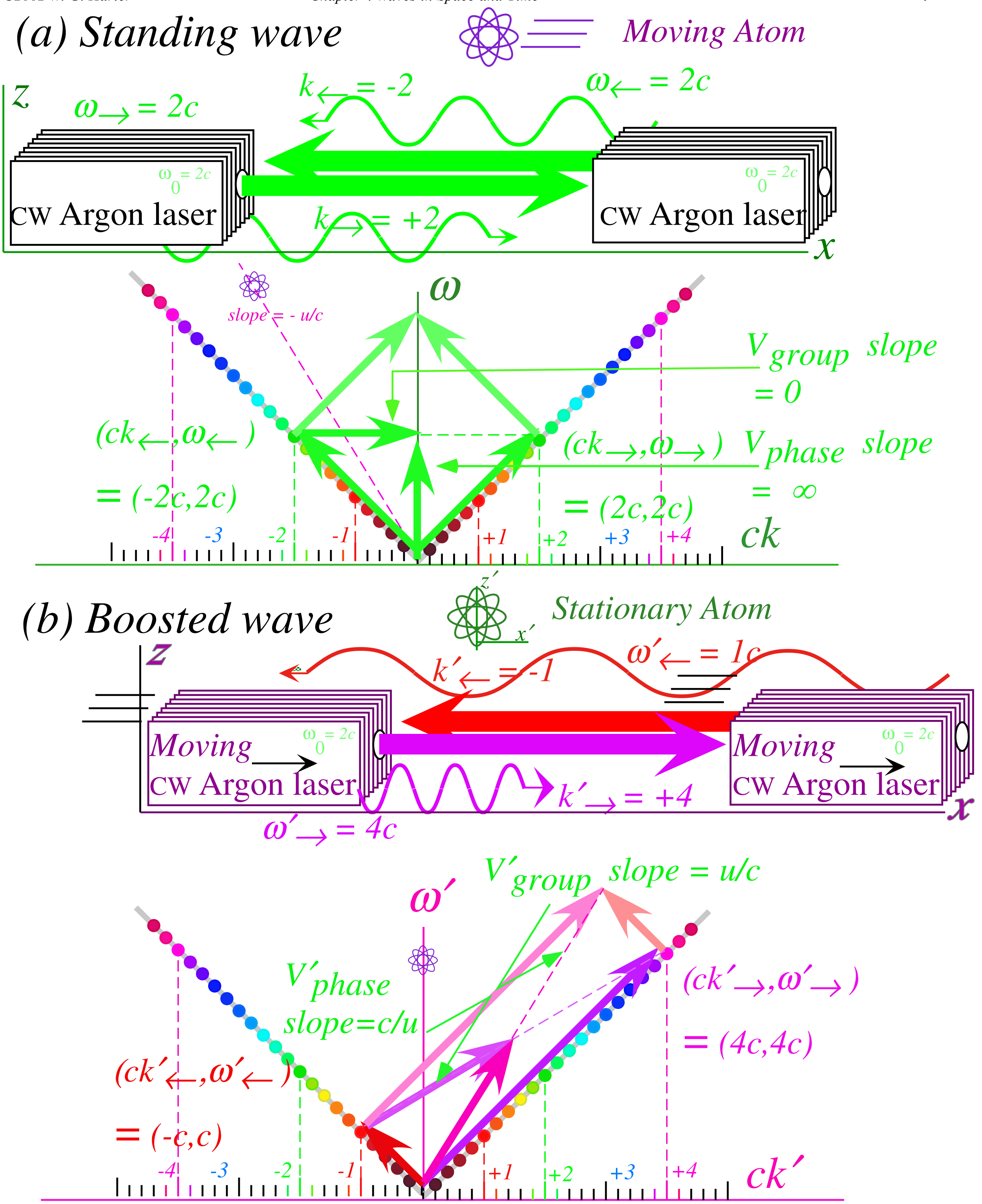

Fig. 4.3.2 Wave (ck-omega)-vector analysis of laser wave group and mean phase velocity.

(b) How'd we get relativity so quickly? Follow the zeros!

Let us look at spacetime plots (by *BohrIt*) of the waves as seen by the lasers that are making them in their own frame, and compare that to the plot of the wave seen by the atom. The first plot, a laser view, is shown in Fig. 4.3.3(a). Notice an orderly square space-time graph grid made by the zeros of the real part of the wave (4.3.2). The imaginary part can be used just as well. (In fact, that's the one plotted to get a zero going through origin $x=0$ at time $t=0$. A sine-envelope wave is needed to do that.)

Here the time or *ct-axis* is vertical as are its companion grid lines representing the stationary-in-laser-frame envelope nodes. Those lines have zero group velocity and zero *x-versus-ct* slopes.

On the other hand, the space or *x-axis* and its parallel companions are horizontal and represent brief moments when the mean phase is zero and the real wave (electric field) is zero everywhere. The space axis lines have infinite mean phase velocity and infinite *x-versus-ct* slope.

The zeros and infinities go away according to the atom in a frame made of a bent-egg-crate of grid lines in Fig. 4.3.3(b). The Cartesian grid in Fig. 4.3.3(a) is replaced by lines running with the slope of the wave group velocity including the new *atomic time* *ct′-axis* crossing the new *atomic space* *x′-axis* whose slope is the mean phase velocity. This is the Lorentz-Minkowski spacetime coordinate grid given by (4.3.5e). End of story! Well, not quite. Such a view opens up a *lot* of questions.

The first is, "Where are Einstein's meter rods and cuckoo clocks?" They're in a museum and good riddance! They never worked very well. The *Global Positioning System (GPS)* uses waves and is trillions of times more precise. Waves are more accurate and intuitive spacetime meter rods and clocks. The key is wave phase invariance of the "readings" on real *vs.* imaginary wave phasor clocks in Fig. 4.2.10. Since about 1960, all CW lasers have had precise Einstein-Minkowski wave coordinates hidden in them.

Phase invariance: Keep the phase!

Wave nodes and zeros are key indicators and measuring tools in physics, optics, and electrical engineering. The white regions that define the grid lines in Fig. 4.3.3 are regions of low or zero electric field where the real part $\mathrm{Re}\Psi \sim \mathrm{Re}E$ of the wave is small. Zero-$\mathrm{Re}\Psi$ means phase is zero modulo $\pi/2$, and the Ψ–phasor clock has struck *12 o'clock* or *6 o'clock* while $\mathrm{Re}\Psi$ is changing its *(±)*-sign.

Each strike of the phasor clock, indeed any tick, can be regarded as a relativistic *event*. It could be arranged that each zeroing of field resulted in a tiny "pop" with the clock's reading, say, $\Phi = 1012\pi$ printed out at that point. Each "pop" and its *phase* reading is a *proper invariant* whose existence and value must be agreed upon by all competent observers though they may disagree about time and spatial location of it. Traveling at high speed alters space *(x meters)*, time *(t sec.)*, *k*-vector *(k per meter)*, and frequency *(ω per-second)* but cannot cause a piece of silicon stamped 1012π to read 2101π or 1012.1π instead!

If there is a simpler or more powerful axiom than the *Colorful Relativity Axiom* (4.3.1) then it would probably be an axiom of phase invariance. We shall take up this idea shortly.

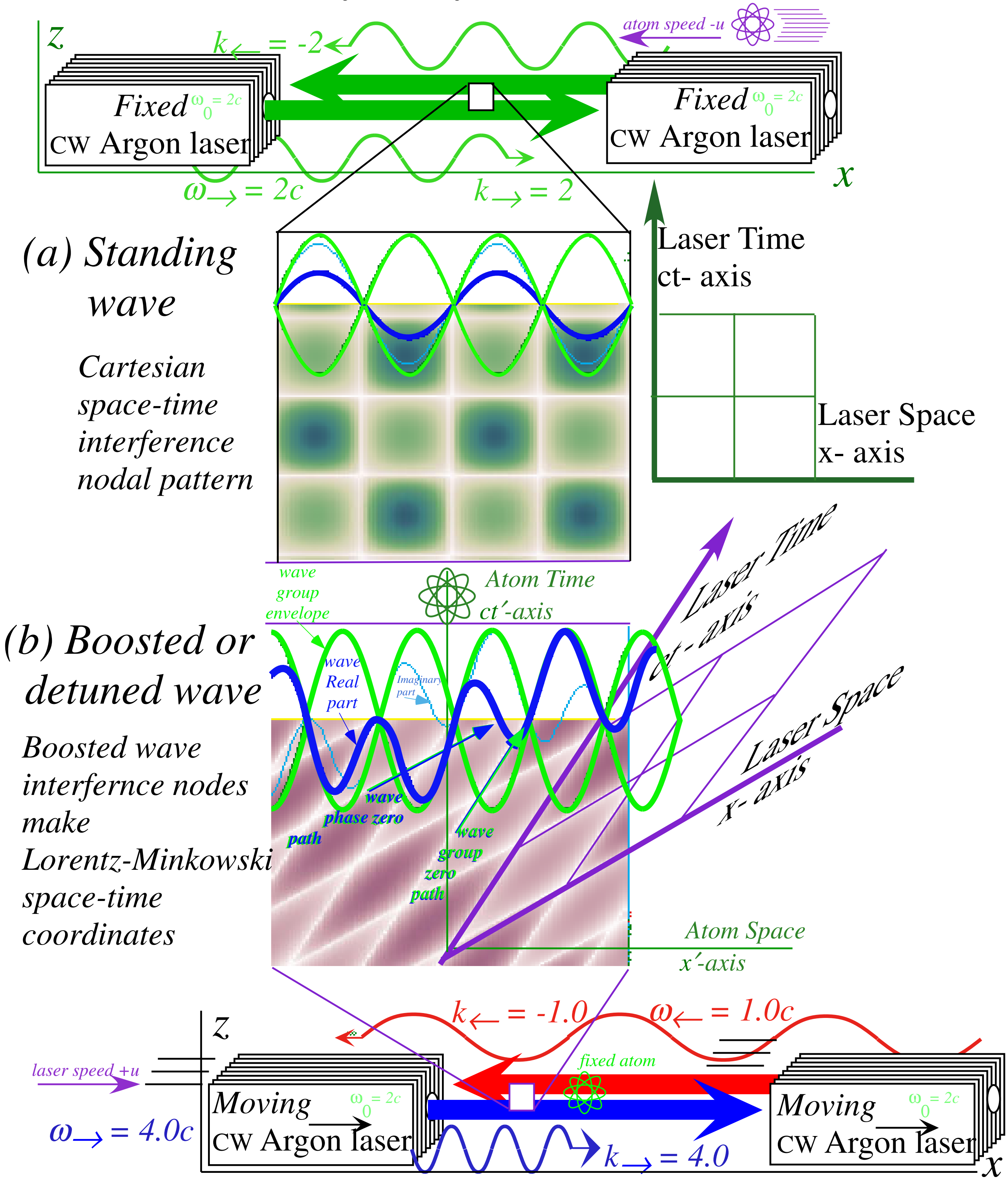

Fig. 4.3.3 Lasers do Cartesian (x,ct)-wave frame for themselves but Minkowski (x′,ct′)-frame for atom. (a) (x,ct) frame: fixed lasers, atom goes –u=-3c/5. (b) (x′,ct′)-frame: lasers go +u=3c/5, atom fixed .

Colorful Relativitistic logic: Simpler or not?

A postulate of relativity for a continuous wave (CW) theory is stated in (4.3.1). Simply put, it says, "*All colors go the same speed c*." The usual relativity postulate uses light flashes or optical pulse trains (OPT) which all go the same speed. The two axioms are equivalent, but a CW approach, with just two frequencies, has a power and simplicity that an OPT approach, with innumerable frequencies, lacks.

The idea that a light pulse appears to have the same speed for all observers, be they fast or slow, is counter-intuitive. Invariant light pulses that can't be approached seem mythical. Instead, we propose a more intuitive idea that a continuous 200THz light wave has different frequency (*color*) for different speeds, say, 400Thz approaching and 100Thz going away. Indeed, the Doppler shift, in one form or another, has been taught since Christian Doppler introduced it in the 1600's.

Still, electromagnetic waves have a unique but simple property: CW radiation of, say, 400Thz is the same as 400Thz light made by an approaching 200Thz source, or by you approaching that source, or by a fixed source tuned up to 400Thz, or by a slowly approaching 399THz source, and so on. In contrast, sound waves of, say, 400Hz heard coming from a car horn approaching is not the same as another 400Hz wave heard while approaching that fixed source. The wavelength and speed of one 400Hz sound wave will differ from the other because the speed of a sound wave depends on the relative speed of a mechanical medium (wind, liquid, or solid) carrying it. Not so for light in a vacuum. It seems not to have anything to help "blow it along."

So while the speed c and wavelength λ of a given frequency-ν sound wave might vary between, say, $c = \lambda\nu$ and $c' = \lambda'\nu$, a ν=400THz red light will always be seen to possess the same speed c and wave length λ by any observer as it beams through a vacuum devoid of interfering mechanical media. That is part of a CW relativistic postulate: allowing only one wavelength $\lambda(\nu)$ for each frequency ν, or stated conversely, only one frequency $\nu(\lambda)$ for each wavelength λ. That is simpler and less surprising than the alternative, having different "kinds" of light for each ν, a much more complicated situation.

It turns out that quantum matter waves also have a definite frequency $\nu(\lambda)$ assigned to each λ by a function called a *dispersion function*. Dispersion functions $\nu(\lambda)$ or $\omega(k)$ are the end-all-be-all for any wave theory; $\omega(k)$ determines how a wave pulse disperses or spreads as it propagates. The optical dispersion function is simplest of all, a linear relation $\omega(k)=ck$, or equivalently, a single wave speed $c = \lambda\nu = \lambda'\nu'$ for all frequencies or wavelengths $(c = \lambda\nu = constant = 2.99792458E8ms\text{-}1)$.

Constant c completes the CW postulate: *All colors go the same speed in a vacuum for any observer*. It is simple, less surprising, and in accordance with the best frequency experiments showing non-dispersal of vacuum light pulses. But, the CW postulate, however logical or conventional it might now seem, still appears to imply a mythical invariant pulse having an unapproachable speed c. In fact, this *is* a myth that needs closer examination as will be done in the following chapters.

(c) Phase invariance in spacetime (x,ct) or per-spacetime (ck,ω) plots

The colorful axiom (4.3.1) says light phase velocity is invariant. We now argue that each plane $e^{i(kx-\omega t)}$-wave has an *invariant phase* $\Phi=kx-\omega t$. No matter who sees different (Doppler shifted) values $[(ck,\omega),(ck',\omega'),(ck'',\omega''),\ldots]$ for k-vector (or wavelength $\lambda=2\pi/k$) and frequency (or period $\tau=2\pi/\omega$) and Lorentz transformed values $[(x,ct),(x',ct'),(x'',ct''),\ldots]$ of space and time, they must come up with the same value for each "strike" Φ on a wave phase clock. (Otherwise they're ruled incompetent!)

$$\Phi = kx - \omega\, t = k'x' - \omega'\, t' = k''x'' - \omega''\, t'' = \ldots \qquad (4.3.6a)$$

Does this axiom hold for any given wave at all its spacetime points? Suppose we ask, "How fast goes the 12 o'clock *(phase $\Phi=0$)* strike?" If phase Φ is invariant, each observer answers, in turn,

$$\Phi = 0 = kx - \omega\, t = k'x' - \omega'\, t' = k''x'' - \omega''\, t''\ldots \quad \text{or :} \quad \frac{x}{t} = \frac{\omega}{k},\quad \frac{x'}{t'} = \frac{\omega'}{k'},\quad \frac{x''}{t''} = \frac{\omega''}{k''},\ \ldots \qquad (4.3.6b)$$

That would just be their readings of the wave's phase velocity. For a lightwave they all say, *"c!"* Phase-invariance axiom (4.3.6a) is consistent with *"All colors go c"*-axiom (4.3.1) or (4.3.3), but, it is much deeper. It applies to the mean phases and group phases in (4.3.5d). Indeed, it applies to *all* waves and *all combinations of all waves* including quantum matter waves of which we are made! How can this be?

This requires linearity of Lorentz transformation (4.3.5e) and its inverse *($\beta\to-\beta$ or $\rho\to-\rho$)*

$$\begin{aligned} x &= x'\cosh\rho - ct'\sinh\rho \\ ct &= -x'\sinh\rho + ct'\cosh\rho \end{aligned} \quad (4.3.7a) \qquad \begin{aligned} x' &= x\cosh\rho + ct\sinh\rho \\ ct' &= x\sinh\rho + ct\cosh\rho \end{aligned} \quad (4.3.7b)$$

Modern notation uses hyperbolic functions of *relativistic rapidity* ρ. (The geometry of the rapidity "angle" ρ is clarified in Sec. 4.4 (b). Here it's just a shorthand notation based on an identity $\cosh^2\rho - \sinh^2\rho = 1$.)

$$\cosh\rho = \frac{1}{\sqrt{1-\beta^2}} \quad (4.3.7c) \qquad \sinh\rho = \frac{\beta}{\sqrt{1-\beta^2}} \quad (4.3.7d) \qquad \tanh\rho = \beta = \frac{u}{c} \quad (4.3.7e)$$

The laser frame x-unit *($x=1$, $ct=0$)* transforms by (4.3.7b) to an atom-frame point *($x'=\cosh\rho$, $ct'=\sinh\rho$)*.

$$x' = x\cosh\rho + ct\sinh\rho = \cosh\rho \qquad ct' = x\sinh\rho + ct\cosh\rho = \sinh\rho. \quad (4.3.7f)$$

Phase invariance (4.3.6a) applies to <u>*any*</u> k-vector-frequency pair *(k,ω/c)* or spacetime *(x,ct)* pair. Let us take a pair *(x,ct)=(1,0)* that implies *($x'=\cosh\rho$, $ct'=\sinh\rho$)* and a pair *(x,ct)=(0,1)* that implies *($x'=\sinh\rho$, $ct'=\cosh\rho$)*

$$k = kx - \omega t = k'x' - \omega' t' = k'\cosh\rho - \frac{\omega'}{c}\sinh\rho \qquad \text{for: } x=1 \text{ and: } ct = 0. \quad (4.3.8)$$

$$-\frac{\omega}{c} = kx - \omega t = k'x' - \omega' t' = k'\sinh\rho - \frac{\omega'}{c}\cosh\rho \qquad \text{for: } x=0 \text{ and: } ct = 1. \quad (4.3.9)$$

So, relations (4.3.7b) make each *(ck, ω)*-per-spacetime pair transform just like spacetime *(x,ct)*.

$$\begin{aligned} ck &= ck'\cosh\rho - \omega'\sinh\rho \\ \omega &= -ck'\sinh\rho + \omega'\cosh\rho \end{aligned} \quad (4.3.10a) \qquad \begin{aligned} ck' &= ck\cosh\rho + \omega\sinh\rho \\ \omega' &= ck\sinh\rho + \omega\cosh\rho \end{aligned} \quad (4.3.10b)$$

So does a sum $(ck_{phase}, \omega_{phase}) = \left((ck_1+ck_2),(\omega_1+\omega_2)\right)/2$ for a wave of speed $V_{phase} = (\omega_1+\omega_2)/(k_1+k_2)$ or a difference $(ck_{group}, \omega_{group}) = \left((ck_1-ck_2),(\omega_1-\omega_2)\right)/2$ for a wave of speed $V_{group} = (\omega_1-\omega_2)/(k_1-k_2)$. In fact, any linear combination $(ck_{12}, \omega_{12}) = A(ck_1,\omega_1) + B(ck_2,\omega_2)$ of optical *(ck, ω)*-pairs transforms this way.

$$\begin{aligned} ck_{12} &= ck'_{12}\cosh\rho - \omega'_{12}\sinh\rho \\ \omega_{12} &= -ck'_{12}\sinh\rho + \omega'_{12}\cosh\rho \end{aligned} \quad (4.3.10c) \qquad \begin{aligned} ck'_{12} &= ck_{12}\cosh\rho + \omega_{12}\sinh\rho \\ \omega'_{12} &= ck_{12}\sinh\rho + \omega_{12}\cosh\rho \end{aligned} \quad (4.3.10d)$$

Pair (ck_{12}, ω_{12}) may lie on $\pm c$-lightcone line or else on *hyperbolic invariant* curves above or below them.

$$\omega^2_{12} - \left(ck_{12}\right)^2 = \omega'^2_{12} - \left(ck'_{12}\right)^2 = (2AB)\,\frac{D}{c} \quad (4.3.11a)$$

Locus of (ck_{12}, ω_{12}) depends on an invariant *wave-propagation discriminant* D. (Recall also (4.2.11).)

$$D = \mathbf{K}_1 \times \mathbf{K}_2 = \omega_1 ck_2 - \omega_2 ck_1 = \omega'_1 ck'_2 - \omega'_2 ck' = \begin{cases} 2c\omega_1\omega_2 = 2c\omega_0^2 & (\text{Counter-propagate}) \\ 0 & (\text{Co-propagate}) \end{cases} \quad (4.3.11b)$$

Co-propagation ($\omega_1/k_1=\omega_2/k_2=\pm c$) has $D=0$ in (4.3.11) so wave lattices collapse onto ±*45°* lines $\omega_{12}=\pm c\, k_{12}$ as in Fig. 4.2.12. Counter-propagation ($\omega_1/k_1=-\omega_2/k_2=\pm c$) turns a wave lattice in Fig. 4.2.11 into a Lorentz grid of Fig. 4.3.4. (4.3.11a) is a hyperbola that crosses ω-axis at $\pm\omega_1$ for *($A=1/2=B$)* or ck-axis for *($A=1/2=-B$)*.

$$\omega^2_{12} - \left(ck_{12}\right)^2 = \begin{cases} +\omega_0^2 & \mathbf{K}_{\text{phase}} \text{ wave:}(A = 1/2 = +B) \\ -\omega_0^2 & \mathbf{K}_{\text{group}} \text{ wave:}(A = 1/2 = -B) \end{cases} \quad (4.3.12)$$

Recall that the Doppler relations (4.3.3), by time reversal, give blue shift $\omega_1 = b\omega_0$ inverse to red shift $\omega_2 = 1/b\omega_0$ so the product $\omega_1\omega_2 = \omega_0^2 = \omega'_1\omega'_2$ is frame-invariant. Area D=$\mathbf{K}_1 \times \mathbf{K}_2$ is thus invariant.

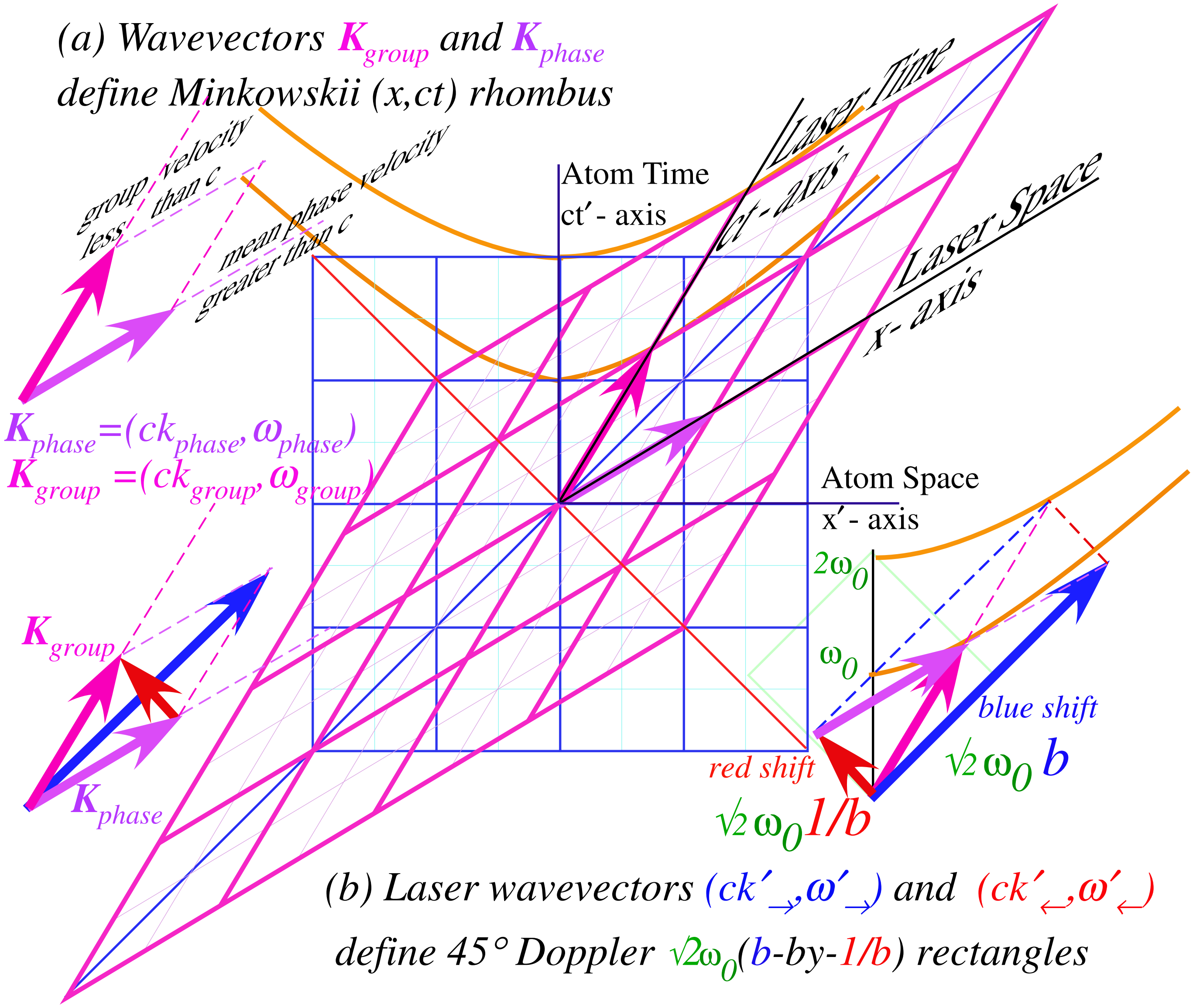

Fig. 4.3.4 Spacetime paths of laser standing wave zeros using (a) V_{group} and V_{phase}. (b) Doppler shifts.

Rhombic spacetime wave lattice paths shown above in Fig. 4.3.4 reconstruct the ones in Fig. 4.3.3(b). Fig. 4.3.4(a) shows the V_{group} and $V_{mean\ phase}$ slopes u/c and c/u (V_{group} is slower than c and $V_{mean\ phase}$ is faster than c) of a rhombic (x,ct)-lattice based on $(ck'_{group}, \omega'_{group})$ and $(ck'_{phase}, \omega'_{phase})$ vectors. These are half-diagonals of $45°$-tipped rectangles shown in Fig. 4.3.4(b). Each rectangle has a longer side of length $b\sqrt{2}\omega_0$ that is the blue shifted laser wave vector $(ck'_{\rightarrow}, \omega'_{\rightarrow})$ and a shorter side of length $1/b\ \sqrt{2}\omega_0$ that is the red shifted wave vector $(ck'_{\leftarrow}, \omega'_{\leftarrow})$ of the oppositely moving laser. (Here, $b=2$ again.) Rhombic cell vectors frame an invariant area ω_0^2 and lie on hyperbolas of radius ω_l as given by (4.3.12). The rhombic cells have half the area $(2\omega_0^2)$ of their enclosing $b\sqrt{2}\omega_0$-by-$1/b\ \sqrt{2}\omega_0$ rectangle whose diagonal lies on an invariant hyperbola of double-radius $2\omega_l$, twice that of the rhombic half-diagonal's hyperbola.

Fig. 4.3.4 emphasizes continuous wave (CW) phase paths. The following Fig. 4.3.5 shows pulsed wave (PW) paths that we might see if the lasers just spat out Newtonian corpuscles or incoherent pulses.

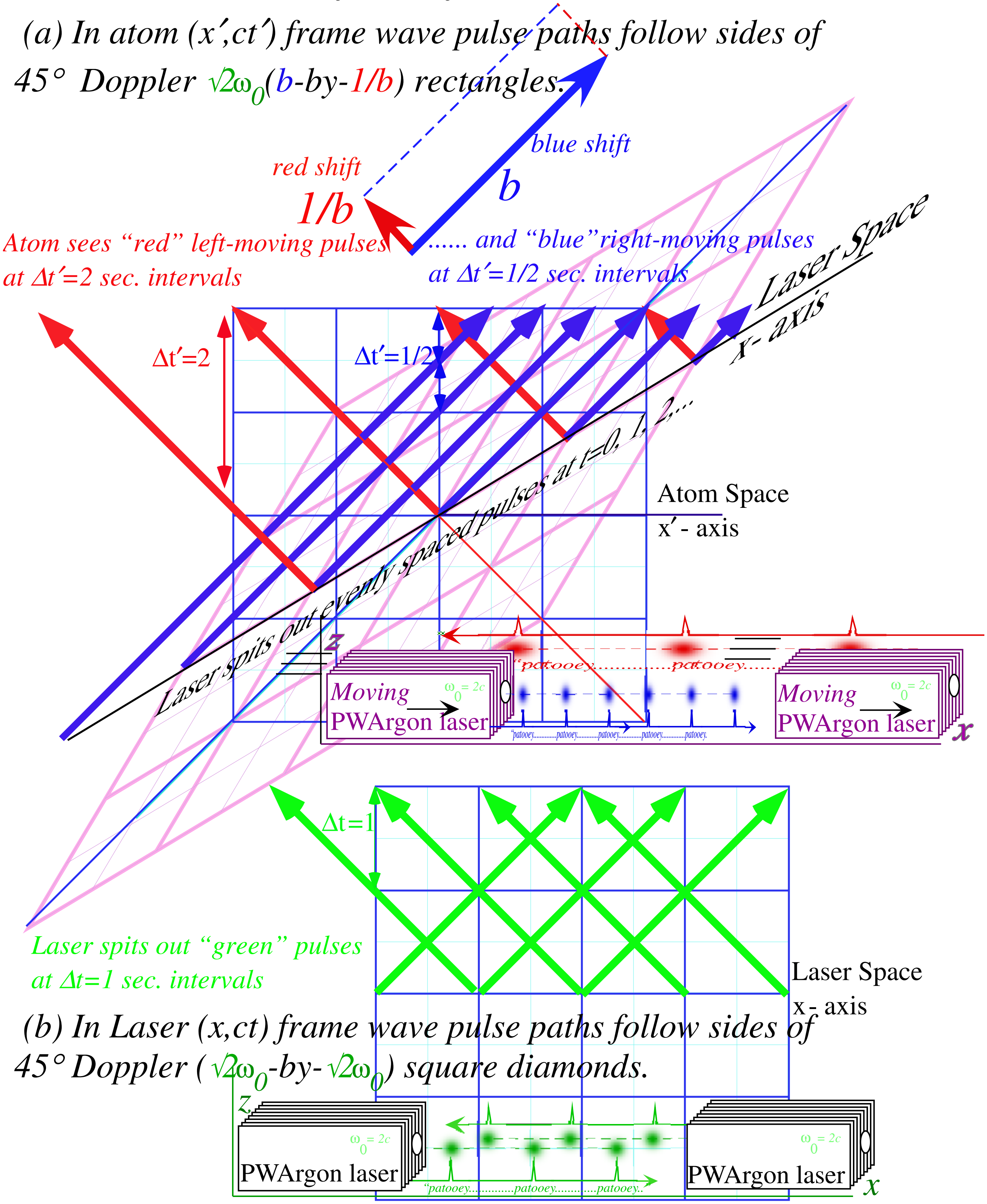

Fig. 4.3.5 Spacetime paths of laser pulses or "particles" as seen by (a) Atom frame. (b) Laser frame.

(d) Pulsed Wave (PW) and "particle" paths *versus* Continuous Wave (CW) laser

If the lasers in the preceding figures were to spit out pulses at *1 sec*. intervals, then the Minkowski wave interference grid of Fig. 4.3.3 and Fig. 4.3.4 is replaced by a latticework of *45°* rectangles that may be thought of as pulse or particle paths as noted in Fig. 4.2.11. Rectangle aspect ratio is that of the Doppler *b*-shift squared, that is, $b^2=4$ or *4-to-1* in the case shown in Fig. 4.3.5(a).

Such paths result from the lasers emitting pulses at *1 sec.* intervals in both directions as shown in Fig. 4.3.5(b). Newton viewed light as a beam of "corpuscles" that occasionally has "fits" (his term for what later was seen as wave interference.) The "corpuscles" of modern quantum theory are called *photons* but are not simply wave pulses. Nevertheless, we may imagine photons follow pulse paths.

The atom frame sees Doppler shifted rates of pulse production just as it saw the color frequencies shifted by the same *b*-factor of *2* on the "blue" side and *1/2* on the "red" side. The quotes around the color names are to remind us that very sharp pulses are "white" combinations of many colors interfering all at once as will be explained later. Fig. 4.3.5 shows broad pulses, say $\Delta t\sim 10^{-2}$ second, plotted once a second on a length scale of light-seconds. Such broad pulses do not compromise their "color" significantly as shown in simulations of Fig. 5.3.2 in the following Chapter 5.

The "Now" line(s)

At each instant of time in each frame there is a line of points that the frame calls *NOW*. For the atom (x',ct')-frame in Fig. 4.3.5(a) the *NOW* line for $(x',ct'=0)$ is the horizontal x'–axis. Meanwhile, for the laser (x,ct)-frame in Fig. 4.3.5(a), the *NOW* line for $(x,ct=0)$ is the x–axis which is tipped up at the velocity slope u/c. The laser would prefer to plot its frame as shown in Fig. 4.3.5(b) with its *NOW* line horizontal. Then the atom *NOW* line for $(x',ct'=0)$ and x'–axis would tip *down* at slope $-u/c$.

If the laser spits out pulses at equal space intervals along its $(t=0)$-*NOW* line as shown in Fig. 4.3.5(b) then the pulses go off at speed $\pm c$ and are seen to pass any space point at equal time intervals regardless of direction of travel. Not so, according to the atom frame as plotted in Fig. 4.3.5(a). The atom faults the laser for not releasing those pulses on a *NOW* line belonging to the atom and thereby causing the right-moving blue pulses to "pile-up" and hit rapidly like "*clink, clink, clink, clink, clink,…*" while the left moving red pulses spread out and hit less often like "*clunk,…., clunk,….*"

The delay of the "clunkers" is made worse for the atom by the fact that their release locations are stretched out from, say, laser point $(x=1,ct=0)$ to atom point $(x'=\cosh\beta,\ ct'=\sinh\beta)$ as given by (4.3.7f). In order to appreciate the ways that time definition may seem out-of-whack, we need to explore further the geometry of the wave and pulse path coordinate systems. This is addressed in the following section.

4.4 Geometry and Invariance in Lorentz transformations

The Lorentz transformations (4.3.7) relate the two coordinate systems in Fig. 4.3.3 and Fig. 4.3.5. To check (4.3.7a) note that the time axis $x= 0 = x'-\beta ct'$ gives a line $x'=\beta ct'=ut'$ consistent with the figures having a laser traveling positively at velocity $u=\beta c$. Fig. 4.4.1 shows a close-up view of the *(+,+)* quadrant including the geometry of the well-known *Einstein time dilation* Δt (which is *125%* for $\beta=3/5$)

$$\Delta t' / t' = \frac{1}{\sqrt{1-\beta^2}} = \cosh\rho \approx 1 + \frac{\rho^2}{2} \quad (\text{for } \rho \approx \beta << 1), \tag{4.4.1a}$$

and the well known *Lorentz-Fitzgerald length contraction* ΔL (which is *80%* for $\beta=3/5$).

$$\Delta L' / L' = \sqrt{1-\beta^2} = \operatorname{sech}\rho \approx 1 - \frac{\rho^2}{2} \quad (\text{for } \rho \approx \beta << 1) \tag{4.4.1b}$$

These are each second order effects for small velocity while the *Doppler shift* $\Delta\omega$ is a *first* order one.

$$\Delta\omega' / \omega' = \frac{\sqrt{1+\beta}}{\sqrt{1-\beta}} = \frac{1+\beta}{\sqrt{1-\beta^2}} = e^{\rho} \approx 1 + \rho \quad (\text{for } \rho \approx \beta << 1) \tag{4.4.2}$$

While Lorentz length contraction and Einstein time dilation are the first topics in most old-fashioned relativity treatments, the Doppler shifts are far greater effects. Also, Doppler is the primary concept for wave relativity. Its derivation (4.3.5) is comparatively clear and simple. Anyone who has gotten a speeding ticket from a Doppler meter-yielding cop has felt its effects. To feel the second-order dilation or contraction effects would involve, at the very least, an astronomical speeding ticket!

As discussed in Sec. 4.3.(c), $\beta = 3/5$ Doppler blue and red shifts correspond to *(+,+)* diagonal expansion of *200%* and *(+,–)*-diagonal foreshortening of *50%* , respectively. As shown in Fig. 4.4.1, the quantities $\Delta L'$ and $\Delta t'$ correspond, respectively to only *80%* and *125%* Minkowski graph projections from the unit grid markers *(x=1.0) and (ct=1.0)* in the laser frame onto the atom's *(x') or (ct')* axes.

The atom says, "Laser's unit length has contracted to *0.8*, but his unit time has dilated to *1.25*!" However, projections from *(x'=1.0,ct'=1.0)* in the atom frame to the laser's *(x,ct)* axes tell a seemingly contradictory story. The laser says, "No! It's the atom's unit length which has contracted to *0.8*, and it's the atom's unit time that has dilated to *1.25*!" It gets to be a serious argument because *they are both right*!

The resolution of this paradox centers on the definition of *now* or *simultaneity.* The projections in Fig. 4.4.1 respect the *NOW*-line of the atom that is always parallel to his horizontal *x'*-axis in this graph. He asks, "Along what horizontal now-line is the laser tick *ct=1.0*?" (At atom now-line *ct'=1.25*.)And, "What is the distance between the laser's rear *(x=0)* and front *(x=1.0)* along my *ct'=0* now-line?" (The distance is $\Delta L=0.8$ along any of the atom's now-lines.)

However, the laser's now-line is always parallel to his *x*-axis so it slopes up by *3/5* in Fig. 4.4.1. (Presumably, *x* would be horizontal if you asked laser people to draw the graph, but, then the atom's *x'*-axis would tip down.) So the laser's projections also show a *1.25* time dilation and a *0.8* length contraction, just like those claimed by the atom in Fig. 4.4.1. (The space and time grid markers follow invariant hyperbolas (4.3.12) shown in the figure. Invariants are discussed at length in the following chapter.)

Perhaps, it is surprising that old-fashioned texts do not mention the reverse of the Lorentz length contraction and Einstein time dilation. Just as real and present in Fig. 4.4.1 are *length dilation* and *time contraction* effects which the atom frame records for a speeding laser system.

Dropping a perpendicular (not shown in Fig. 4.4.1) from the laser point $(x=1.0, ct=0.0)$ to the atom's x'-axis shows that the laser unit length at its zero-time $(ct=0)$ has dilated by 125% to $x'=1.25$ at atom time $ct'=0.75$. (By that time the laser origin has moved to $x'=(3/4)(4/5)=0.45$ leaving the old Lorentz contracted length of exactly $1.25-0.45=0.8$. But, whom are you going to believe here?)

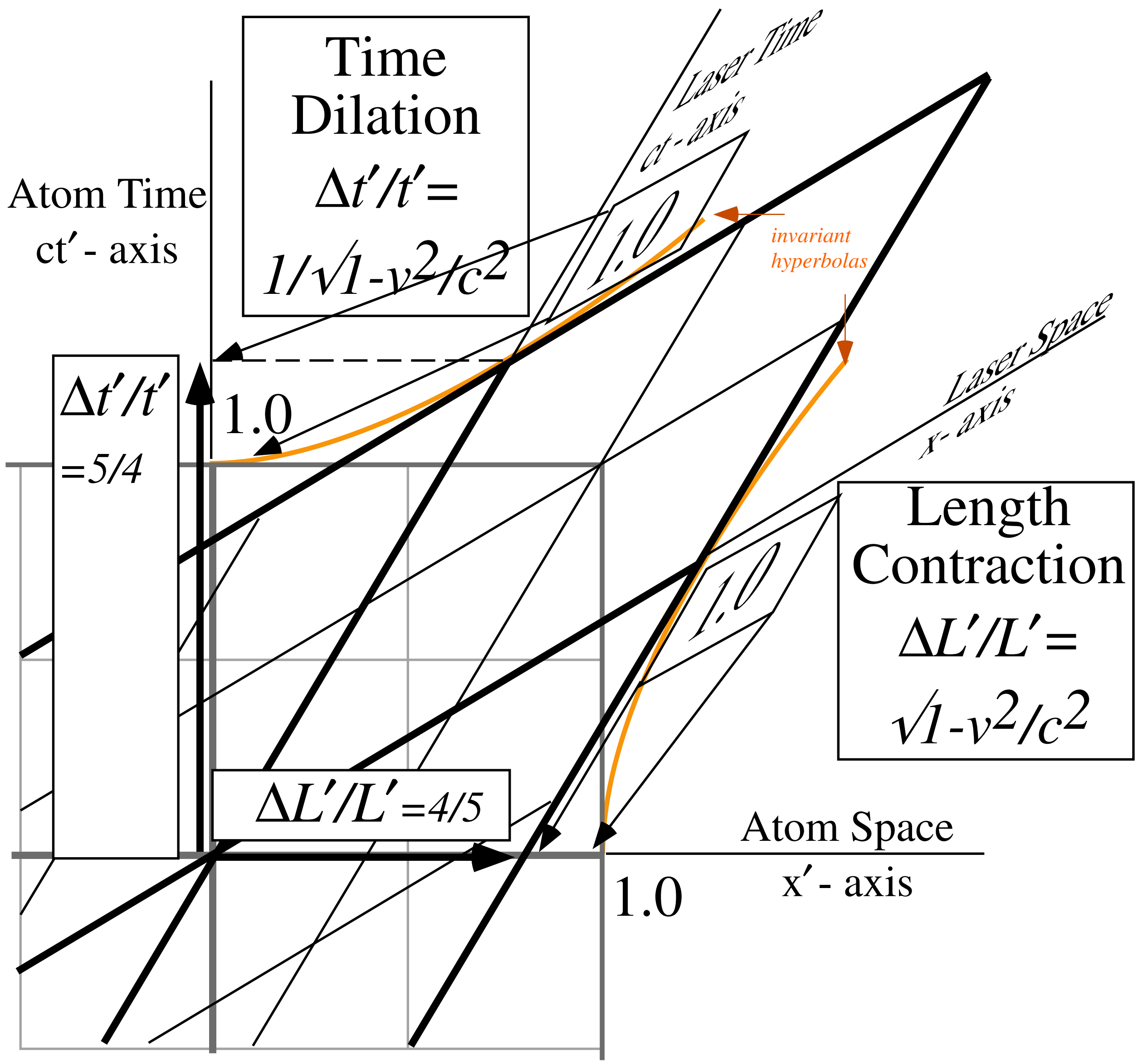

Fig. 4.4.1 Minkowski plot showing time dilation and Lorentz contraction effects at u=3c/5.

Time contraction is relevant to the atom who asks, "When do I experience a laser phasor ticking its unit time $ct'=1.00$?" That time point at the atom's origin $(x=0)$ is a "contracted" time of $ct=0.8$. But, the laser *origin* doesn't tick *1 o'clock* until the old dilated atom time of $ct=1.25$. It's all relative!

(a) Geometric construction of relativistic variables and invariants

Fig. 4.4.2 shows a geometric construction of relativistic quantities in the order that they are normally introduced in conventional algebraic treatments starting with velocity u/c in Fig. 4.4.2(a) then followed by Lorentz contraction factor $\sqrt{1-u^2/c^2}$ and *stellar aberration angle* σ in Fig. 4.4.2(b).

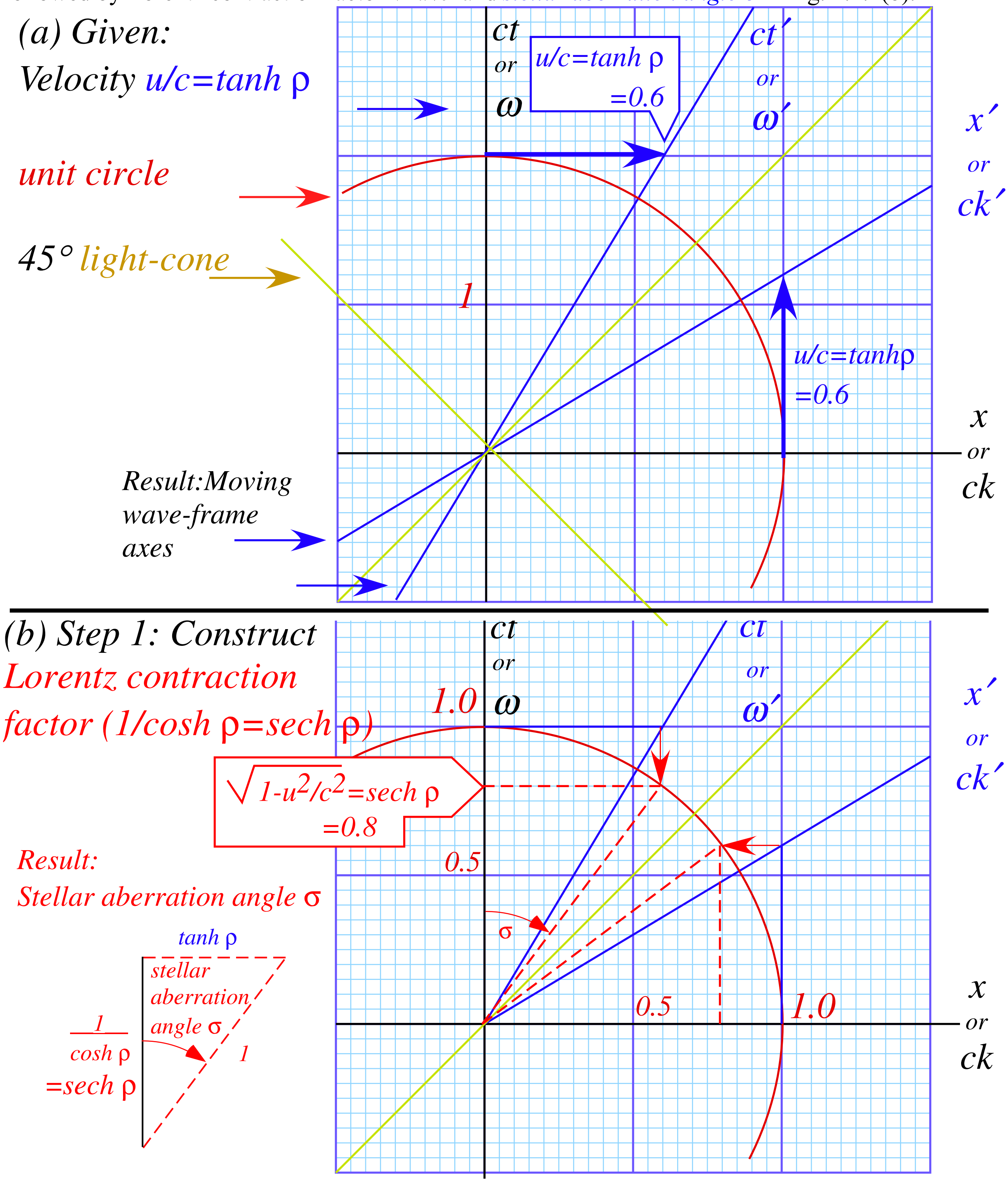

Fig. 4.4.2 Geometry of relativistic quantities. (a) Velocity u/c=3/5. (b) Related Lorentz contraction.

Lorentz contraction and aberration angle

The *stellar aberration angle* (σ=*atan(sinh* ρ*)*) is the angle a telescope must tip to catch starlight coming in normal to the telescope's direction of motion. This is discussed more fully in the development of three-dimensional space and four-dimensional wave coordinates. (See Chapter 6.)

The physical significance of *Lorentz contraction factor* $sech\ \rho$ has been noted in the discussion of Fig. 4.4.1. Here in Fig. 4.4.2(b) the plane geometric construction starts by dropping a perpendicular from the unit abscissa (or ordinate) toward the unit circle. The intercept is the altitude (or base) of the stellar aberration triangle whose hypotenuse is unity and base (or altitude) is the Lorentz contraction factor.

Lorentz-Einstein factors

Lorentz-Einstein *asimultaneity factor* $sinh\ \rho$ and *time-dilation factor* $cosh\ \rho$ are obtained geometrically in Fig. 4.4.2(c). Asimultaneity coefficient $sinh\ \rho$ is found by extending the stellar-aberration hypotenuse from the unit circle back to the unit abscissa (or ordinate) where the intercept distance is $sinh\ \rho$. Finally, a line perpendicular to the unit line intercepts the space (or time) axis at a point whose coordinates ($sinh\ \rho$, $cosh\ \rho$) (or ($cosh\ \rho$, $sinh\ \rho$)) include the time-dilation $cosh\ \rho$, as well.

Both coefficients $sinh\ \rho$ and $cosh\ \rho$ approach half-exponential functions $e^{+\rho}/_2$ for large ρ, with dilation $cosh\ \rho$ bigger than asimultaniety $sinh\ \rho$ by $e^{-\rho}$, the red-shift. So, the *(*$sinh\ \rho$, $cosh\ \rho$*)*-triangle slope can only approach the $45°$ or unit slope that represents the speed-of-light horizon. However, only zero and ±infinity limit the slope of the stellar-aberration hypotenuse. As speed approaches c, stars appear to swing in front arbitrarily close to the direction of travel.

In the non-relativistic limit of low speeds $(u<<c)$, the asimultaneity factor $sinh\ \rho$ is first order in velocity u or rapidity ρ while the time-dilation factor $cosh\ \rho$ remains equal to 1 and grows only by second order term $(u/c)^2/_2$. Having $cosh\ \rho \sim 1$ and $sinh\ \rho \sim \rho \sim u/c$ simplifies the construction in Fig. 4.4.2(c). In this limit the stellar aberration $(tanh\ \rho\ , 1)$-triangle reduces to a $(u/c,1)$-triangle and becomes equal to the coordinate $(sinh\ \rho\ , cosh\ \rho)$-triangle that reduces to a $(u/c,1)$-triangle, too.

For speeds low enough to ignore time dilation, there is only one pair of triangles: a $(u/c,1)$-triangle defining the time axis and a $(1, u/c)$-triangle defining the space axis. The non-relativistic limit is *not* the same as the so-called Galilean limit that has no asimultaneity factor $sinh\ \rho$ at all and would fail to tip the space axis $(1, u/c)$. The asimultaneity factor is a *first* order one giving $sinh\ \rho \sim u/c$ and *not* zero.

Doppler factors

Both Doppler factors $b=e^{+\rho}$ and $b^{-1}=e^{-\rho}$ are first order in u and are fundamental to the wave based development stated by (3.2.5). Here $e^{+\rho}$ and $e^{-\rho}$ are the last to appear in the construction ending with Fig. 4.4.2(d). This last step simply strikes an arc of radius $sinh\ \rho$ from the time dilation point $cosh\ \rho$ so as to locate the sum $e^{+\rho}= cosh\ \rho + sinh\ \rho$ and difference $e^{-\rho}= cosh\ \rho - sinh\ \rho$ that are the Doppler factors.

The construction is quite straightforward as presented by Fig. 4.4.2(a-d), but it is even simpler if the Doppler factor b is given first. A lattice of b-by-b^{-1} rectangles defines the Doppler pulse-paths in Fig. 4.4.2(d). Then the rectangle diagonals give the $(sinh\ \rho\ , cosh\ \rho)$-triangles directly and the rest follows.

(c)

Step 2: Construct Lorentz factors (sinh ρ , cosh ρ)

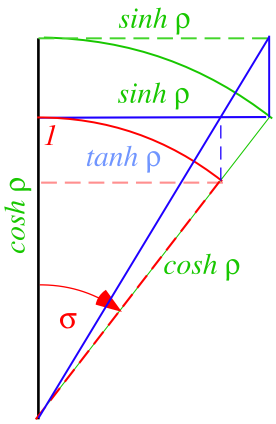

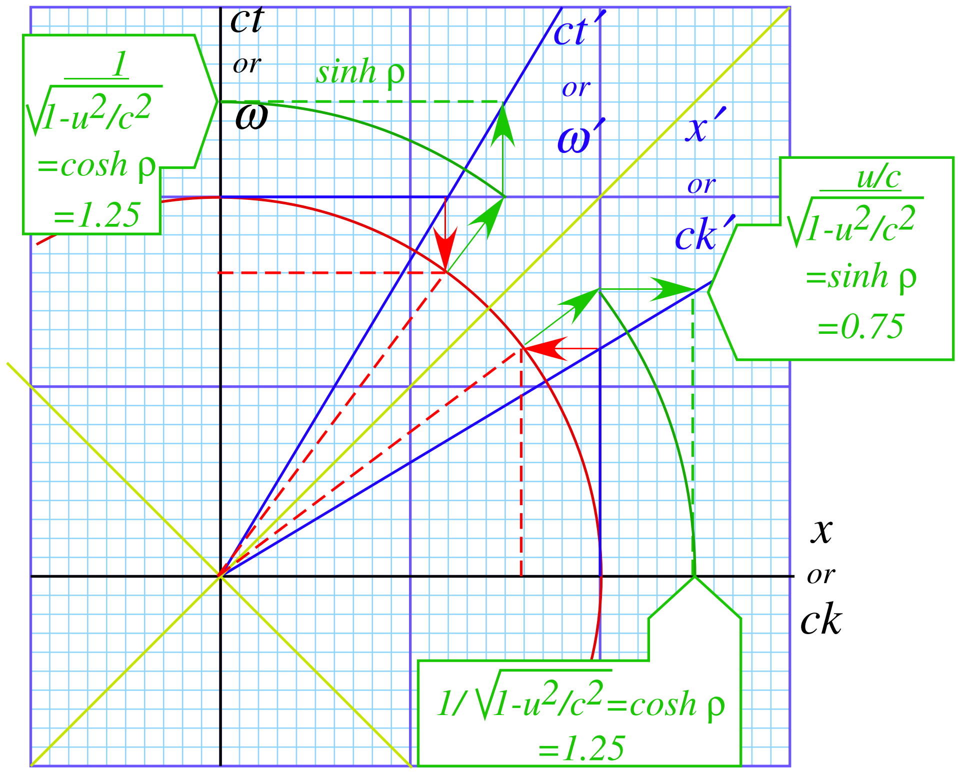

(d)

Step 3: Construct Doppler factors ($e^{+\rho}$, $e^{-\rho}$) and paths.

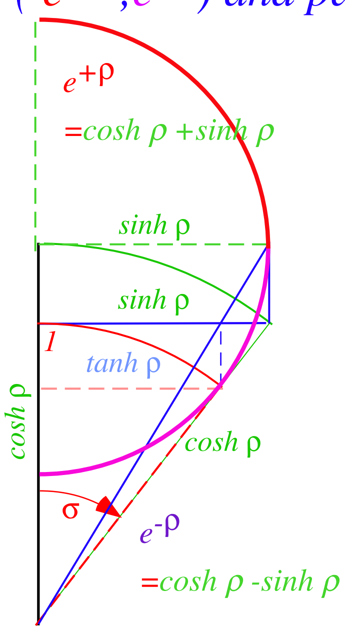

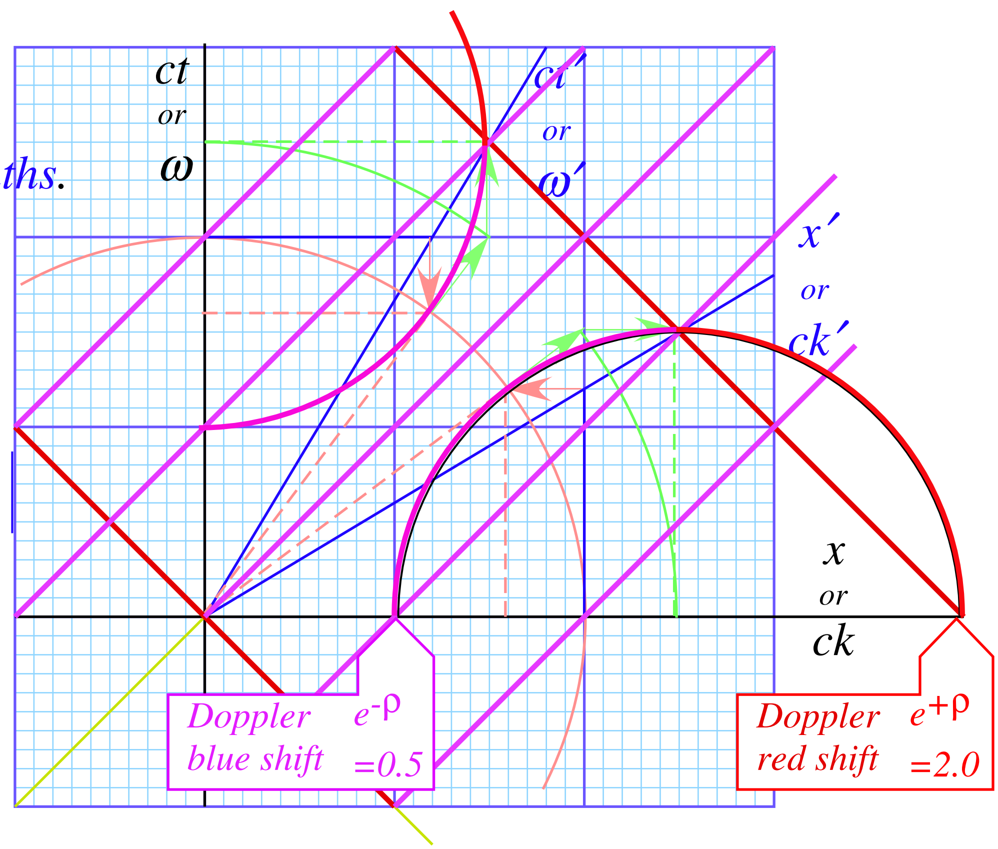

Fig. 4.4.2 (contd.) (c) Einstein-Lorentz time-dilation and asimultaniety factors.
(d) Doppler shift factors and particle-pulse paths.

Coordinate lines and invariants for waves or pulses: Baseball diamond geometry

Both the geometric construction and algebraic development of relativity and quantum wave mechanics is simplified and clarified by starting with wave Doppler factors. As shown in Fig. 4.4.2(d) (also in Fig. 4.3.5), the Doppler factors b and b^{-1} are the intercept intervals of the $\pm 45°$ trajectories of optical pulses in a moving frame. (In all cases illustrated, the Doppler factor is $b=2.0$ for a frame is moving at $u=3c/5$.)

The fundamental geometry of b-by- b^{-1} Doppler rectangles given in Fig. 4.4.2(d) is repeated in Fig. 4.4.3(a) that also shows the rectangle diagonals defining space and time axes and grid lines. Each figure has an inset sketch of its fundamental geometry. The inset in Fig. 4.4.3(a) is the simpler of the two because it is based on the b-by- b^{-1} Doppler rectangle. If there is a single geometric construction that represents modern physics as we currently understand it, then this must be the one. It is a “slide rule” for relativistic spacetime and quantum wave mechanics based entirely upon properties of light.

The Doppler rectangle is a distortion of a square diamond quite like a baseball diamond. It starts out with equal right and left arms (the “first” and “third” baselines) of length $\omega_0\sqrt{2}$ intersecting at origin or “home plate” at the bottom. The diamond center $(0, \omega_0)$ is the “pitcher’s mound.” At the top $(0, 2\omega_0)$ of the diamond shaped “infield” is the “2nd base” vector that is the sum of the “1st ” and “3rd ” base vectors.

Doppler blue shift b causes the home-to-first baseline to stretch by b, but it must remain on the $+45°$ right “foul-ball-line” by the rule of the *Colorful Axiom* (3.3.1) that demands constant lightspeed. The time reversal axiom then requires that the home-to-third baseline to shrink to $1/b$ (the Doppler red-shift factor) while staying on the $-45°$ left “foul-ball-line” according (3.3.1). The central pitcher mound and the second base vector lie on the sum of 1st and 3rd base vectors that tips as blue shift b increases.

When b is only slightly greater than one, the distance from home to the pitcher’s mound or to 2nd base grows only to *2nd order*. (This is the non-relativistic limit mentioned earlier.) However, as b grows without limit so do the distances to 1st and 2nd base as 2nd base follows a mass-shell hyperbola that brings it ever closer to 1st base but takes both of them deep into the “outfield” near the foul-ball-line.

Finally, the distance $1/b$ between 1st and 2nd base (and between home and 3rd) shrinks to a tiny value. This is known as the *ultra-relativistic limit*. Then the mass-shell point (2nd base) is quite like the right-moving photon point (1st base) and both have huge frequency and wavevector. Meanwhile, the left-moving photon wave (3rd base) has lost practically all its frequency and wavevector.

At this point, you may wish to skip to the beginning of Chapter 5 where it is seen that this “baseball diamond” also describes relativistic energy-momentum relations. The horizontal hyperbolas in Fig. 4.3.5(b) are called “mass shells” and vertical hyperbolas are constant-acceleration trajectories. Indeed, this little baseball diamond jewel of a construction is a Rosetta stone for the foundation of all of classical and quantum mechanics. What a simple rule-and-compass derivation of spacetime wave mechanics!

This is not to say the rest of Chapter 4 may be ignored. It contains important details about this wave based approach, and as Freeman Dyson is supposed to have said, “The devil is in the details!”

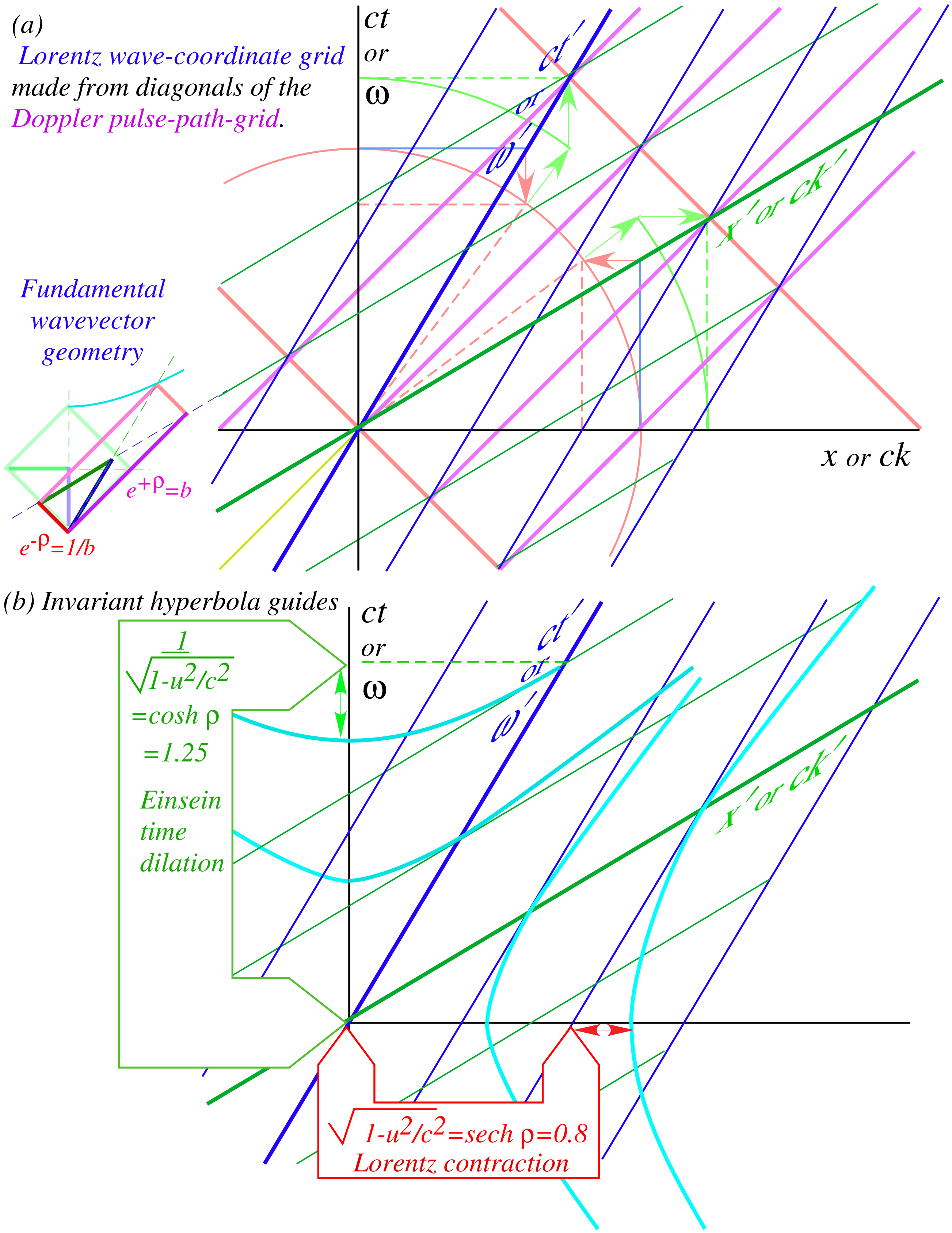

Fig. 4.4.3 Geometry of (a) Lorentz coordinates and (b) invariant hyperbolas

(b) Comparing Circular and Hyperbolic Functions

Quantum theory and relativity make frequent use of trigonometric circular functions (sinϕ , cosϕ , etc.) and hyperbolic functions (sinhϕ , coshϕ , etc.), and so it helps to be familiar with some tricks and definitions. To aid this, Fig. 4.4.3 presents a comparison of the circular and hyperbolic geometric ϕ definitions. First, it should be noted that both types of function are defined in terms of an area ϕ subtended by a rotating diameter, the gray area ϕ in Fig. 4.4.4 (a-b). (Note it is twice that subtended by the radius.) For circular functions, ϕ is also the usual rotational polar angle in radians ($-\pi<\phi<\pi$), but no such simple equivalent exists for hyperbolic ϕ geometry. As derived below, the area ϕ swept by a hyperbolic diameter is the rapidity ρ of Lorentz transformation (4.3.7a) or (4.3.7b).

A key idea here is that areas can be added to combine transformations. Transformation by ϕ_{AB} from frame *A* to *B* followed by a transformation by ϕ_{BC} from frame *B* to *C* equals a transformation by

$$\phi_{AC} = \phi_{AB} + \phi_{BC} \tag{4.4.3a}$$

from frame *A directly* to *C*. Relativistic velocities $u/c = \beta = tanh\phi$ add through hyper-tangents.

$$\tanh(\phi_{AB}+\phi_{BC}) = \frac{\tanh(\phi_{AB})+\tanh(\phi_{BC})}{1+\tanh(\phi_{AB})\cdot\tanh(\phi_{BC})} \quad \text{implies:} \quad \beta_{AC} = \frac{\beta_{AB}+\beta_{BC}}{1+\beta_{AB}\cdot\beta_{BC}} \tag{4.4.3b}$$

Adding angles is well known; but "slope-addition" is not an easy way to combine rotations! Adding velocities like (4.4.3b) takes some getting used to, too. Before relativity came along, we thought like Galileo that adding velocities directly ($u_{AC} = u_{AB} + u_{BC}$) was the way to transform them, and for small velocities, this is what (4.4.3b) gives. But, simple rapidity summing using (4.4.3a) is safe at any speed.

Let us prove that area ϕ swept by hyperbolic diameter *(x=cosh ρ, y=sinh ρ)* in Fig. 4.4.4(b) is ρ. By symmetry, the radially swept area in just one hyperbolic quadrant of $y=+\sqrt{1-x^2}$ is half that value.

$$\begin{aligned}\frac{\phi}{2} = \underset{\text{area}}{\text{triangle}} - \underset{\text{hyperbola}}{\text{area under}} &= \frac{1}{2}x\cdot y - \int_{x=1}^{x} y\cdot dx = \frac{1}{2}\sinh\rho\cdot\cosh\rho - \int_{\rho=0}^{\rho}\sinh\rho\cdot d(\cosh\rho) \\ &= \frac{1}{4}\sinh 2\rho - \int_{\rho=0}^{\rho}\sinh^2\rho\cdot d\rho\end{aligned} \tag{4.4.4a}$$

Using $\sinh^2\rho = \left(e^{\rho}-e^{-\rho}\right)^2/4 = \left(\cosh 2\rho - 1\right)/2$ shows the equality of ϕ and ρ.

$$\frac{\phi}{2} = \frac{1}{4}\sinh 2\rho - \int_{\rho=0}^{\rho}\frac{1}{2}\left(\cosh 2\rho - 1\right)\cdot d\rho = \frac{\rho}{2} \tag{4.4.4b}$$

The ϕ–area or rapidity $\rho = \ln b$ is unlimited. There is an infinite amount of area in a hyperbola's asymptote. For example, at $\beta=0.99999999$ the blue Doppler factor $b=e^{\rho}$ and ϕ are approximated easily.

$$b = \sqrt{\frac{1+\beta}{1-\beta}} \xrightarrow[\beta\to 1]{} \sqrt{\frac{2}{1-\beta}} = \sqrt{\frac{2}{10^{-8}}} = 10^4\sqrt{2}, \qquad \phi = \ln b \cong \ln\sqrt{\frac{2}{1-\beta}} = \ln\left(10^4\sqrt{2}\right) = 9.6 \tag{4.4.5}$$

But, the hyperbolic area ϕ grows slowly with *b* or β, roughly as the number of 9's in β. It shows that approaching the speed of light is like approaching an out of reach horizon.

(a) Geometry of Circular Functions

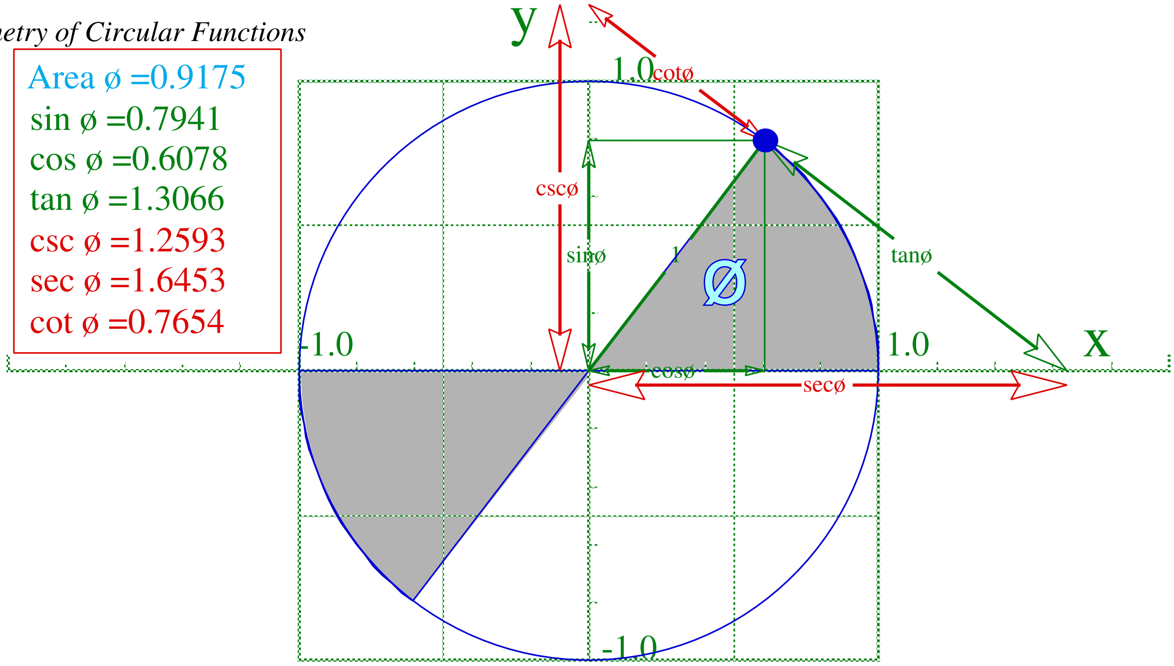

(b) Geometry of Hyperbolic Functions

(b) Geometry of Hyperbolic Functions

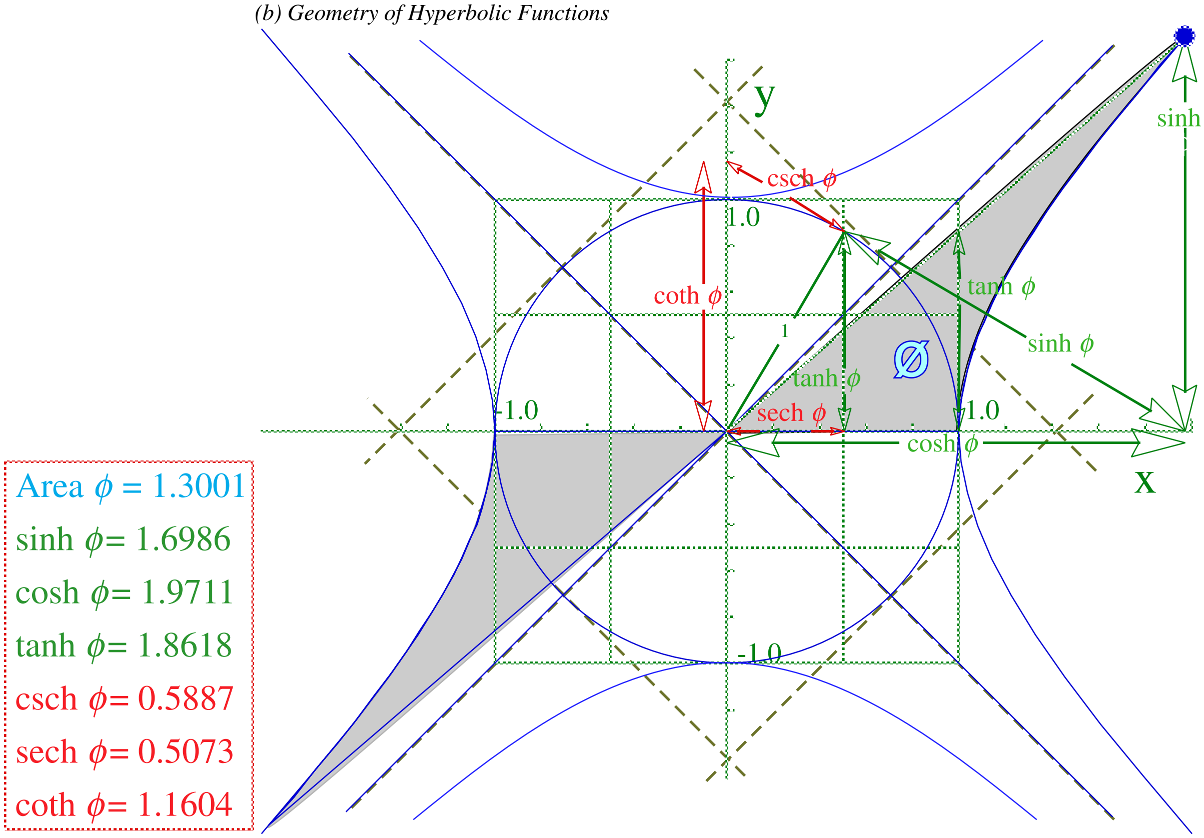

Fig. 4.4.4 Geometry and trigonometry of exp() functions (a)Circular and (b)Hyperbolic.(From RelativI*t)*

4.5. When Lightwaves Dance: Superluminal phase

The preceding relativistic quantum wave development was actually discovered in connection with a little known but quite striking wave interference phenomenon called *galloping*. The spacetime wave-zero coordinates displayed in the laser trap of Fig. 4.3.3 are each due to an extreme form of galloping in which phase velocity repeatedly or persistently exceeds the speed of light. Galloping is not restricted to γ-waves (light) but appears in virtually all wave phenomena including the μ-waves (matter) derived in Chapter 5.

A related but more complex wave phenomena called *revivals* is another striking interference effect that occurs in matter waves or in light confined by a waveguide. Revivals are most prevalent and persistent if the dispersion function is purely quadratic as it is for a DeBroglie-Bohr-Schrodinger wave described by the low-k-vector μ-wave case outlined in Chapter 5.

(a) Galloping waves and Standing Wave Ratio (SWR)

For counter-propagating laser beams such as in Fig. 4.3.3(a), galloping waves are the rule rather than the exception. In fact the only way to squelch galloping is to turn off one of the lasers! Turning off the right laser gives a pure *right-moving wave* $e^{i(kx-\omega t)}$ that traces *45°* wave zero lines going at a constant lightspeed c as shown in the spacetime plot of Fig. 4.5.1(a). Turning on even a small amount of *left-moving wave* $e^{i(-kx-\omega t)}$ results in galloping paths as shown in Fig. 4.5.1(b-e). The real part $Re\Psi$ of the wave gallops faster than light once each half-cycle just *1/4*-cycle behind a similarly galloping $Im\Psi$.

As the relative amount of left moving wave increases, galloping becomes more pronounced, and then, for equal left and right amplitudes, the zeros of the real standing wave gallop infinitely fast at each moment $Re\Psi$ is zero everywhere. (Being everywhere is tantamount to going infinitely fast!) This is the special case that gives a Cartesian *(x,ct)* grid shown in Fig. 4.3.3(a). Finally, for dominant left-moving amplitudes, the galloping reverses sign and subsides as in Fig. 4.5.1(e-f).

Counter-propagating laser waves in Fig. 4.5.1 have the following wave zeros of $Re\Psi$.

$$\begin{aligned}0 = \mathrm{Re}\,\Psi(x,t) &= \mathrm{Re}\left[A_{\rightarrow}e^{i(k_0x-\omega_0 t)} + A_{\leftarrow}e^{i(-k_0x-\omega_0 t)}\right]\\ &= A_{\rightarrow}\left[\cos k_0x\ \cos\omega_0 t + \sin k_0x \sin\omega_0 t\right] + A_{\leftarrow}\left[\cos k_0x\ \cos\omega_0 t - \sin k_0x \sin\omega_0 t\right]\\ &= \left(A_{\rightarrow} + A_{\leftarrow}\right)\left[\cos k_0x\ \cos\omega_0 t\right] + \left(A_{\rightarrow} - A_{\leftarrow}\right)\left[\sin k_0x \sin\omega_0 t\right]\end{aligned}$$

Galloping varies according to a *Standing Wave Quotient SWQ* or its inverse *Standing Wave Ratio SWR*.

$$\tan k_0x = -SWQ\cdot\cot\omega_0 t \quad (4.5.1a) \qquad \text{where: } SWQ = \frac{A_{\rightarrow}+A_{\leftarrow}}{A_{\rightarrow}-A_{\leftarrow}} = \frac{1}{SWR} \quad (4.5.1b)$$

The time derivative gives upper and lower speed limits in terms of $V_{phase} = \frac{\omega_0}{k_0} = c$ and SWQ or SWR.

$$\frac{dx}{dt} = c\cdot SWQ\frac{\csc^2\omega_0 t}{\sec^2 k_0 x} = \frac{c\cdot SWQ}{\sin^2\omega_0 t + SWQ^2\cdot\cos^2\omega_0 t} = \begin{cases} c\cdot SWR & \text{for: } t = 0,\ \pi,\ 2\pi\ldots \\ c\cdot SWQ & t = \pi/2,\ 3\pi/2,\ldots\end{cases} \quad (4.5.1c)$$

The functional dependency (4.5.1) might have been a familiar one to Galileo and Kepler who analyzed orbits of swinging lamps and planets using elliptical geometry sketched in Fig. 4.5.2. This analogy is examined in the following section.

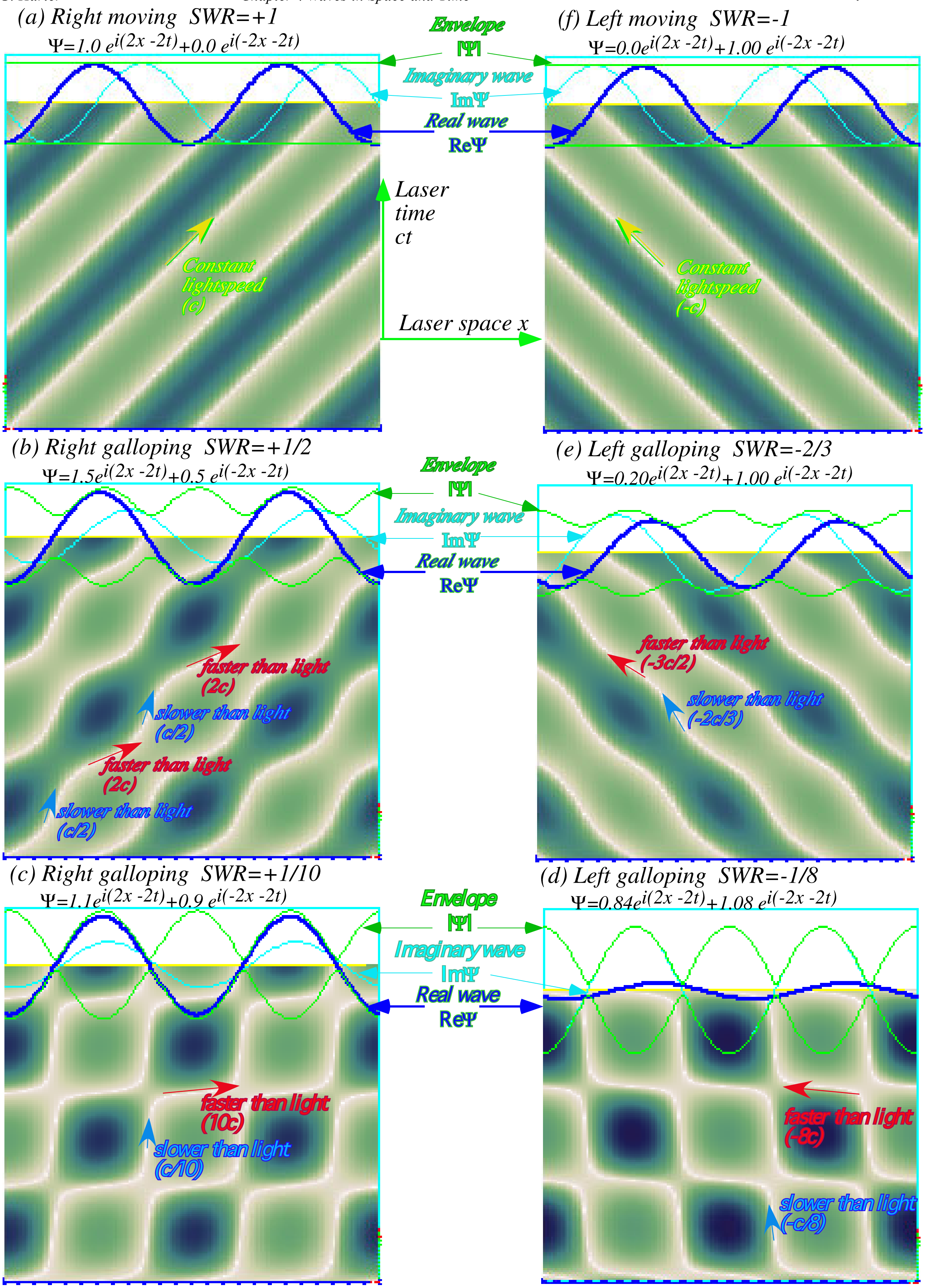

Fig. 4.5.1 Spacetime plots of monochromatic waves of varying Standing Wave Ratio (SWR).

(b) Kepler's Law for galloping

Galloping wave velocity (4.5.1c) is directly related to Kepler's Law for isotropic force field orbits, such as in a 2D oscillator orbit constructed by Fig. 4.5.2. (Recall also Fig. 1.3.6.) If polar angle $\phi(t)$ of ellipse-orbiting point $P=(x=a\sin\omega t,\ y=a\cos\omega t)$ is read clockwise like orbital phase ωt, then they relate by

$$\tan\phi(t) = \frac{y}{x} = -\frac{b}{a}\cdot\cot\omega t\,. \qquad (4.5.2)$$

This resembles the galloping wave equation (4.5.1a) with the ellipse aspect ratio b/a replacing a standing wave ratio. To conserve orbital angular momentum **r**x**v** in the absence of torque, the orbital velocity $v(r)$ gallops to a faster $v(b)$ at perigee $(r=b)$ and a slower $v(a)$ at apogee $(r=a)$. In the same way waves in Fig. 4.5.1 gallop faster through smaller parts of their envelope and slow down as their amplitudes grow.

Analogy of laser wave dynamics (4.5.1) to classical orbital mechanics (4.5.2) has physical as well as historical use. Wave galloping shown in Fig. 4.5.1 happens equally in systems with open or infinite boundaries as it does in closed or periodic (ring laser or Bohr-ring) systems. In fact, Fig. 4.5.2 are pictures of 2nd lowest $(k_m=\pm 2)$-modes of a micro-ring-laser or the 2nd excited Schrodinger $(m=\pm 2)$-waves on a Bohr-ring. Exactly two wavelengths fit in each space frame and two periods fit in each time frame. (While Bohr dispersion $\omega_m=Bm^2$ in Fig. 4.5.1(b) differs from optical dispersion $\omega_m=|ck_m|$, that does not affect Fig. 4.5.1. Right and left moving waves have the same frequency in either case, and time is scaled accordingly.)

Analogy with polarization ellipsometry

If a frame in Fig. 4.5.1 were drawn instead for 1st or fundamental $(m=\pm 1)$-waves or $(k_m=\pm 1)$-modes of either ring system it would just be a *1/4*-area square section with only one sine wave per frame. (Recall Fig. 4.2.10(c).) Such a wave has an average dipole moment $\mathbf{p}=\langle p\rangle$ that orbits an ellipse like radius **r** in Fig. 4.5.2 and is analogous to a polarization figures used to depict states in optical ellipsometry.

In the polarization analogy, purely right-moving $(m=+1)$ or purely left-moving $(m=-1)$ wave states e^{+ikx} and e^{-ikx} are analogous, respectively, to right or left circular polarization states. Equal combinations $e^{+ikx}+e^{-ikx}=2\cos kx$ or $e^{+ikx}-e^{-ikx}=2i\sin kx$ are analogous, respectively, to x-plane or y-plane polarization. Most arbitrary combinations $ae^{+ikx}+be^{-ikx}$ are analogous to elliptical polarization. A polarization vector for elliptic states enjoys the same Kepler galloping described by Fig. 4.5.2.

Perhaps the simplest explanation of wave galloping in Fig. 4.5.1 uses an analogy with the elliptical polarization states as in Fig. 4.5.3. The uniformly spaced ticks on the circular polarization circles are crowded into a traffic jam at the long axes of their elliptic orbits as the aspect ratio b/a or SWR approaches zero. The ticks near the short axes maintain their spacing in the Kepler geometry. Like a uniformly turning lighthouse beacon viewed edge-on, the beam is seen to gallop by quickly and then slow to a crawl as it swings perpendicular to the line of sight.

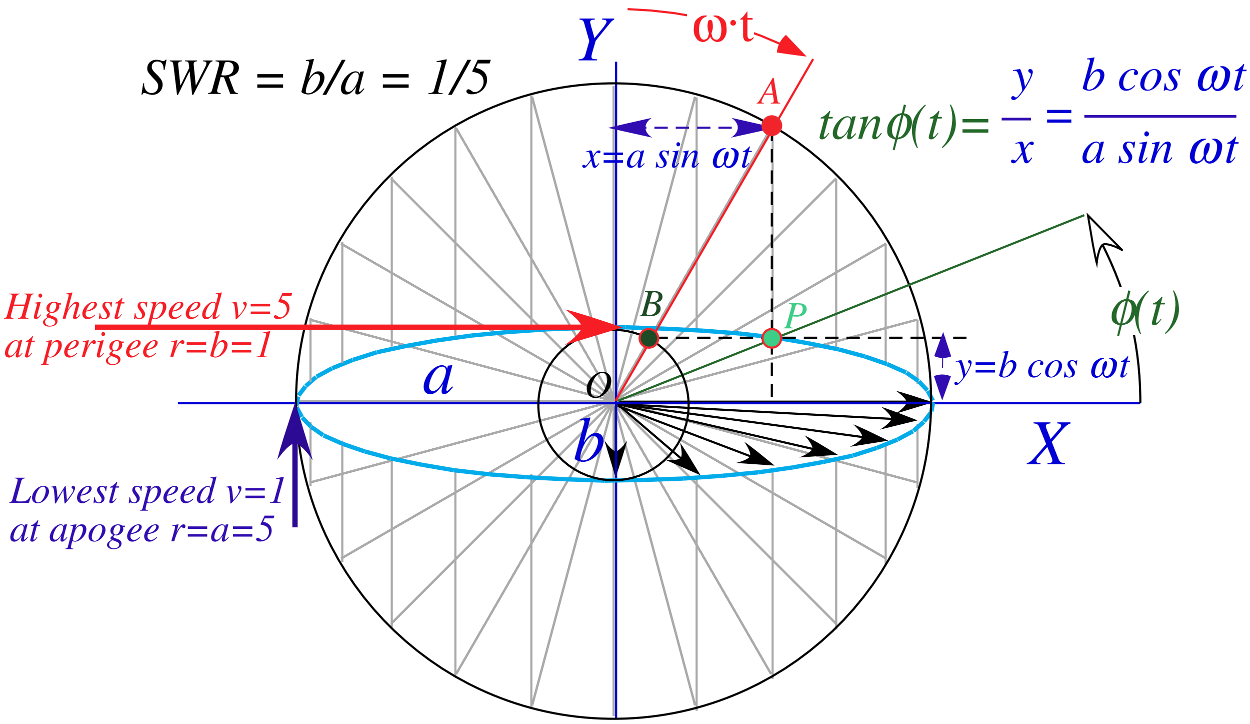

Fig. 4.5.2 Elliptical oscillator orbit and a Kepler construction

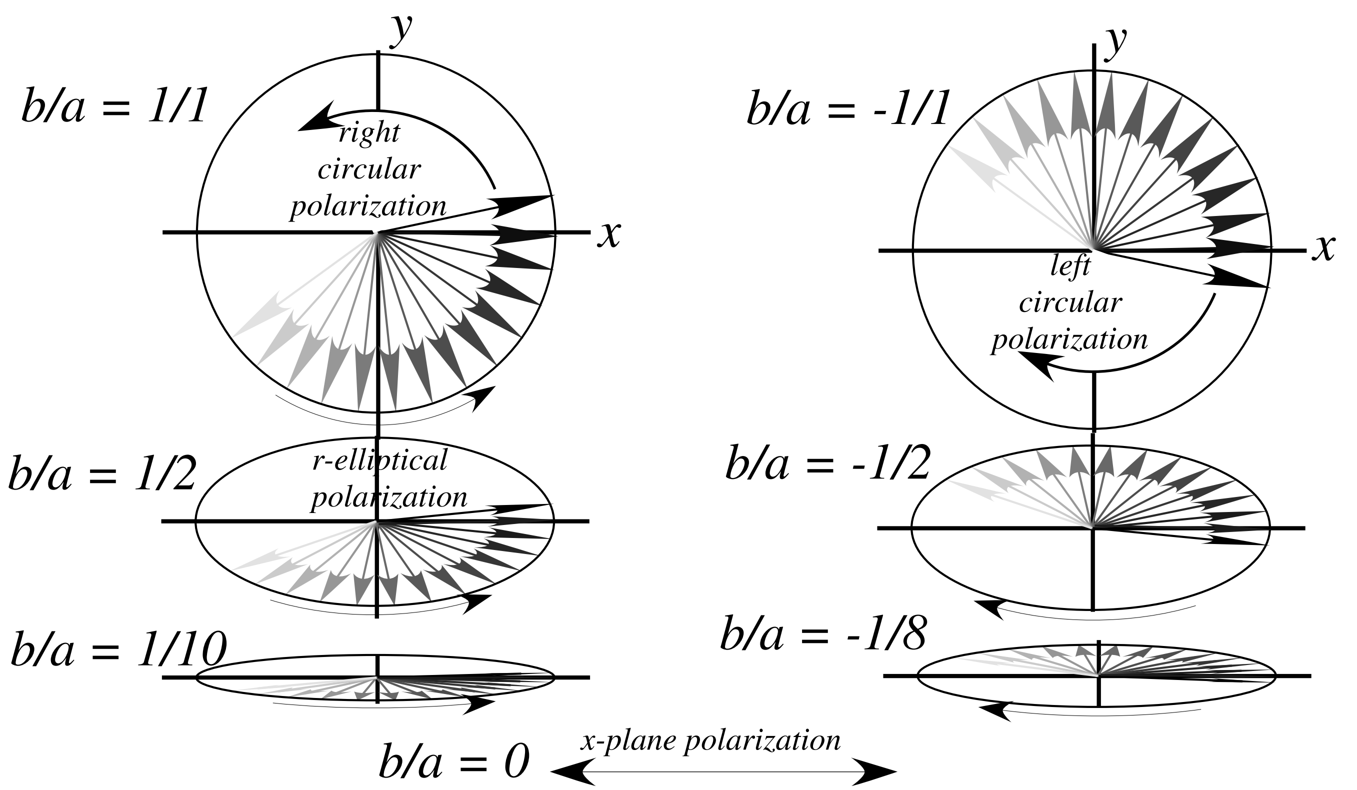

Fig. 4.5.3 Elliptical polarization states of varying aspect ratio a/b or standing wave ratio SWR. This figure is analogous to Fig. 4.5.1 according to the Keplerian geometry of Fig. 4.5.2.

(c) SWR algebra and geometry

The galloping waves $Re\Psi(x,t)$ and $Im\Psi(x,t)$ in Fig. 4.5.4(b-e) are speeding or galloping inside stationary envelopes $e=\pm|\Psi|=\pm\sqrt{(\Psi^*\Psi)}$ that serve as the "skin" of the wave. The bounding skin $\pm|\Psi|$ is a pair of square roots of the probability function $\Psi^*\Psi$ for a general galloping wavefunction

$$\Psi(A_\rightarrow,\omega_\rightarrow,k_\rightarrow;A_\leftarrow,\omega_\leftarrow,k_\leftarrow)=A_\rightarrow e^{i(k_\rightarrow x-\omega_\rightarrow t)}+A_\leftarrow e^{i(k_\leftarrow x-\omega_\leftarrow t)}. \qquad (4.5.3)$$

The envelope function is worked out below assuming real amplitudes $A_\leftarrow^*=A_\leftarrow$ and $A_\rightarrow^*=A_\rightarrow$.

$$e(x,t)=\left|\Psi(A_\rightarrow,\omega_\rightarrow,k_\rightarrow;A_\leftarrow,\omega_\leftarrow,k_\leftarrow)\right|=\sqrt{\Psi^*\Psi}$$

$$=\sqrt{\left(A_\rightarrow^* e^{-i(k_\rightarrow x-\omega_\rightarrow t)}+A_\leftarrow^* e^{-i(k_\leftarrow x-\omega_\leftarrow t)}\right)\left(A_\rightarrow e^{i(k_\rightarrow x-\omega_\rightarrow t)}+A_\leftarrow e^{i(k_\leftarrow x-\omega_\leftarrow t)}\right)}$$

$$=\sqrt{A_\rightarrow^*A_\rightarrow+A_\leftarrow^*A_\leftarrow+A_\leftarrow^*A_\rightarrow e^{i[(k_\rightarrow-k_\leftarrow)x-(\omega_\rightarrow-\omega_\leftarrow)t]}+A_\leftarrow A_\rightarrow^* e^{-i[(k_\rightarrow-k_\leftarrow)x-(\omega_\rightarrow-\omega_\leftarrow)t]}} \qquad (4.5.4a)$$

$$=\sqrt{A_\rightarrow^2+A_\leftarrow^2+2A_\rightarrow A_\leftarrow\cos[(k_\rightarrow-k_\leftarrow)x-(\omega_\rightarrow-\omega_\leftarrow)t]}\quad\text{(for real } A_\rightarrow \text{ and } A_\leftarrow) \qquad (4.5.4b)$$

$$=\sqrt{A_\rightarrow^2+A_\leftarrow^2+2A_\rightarrow A_\leftarrow\cos[2kx]}\quad\text{(for: } k_\rightarrow=k=-k_\leftarrow \text{ and: } \omega_\rightarrow=\omega=\omega_\leftarrow) \qquad (4.5.4c)$$

For monochromatic $(\omega_\leftarrow=\omega_\rightarrow)$ counter-propagating $(k_\leftarrow=-k_\rightarrow)$ waves, the envelope is a stationary or standing wave pattern. The envelope is a *two-component quantum interference function* similar to one first introduced in (1.3.10). Its min-max values give the amplitude peaks and valleys in Fig. 4.5.4a.

$$\begin{aligned} e_{MIN}&=\sqrt{|A_\rightarrow|^2+|A_\leftarrow|^2-2|A_\rightarrow||A_\leftarrow|}=|A_\rightarrow|-|A_\leftarrow| \\ |e_{MAX}|&=\sqrt{|A_\rightarrow|^2+|A_\leftarrow|^2+2|A_\rightarrow||A_\leftarrow|}=|A_\rightarrow|+|A_\leftarrow| \end{aligned} \qquad (4.5.5)$$

The ratio of interference maxima (where amplitudes $A_\rightarrow$ and $A_\leftarrow$ add constructively) to minima (where they subtract or interfere destructively) is called the *standing wave ratio (SWR)*.

$$-1\le SWR=\frac{e_{MIN}}{e_{MAX}}=\frac{|A_\rightarrow|-|A_\leftarrow|}{|A_\rightarrow|+|A_\leftarrow|}\le 1 \qquad (4.5.6)$$

Let us pause to reconsider the simple analogy between galloping waves and optical polarization. This analogy is related to a crowd behavior of American football fans. Whoopee. (Or Woo-pig-sooee.)

Analogy between complex waves and polarization: Stadium circumference waves

Imagine a single-kink $(k=1)$ wave wrapped around a ring like a "football stadium wave" in Fig. 4.5.4. As fans take turns standing up, a "stand-up" wave rotates clockwise around the stadium from $+x$-axis on North side ($r=0$ or *12 o'clock*) to $-y$-axis on East side ($r=3$ or *3 o'clock*) and so on.

The imaginary ("gonna' be standing-up") wave rotates $90°$ ahead from the $-y$-axis in the figure down to the $-x$-axis ($r=6$ or *6 o'clock*). This wave is analogous to a left-circular (clockwise) polarization state: $|L\rangle=|x\rangle - i|y\rangle$ which evolves in time according to $|L(t)\rangle=|L\rangle e^{-i\omega t}$. The real ("is") part of $|L(t)\rangle$ is $\mathrm{Re}|L(t)\rangle = \cos\omega t|x\rangle - \sin\omega t|y\rangle$, the dark arrows rotating clockwise from $|x\rangle$ at $r=0$ or *12 o'clock* toward minus $|y\rangle$ at $r=3$ or *3 o'clock* in the figure above. The blue-gray arrows rotating clockwise from minus $|y\rangle$ at $r=3$ or *3 o'clock* toward minus $|x\rangle$ at $r=6$ or *6 o'clock* depict the imaginary ("gonna'be") part of $|L(t)\rangle$, that is: $\mathrm{Im}|L(t)\rangle = -\sin\omega t|x\rangle - \cos\omega t|y\rangle$.

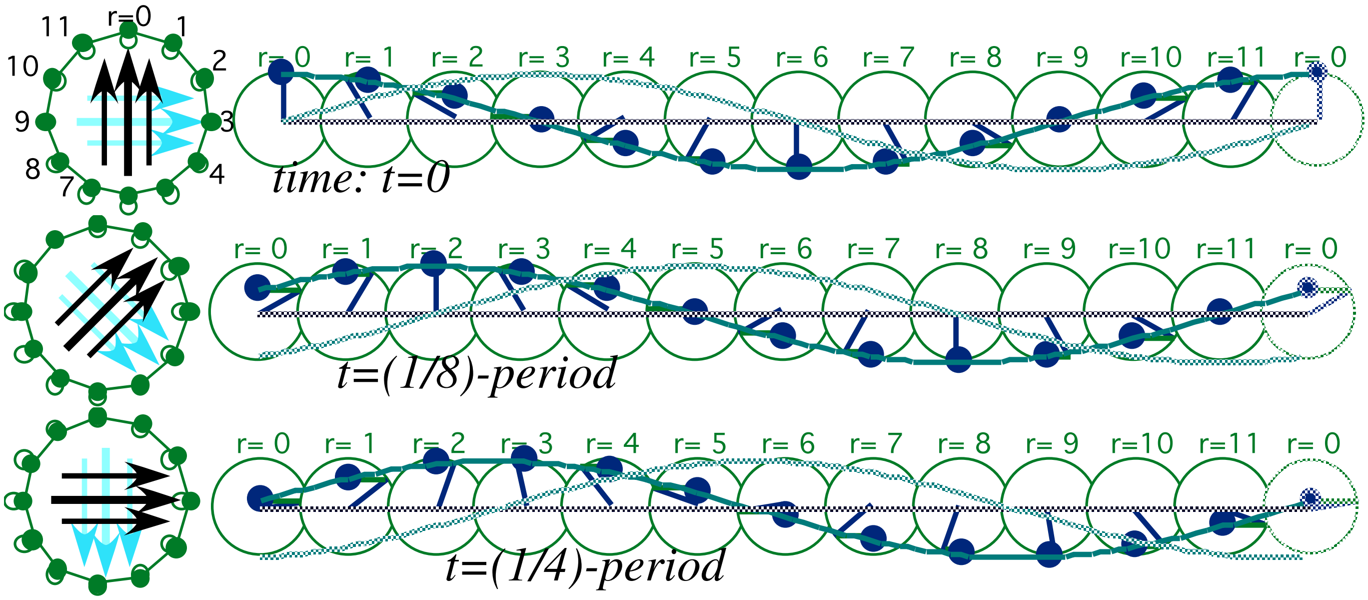

Fig. 4.5.4 Left-polarization state $|L(t)\rangle=(|x\rangle-i|y\rangle)e^{-i\omega t}$ *is like a (k=1) right-moving wave* $\Psi_{\rightarrow}= e^{i(kr-\omega t)}$

Next imagine a *negative*-single-kink *(k=-1)* "football stadium wave" going *anti*-clockwise in Fig. 4.5.5. This is *left*-moving wave $\Psi_{\leftarrow}= e^{i(-|k|r-\omega t)}$ or *right*-hand circular polarization state $|R\rangle=|x\rangle+i|y\rangle$. Because, human hands curl naturally inward (unlike reptiles) the *right* hand tends to point *left*-over-the-top.

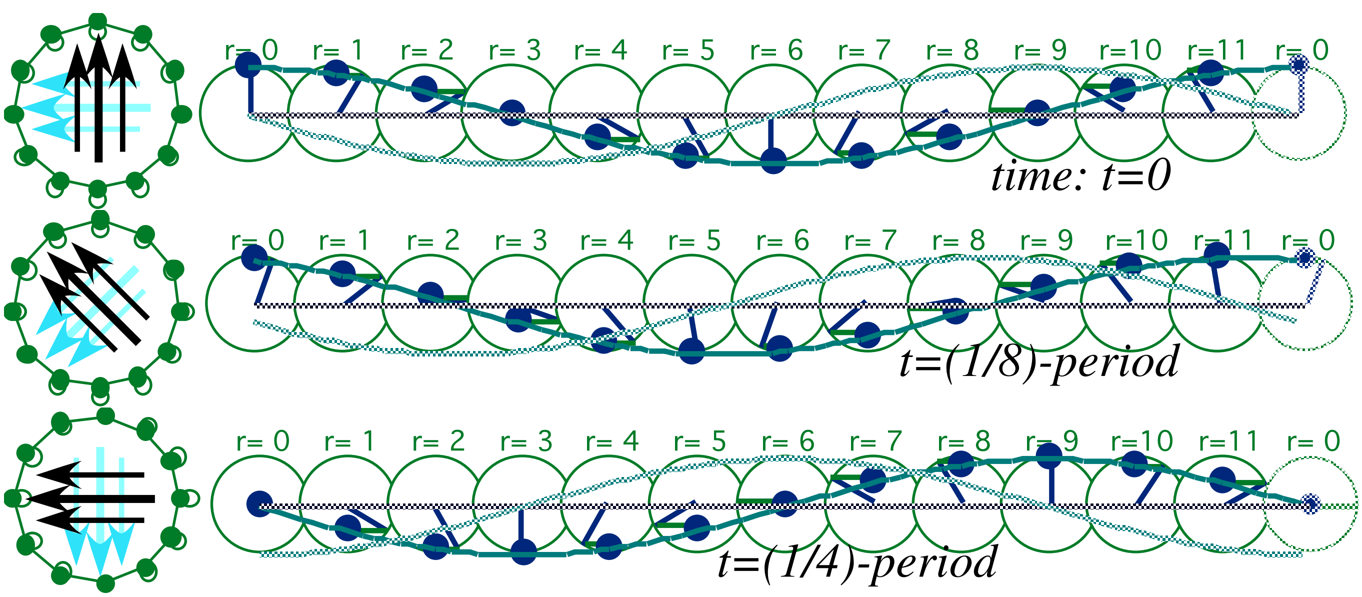

Fig. 4.5.5 Right-polarization state $|R(t)\rangle=(|x\rangle+i|y\rangle)e^{-i\omega t}$ *is like left-moving wave* $\Psi_{\leftarrow}= e^{i(-|k|r-\omega t)}$.

Now consider a 50-50 combination the right-handed and left-handed states.

$(|L\rangle+|R\rangle)/2= (|x\rangle-i|y\rangle+|x\rangle+i|y\rangle)/2 = |x\rangle$ $\quad (\Psi_{\rightarrow}+\Psi_{\leftarrow})/2= (e^{i(kr-\omega t)}+e^{i(-kr-\omega t)})/2 =e^{-i\omega t}\cos kr$

The result is clearly x-polarization or a *cosine standing wave* as shown below in Fig. 4.5.6. Notice that it starts out with a zero imaginary or "gonna'be" part. This predicts (correctly) that the real part is going to die. Notice that it does perish 1/4-cycle later when the real wave "is" zero everywhere. Let this be a lesson to ye of little or no imagination! In this case, however, hope springs eternal; then the "gonna'be" wave predicts a revival in the nether regions (with dubious anthropomorphic implications, however!).

Another 50-50 combination of right-handed and left-handed states is a difference instead of a sum.

$(|L\rangle-|R\rangle)/2=(|x\rangle-i|y\rangle-|x\rangle-i|y\rangle)/2 =-i|y\rangle$ $\quad (\Psi_{\rightarrow}-\Psi_{\leftarrow})/2=(e^{i(kr-\omega t)}-e^{i(-kr-\omega t)})/2 =e^{-i\omega t} i\sin kr$

The result is clearly y-polarization and a *sine standing wave* as seen in Fig. 4.5.7, but it starts $90°$ behind in phase. (Notice the "i" factor.)

The moving $\Psi_{\rightarrow}$ or $|L\rangle$ waves in Fig. 4.5.4 and $\Psi_{\leftarrow}$ or $|R\rangle$ waves in Fig. 4.5.5 represent one extreme while the cosine or x-standing waves in Fig. 4.5.6 and sine or y-standing waves in Fig. 4.5.7 represent another. In between these cases lie the general galloping or elliptic wave states of Fig. 4.5.1(b-d) with polarization that traces elliptical paths of the form sketched in Fig. 4.5.1 and Fig. 4.5.3.

Now we confront a familiar question, "Which came first, the chicken or the egg?" Should we think of plane-polarized states as being made of circular ones, or are circular-polarized states being made from plane old $|x\rangle$ and $|y\rangle$? We have emphasized the latter so far, but the answer is *both* (and which ever you find more convenient). Clearly, other plane polarized states such as $\theta=45°$ polarization bases $|x'\rangle = \cos\theta\, |x\rangle + \sin\theta\, |y\rangle$ and its orthonormal partner $|y'\rangle = -\sin\theta\, |x\rangle+\cos\theta\, |y\rangle$ are best described by good old plain old $|x\rangle$ and $|y\rangle$.

Perhaps, the more general elliptical polarization states and galloping waves beg to be described by circular polarization bases $|L\rangle$ and $|R\rangle$ and moving waves $\Psi_{\rightarrow}$ and $\Psi_{\leftarrow}$.. Nevertheless, all orthonormal and complete bases, including any valid elliptical pair, provide (as the name implies) a complete description according to Axioms 2 through 4, and are themselves completely described by any complete set of bases. It's all relative!

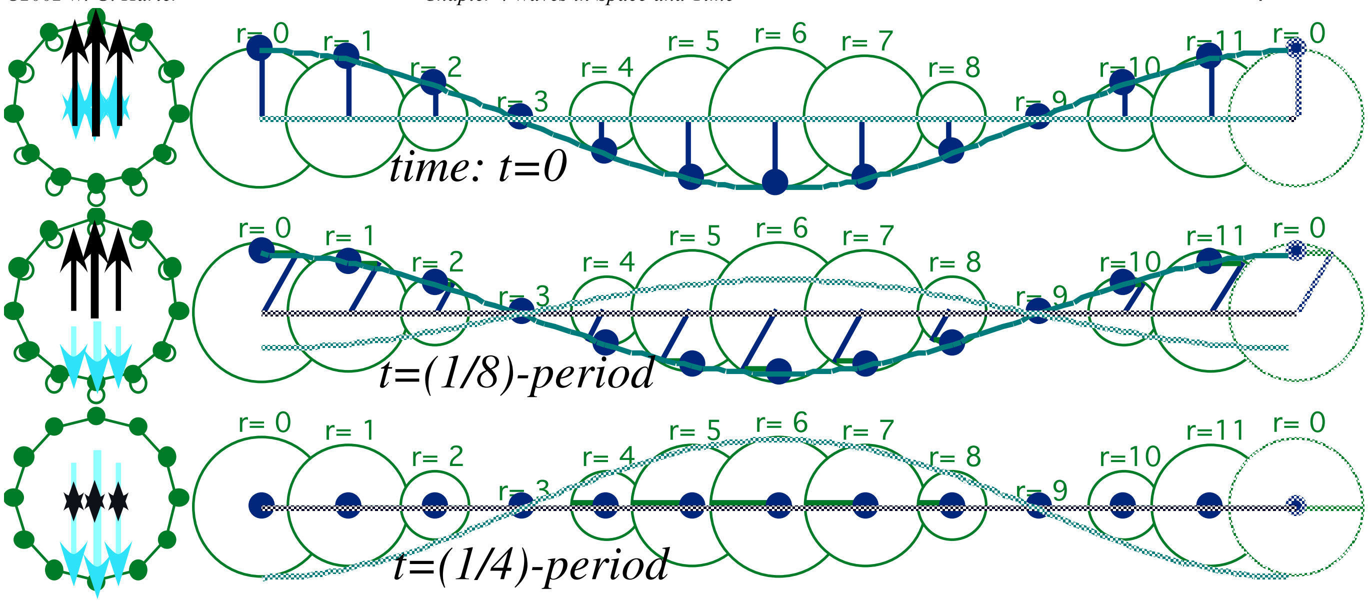

Fig. 4.5.6 x-polarization state |x⟩ is like a (k=1) cosine standing wave $(\Psi_{\rightarrow}+\Psi_{\leftarrow})/2= =e^{-i\omega t}\cos kr$.

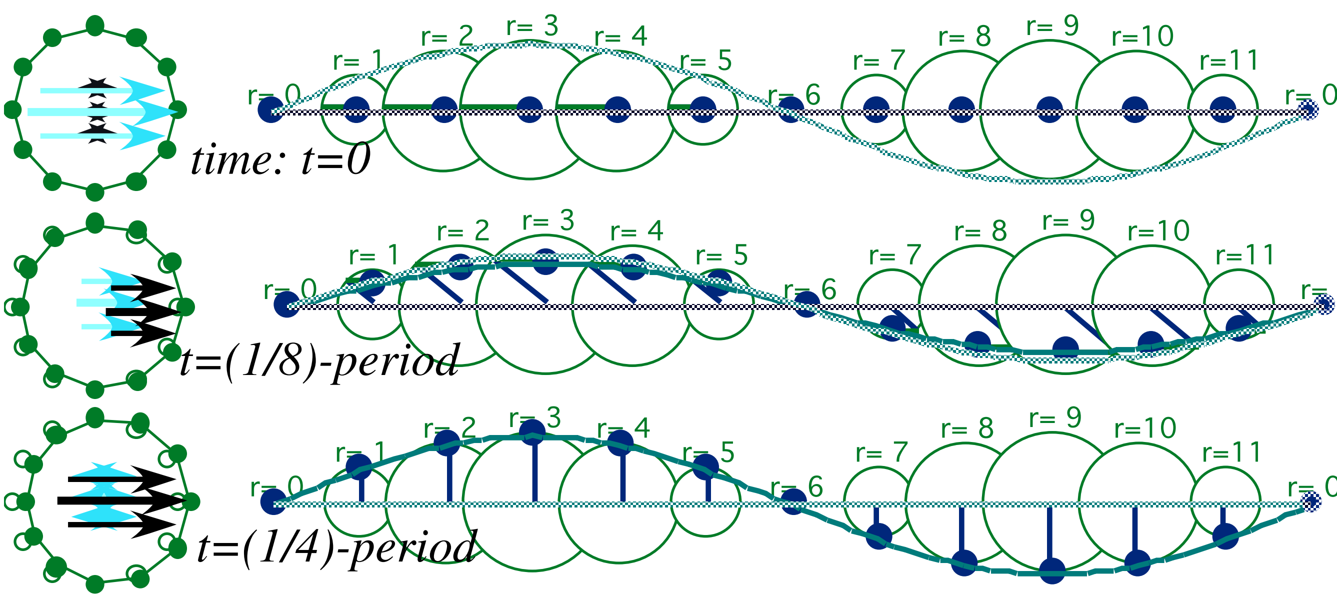

Fig. 4.5.7 y-polarization state |y⟩ is like a (k=1) (i)sine standing wave $(\Psi_{\rightarrow}-\Psi_{\leftarrow})/2= =e^{-i\omega t}i\sin kr$.

4.6 When Lightwaves Go Crazy: Spacetime switchbacks

For most of the waves discussed so far and particularly for the wave coordinates in Fig. 4.5.2 there is phase velocity or "speed of zeros" that exceeds the speed of light. A conventional aphorism, "Nothing can go faster than light." needs a more positive version, "Nothing *CAN* go faster than light!"

Still, as Feynman pointed out, there are consequences (a cosmic speeding ticket, if you will) for having the temerity and the "right stuff" (that is, *NO* stuff) to break this law. The consequences are to be seen undergoing pair creation and then annihilation while following a zigzag spacetime trajectory called a *Feynman-Wheeler switchback*. That is, you are reported to be simultaneously at three or more places!

(a) Wobbly and switchback waves

Each part in Fig. 4.6.1 is an atom-frame view of a corresponding part of Fig. 4.5.2. Recall from Fig. 4.3.3 that atom sees the approaching green laser blue shifted from $\omega_0=2$ to $\omega'_{\rightarrow}=4=2\omega_0$ as in Fig. 4.6.1(a) while the receding laser is seen red-shifted to $\omega'_{\leftarrow}=1=(1/2)\omega_0$ as in Fig. 4.6.1(f). Fig. 4.6.1(b) has a small amount of red light added to the blue *(SWR=1/2)*. The effect is just a small velocity wobble. But, if *SWR* is reduced to almost zero as in Fig. 4.6.1(c), the Minkowski coordinate lines of Fig. 4.3.3(b) emerge.

Each wave in Fig. 4.6.1 (b-e) with non-zero *SWR* has a simple wavefunction.

$$\Psi_{wobbly}= A_{\Rightarrow}\Psi_{\Rightarrow}+A_{\Leftarrow}\Psi_{\Leftarrow} = A_{\Rightarrow}\, e^{\,i\,4x\,-\,i4ct}+A_{\Leftarrow}\, e^{-i\,1x\,-\,i\,1ct} \qquad (4.6.1)$$

For example, the wave in Fig. 4.6.1(c) with *SWR=0.1* has the following *wobbly wavefunction*.

$$\Psi_{wobbly}= 1.1\,\Psi_{\Rightarrow}+0.9\,\Psi_{\Leftarrow} = 1.1\, e^{\,i\,4x\,-\,i4ct}+0.9\, e^{-i\,1x\,-\,i\,1ct} \qquad (4.6.2)$$

A *Minkowski wavefunction* (Recall Fig. 4.3.3(b) where *SWR=0.*) lies between the cases of Fig. 4.6.1 (c-d).

$$\Psi_{Minkowski}= 1.0\,\Psi_{\Rightarrow}+1.0\,\Psi_{\Leftarrow} = 1.0\, e^{\,i\,4x\,-\,i4ct}+1.0\, e^{-i\,1x\,-\,i\,1ct} \qquad (4.6.3a)$$

$$= 2.0\, e^{i(4-1)x/2-i(4+1)ct/2}\cos((4+1)x/2-(4-1)\,ct/2) \qquad (4.6.3b)$$

If *SWR* is negative the low-frequency ($\omega'_{\leftarrow}=1$)-light dominates as in Fig. 4.6.1 (d-e). Then zigzag wave-zero switchback curves appear. The following is a *switchback wavefunction* with *SWR=-0.1*.

$$\Psi_{switch}= 0.9\,\Psi_{\Rightarrow}+1.1\,\Psi_{\Leftarrow} = 0.9\, e^{\,i\,4x\,-\,i4ct}+1.1\, e^{-i\,1x\,-\,i\,1ct} \qquad (4.6.4)$$

Wave-zero-creation is seen each time a minimum point of $\mathrm{Re}\Psi$ dips below the space axis. Creation is followed by wave-zero-annihilation as the faster of the wave-zeros run ahead to annihilate neighboring slow-moving zeros. Later, the slower moving zeros meet the same fate when caught from behind by faster moving zeros to their left. Faster-moving zeros are "anti-zeros" going back in time. Examples of annihilation and creation points are indicated in the upper part of Fig. 4.6.1(d).

An alternative view of the fast-moving zero is that it belongs to a triplet consisting of its "creator" to the left and its "killer" to the right. The triplet is all the same zero, *located three places at one time*. This is sketched in the lower part of Fig. 4.6.1(d).

Waves do things that defy classical intuition. Since the world, as seen by relativity of γ-waves and the quantum theory of μ-waves described in the following Chapter 5, is composed entirely of waves, it may be wise to replace our old "natural" classical intuition with a new and more natural wave-savvy one.

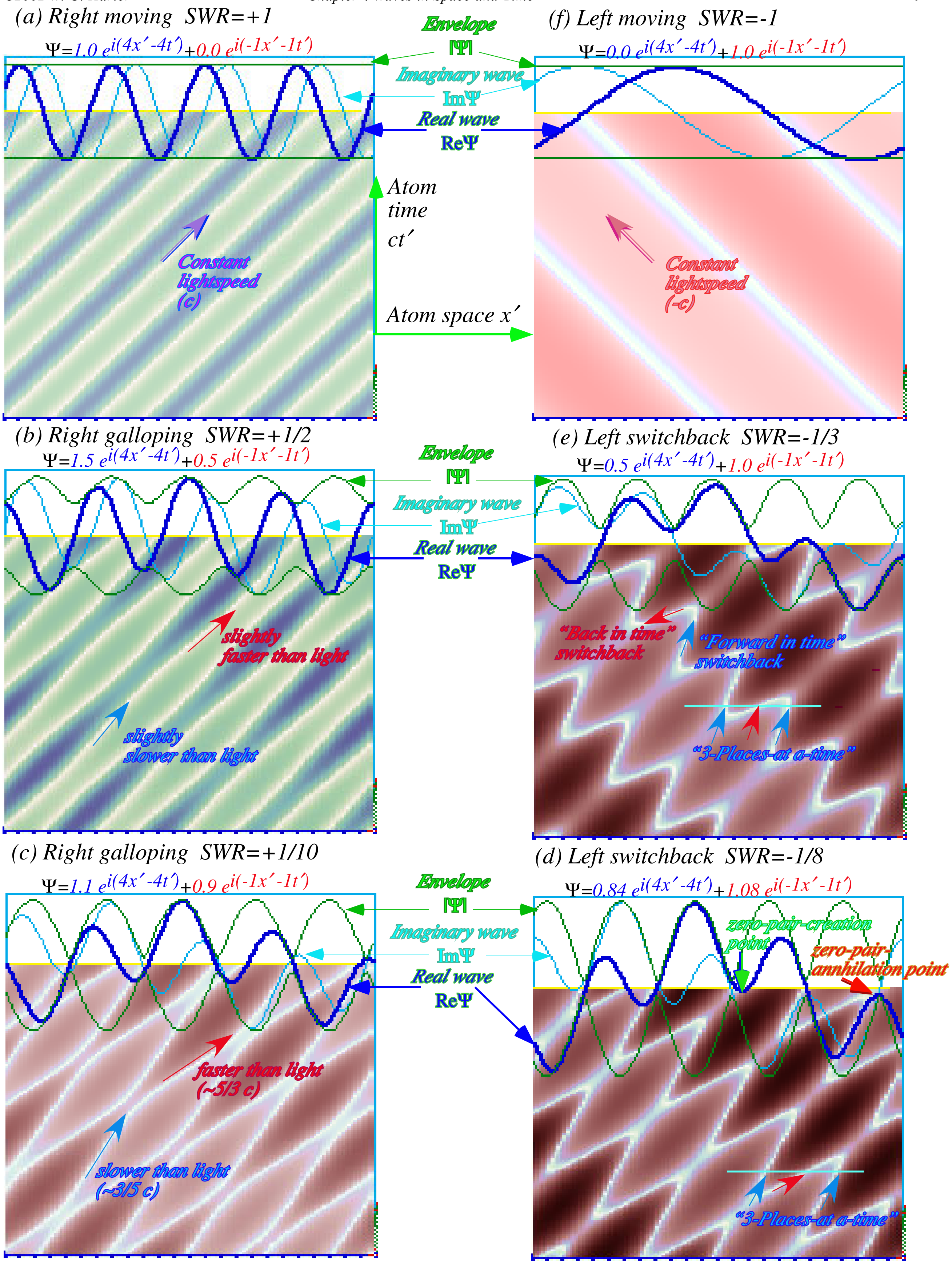

Fig. 4.6.1 Switchback waves (Atom spacetime (x,ct)-view of various galloping waves in Fig. 4.5.1.)

4.7 Co-vs.-Counter propagating waves: Modulation and Beats

Switchback and Minkowski waves (4.6.1) contain *counter-propagating* waves as opposed to *co-propagating* waves in which wavevectors k_1 and k_2 have the same sign as, for example, light waves with $(k_1=1,\ \omega_1=c)$ and $(k_2=4,\ \omega_2=4c)$. In Fig. 4.7.1 k and ω are the same as in Ψ_{switch} (4.6.4) except k_1 is positive so the red wave goes in the *same* direction as the blue k_2 wave. A *group wave* results.

$$\Psi_{group} = 1.1\, e^{i(k_1 x - \omega_1 ct)} + 0.9\, e^{i(k_2 x - \omega_2 ct)}$$
$$= 1.1\, e^{i(x - ct)} + 0.9\, e^{i(4x - 4ct)} = 1.1\,\Psi_{1\Rightarrow} + 0.9\,\Psi_{4\Rightarrow} \qquad (4.7.1a)$$

Time snapshots of the group wave Ψ_{group} shown in Fig. 4.7.1 below may be compared to those of the switchback waves Ψ_{switch} in Fig. 4.6.1. In Fig. 4.7.2 are higher wave frequency values $(k_1=7,\ \omega_1=7c)$ and $(k_2=10,\ \omega_2=10c)$ giving more waves inside each group, but the envelope in Fig. 4.7.2 is the same.

$$\Psi_{group} = 1.1\, e^{i(7x - 7ct)} + 0.9\, e^{i(10x - 10ct)} = 1.1\,\Psi_{7\Rightarrow} + 0.9\,\Psi_{10\Rightarrow} \qquad (4.7.1b)$$

Let us derive the *amplitude modulation (AM) envelope* $|\Psi_{group}|$ or modulus of a group wave.

$$|\Psi group| = \sqrt{\Psi^*\Psi} = \sqrt{\left(A_1 e^{-i(k_1 x-\omega_1 t)} + A_2 e^{-i(k_2 x-\omega_2 t)}\right)\left(A_1 e^{i(k_1 x-\omega_1 t)} + A_2 e^{i(k_2 x-\omega_2 t)}\right)}$$
$$= \sqrt{A_1{}^2 + A_2{}^2 + 2A_1A_2\cos\left[(k_1-k_2)x-(\omega_1-\omega_2)t\right]} \quad \text{(for real } A_1 \text{ and } A_2) \qquad (4.7.1c)$$

The $|\Psi_{group}|$ envelope formula is the same as that of a $|\Psi_{switch}|$ envelope (4.5.4a). Also, Ψ_{group} has the same group velocity V_{group} and phase velocity V_{phase} formulas as (4.3.2) for switchback waves.

$$V_{group} = \frac{\omega_1-\omega_2}{k_1-k_2} = V_{envelope} \qquad (4.7.2a) \qquad\qquad V_{phase} = \frac{\omega_1+\omega_2}{k_1+k_2} = V_{carrier} \qquad (4.7.2b)$$

As before, V_{group} is the *probability distribution velocity* since probability $\Psi^*\Psi$ is the square $|\Psi_{group}|^2$.

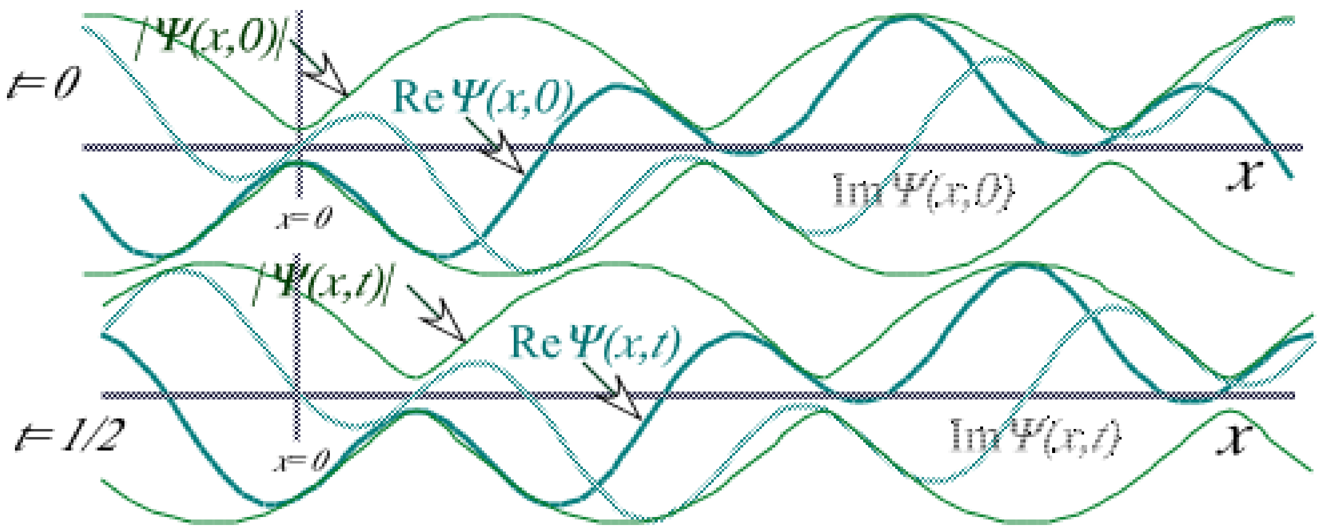

Fig. 4.7.1 Time snapshots of group wave moving in step with its envelope. $(k_1=1,\ \omega_1=c,\ k_2=4,\ \omega_2=4c)$

However, co-propagating light waves satisfy $\omega_1 = ck_1$ and $\omega_2 = ck_2$ with wavevectors k of the same sign (unlike $k_{\leftarrow}$ for Ψ_{switch} in (4.3.20b)), so group and phase velocity both equal the velocity of light.

$$V_{group} = c = V_{phase} \quad \text{(for light in vacuum)}$$

So Ψ_{group} light waves and envelopes march together in lock step at the speed of light for all frequencies ω_1 and ω_2 and amplitudes A_1 and A_2. No negative k is here to cause galloping or SWR dependence.

Recall that Ψ_{switch} is "tamed" by setting *50-50* amplitudes $(|A_1|=|A_2|)$ to get (4.6.3b). The same may be done to Ψ_{group} in Fig. 4.7.2(a) as shown in Fig. 4.7.2(b) where the envelope is "pinched" closed. This is derived algebraically by using an expo-cosine identity (4.2.3a) or (4.3.5a).

$$\Psi_{50\text{-}50group} = 0.5\, e^{i(7x - 7ct)} + 0.5\, e^{i(10x - 10ct)} \tag{4.7.3a}$$

$$= A_1 e^{i(k_1 x - \omega_1 ct)} + A_2\, e^{i(k_2 x - \omega_2 ct)} \tag{4.7.3b}$$

$$\left(\text{for: } A_1 = \frac{1}{2}, A_2 = \frac{1}{2}\right) \qquad = ie^{i\left[\frac{k_1+k_2}{2}x - \frac{\omega_1+\omega_2}{2}ct\right]} \cos\left[\frac{k_1-k_2}{2}x - \frac{\omega_1-\omega_2}{2}ct\right] \tag{4.7.3c}$$

The cosine factor in (4.7.3c) replaces the root-cosine in (4.7.1). Note the sine arguments are half as large as the arguments of the root-cosine. This is due to the half-angle identity: $\cos\frac{a}{2} = \sqrt{\frac{1+\cos a}{2}}$.

$$\sqrt{A_1{}^2 + A_2{}^2 + 2A_1A_2\cos\left[(k_1-k_2)x - (\omega_1-\omega_2)t\right]} = \frac{\sqrt{1+\cos\left[(k_1-k_2)x-(\omega_1-\omega_2)t\right]}}{2}$$
$$\left(\text{for: } A_1 = \frac{1}{2}, A_2 = \frac{1}{2}\right) \qquad = \cos\left[\frac{k_1-k_2}{2}x - \frac{\omega_1-\omega_2}{2}ct\right] \tag{4.7.4}$$

The kinky root-cosine function in Fig. 4.7.2(a) is "tamed" into a cosine envelope that appears to smoothly cross the *x*-axis in Fig. 4.7.2(b). The root-cosine *x*-factor $|k_1 - k_2|=3$ implies that the number of groups is $|10-7|=3$ (per 2π distance across Fig. 4.7.2 frame), but the cosine *x*-factor $|k_1 - k_2|/2=1.5$ indicates half as many or $|10-7|/2=1.5$ groups in the same interval. This is correct since the cosine-groups are exactly twice as long as the root-cosine groups.

Meanwhile, the phase factor $|k_1 + k_2|/2$ in (4.7.3c) indicates the number of half-waves (per 2π frame) being modulated by group envelope is $|10 + 7|/2=17/2$. Note 16 or 17 half-waves in Fig. 4.7.2 lie inside 3 "lumps" or groups that (for Fig. 4.7.2(b)) are 1.5 sine-envelope wavelengths.

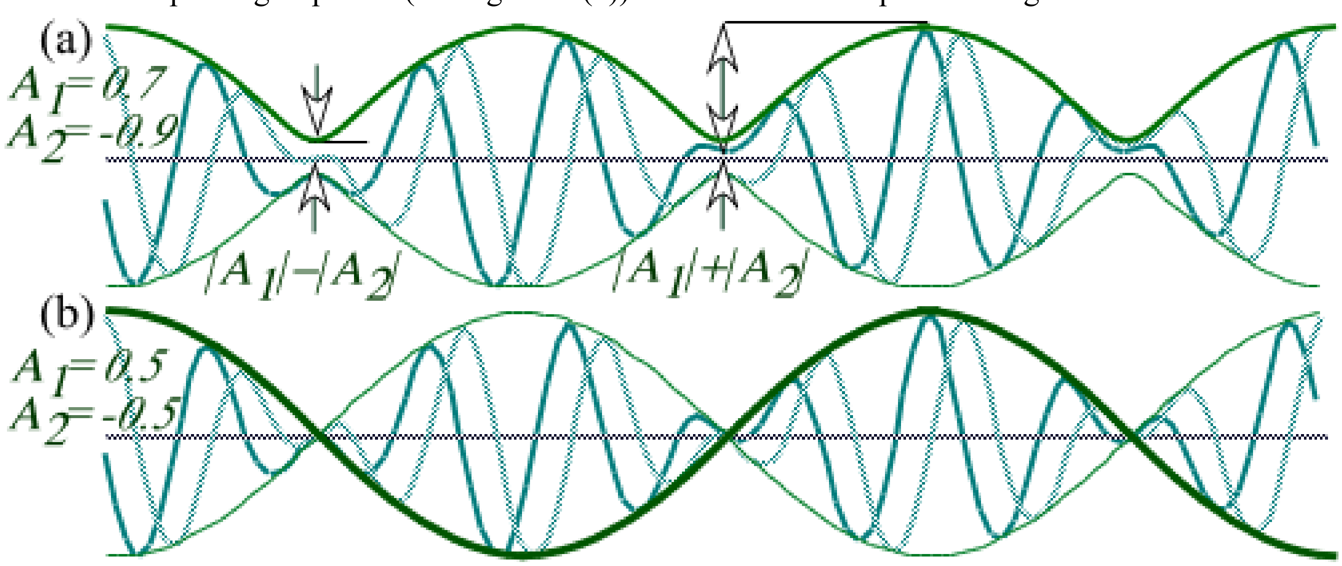

Fig. 4.7.2 Group waves and envelopes.$(k_1=7,\ \omega_1= 7c,\ k_2=10,\ \omega_2= 10$ *(a) Group wave (b) 50-50 group.*

Light waves *en-vacuo* discussed so far are *non-dispersive*, that is, all colors or frequencies travel at the same phase velocity $\omega/k = c$. Most waves (including light waves in many situations) are not so simple. Whenever the velocity $\omega_1/k_1 = v_1$ for one component differs from the velocity $\omega_2/k_2 = v_2$ of its traveling companion, there will be "sparks" between them as one "rubs" by the other at relative velocity $v_2 - v_1$. (Recall the galloping wave components had the same speed but opposite *velocity*.) Then the phase velocity V_{phase} in (4.7.2b) will also differ from the V_{group} in (4.7.2b). Furthermore, dispersive phase velocity will be guaranteed a constant value V_{phase} only for a 50-50 wave such as (4.7.3) and not for general group waves such as given by (4.7.1).

(a). Time and space modulation: Beats and bumps

Plots in Fig. 4.4.2 of two-ω-component light waves look the same plotted vs. distance x or plotted vs. time ct because, for photons: $\omega = kc$. Time amplitude modulation groups are called *beats*. By (4.7.2) the number of *beats* or groups per 2π-time unit is $|\omega_2 - \omega_1| = 3c$, and the number of *carrier* waves inside the group envelope is $|\omega_2 + \omega_1|/2 = 17c/2$ (per 2π-time unit). This is old AM radio jargon. Radio 'messages' (music, voice, gunshots, etc.) are "carried" in the modulation of the amplitude of a fundamental carrier wave running at an assigned radio frequency much higher than that of the message. Ratios of the AM peak amplitudes to the AM valleys, as in Fig. 4.7.2 are for radio an important figure of merit (or lack of merit if it's excessive and results in FCC fines!).The ratio is called an *Amplitude Modulation Ratio (AMR)* or an *Amplitude Modulation Quotient (AMQ)* depending on whether you prefer to deal with a ratio in the range -*1* to +*1* or its inverse outside that range.

$$AMR = \frac{|A_1| - |A_2|}{|A_1| + |A_2|}, \qquad AMQ = \frac{|A_1| + |A_2|}{|A_1| - |A_2|} \tag{4.7.5a}$$

These are analogous to the *Standing Wave Ratio (SWR)* or a *Standing Wave Quotient (SWQ)* for galloping waves that label a pure standing wave with zero *(SWR = 0)* or infinity ($SWQ = \infty$).

$$SWR = \frac{|A_{\rightarrow}| - |A_{\leftarrow}|}{|A_{\rightarrow}| + |A_{\leftarrow}|}, \qquad SWQ = \frac{|A_{\rightarrow}| + |A_{\leftarrow}|}{|A_{\rightarrow}| - |A_{\leftarrow}|} \tag{4.7.5b}$$

For quantum waves, the message or beats are the <u>only</u> thing we can see directly in a $\Psi^*\Psi$ counting experiment as seen by (4.7.1). The phase carrier velocity (4.7.2b) is hidden from our view. Furthermore, the message will be "audible" only if the amplitudes $|A_1|$ and $|A_2|$ are <u>both</u> non-zero. $\Psi^*\Psi$ in (4.7.1) is constant if amplitude product $A_1 A_2$ is zero but is "loudest" for 50-50 amplitudes ($A_1 = A_2$).

The frequency beats or AMR modulation in time of co-propagating waves are analogous to the spatial bumps or SWR groups in space that cause galloping of mono-chromatic (single frequency ω_0) counter-propagating waves as discussed in Sec. 4.5. Two frequency counter-propagating waves such as in Sec. 4.6 may have both beats and moving bumps as may the co-propagating waves here described.

A key quantum principle emerges.

> *The probability distribution $\Psi^*\Psi$ for quantum wave composed of two frequencies ω_1 and ω_2 (or energies $\hbar\omega_1$ and $\hbar\omega_2$) will oscillate at the beat frequency $|\omega_1 - \omega_2|$ with an amplitude that is greatest when the two amplitudes are equal and zero if either one is zero.*

An important corollary of this is due to the Planck factor $e^{-i\omega t}$ being killed in a $\Psi^*\Psi$ product.

> *The probability distribution $\Psi^*\Psi$ for quantum wave composed of a single frequency (or energy) is motionless.*

Single-energy states are called *stationary-states*. They are dead as a doornail, so far as a stationary observer can tell. Galloping motion and phase velocity are not directly observable. Counts come randomly according to the probability $\Psi^*\Psi$ but the statistics stays the same. Phase motion is observable only when there is an interference between two systems, and many many quantum counts are needed to see that.

A common electrical or optical engineering diagnosis is to send a monochromatic input wave of amplitude $A_1 = A_\rightarrow$ down a transmission line and measure the amplitude $A_2 = A_\leftarrow$ that 'echoes' and gallops back using the interference highs and lows whose ratio is the *SWR* in (4.7.5b). This is just what we will be doing with simulated quantum waves later on. The quantum theory of scattering begins by analyzing just such a galloping wave interference problem.

Analogy with Faraday polarization rotation

The complicated motion of atom frame waves in Fig. 4.6.1 has an optical polarization and 2D-oscillator analogy that extends the analogy given for laser frame waves in Fig. 4.5.1. The difference between the two figures is that right and left-moving waves in Fig. 4.6.1 differ in frequency $\omega'_\rightarrow = 4$ and $\omega'_\leftarrow = 1$. So mixtures of them will undergo a quantum beat at their difference frequency $\omega'_\rightarrow - \omega'_\leftarrow = 3$.

The group envelope will rotate around the ring at this beat frequency with velocity u given first in (4.3.5a). That rotation is analogous to what a polarization ellipse undergoes in circular dichroism or *Faraday rotation* due to a difference in frequency of left and right polarization states.

A 2-level or spin-$^1/_2$ or U(2) system has quantum beats and Rabi-like rotation that is maximum at saturation *(SWR=0)*. Galloping and switchback waves are perhaps the oldest *U(2)* systems (~1650) and polarization activity may be the next oldest (~1860). Such analogies serve long and well and should be exploited whenever possible. This is taken up in Chapter 10.

Using (4.7.1) you should be able to show how the shape and location of the *SWR* envelope gives the *complex* echo amplitude $A_\leftarrow = |A_\leftarrow| e^{i\phi}$, that is, *both* its magnitude $|A_\leftarrow|$ and its phase ϕ relative to $A_\rightarrow$.. Note again that monochromatic galloping light speeds range from *(SWR)c* to *(SWQ)c* by (4.5.1).

(b). Group velocity for continuous waves

We may approximate the formula (4.7.2a) for group velocity by a derivative relation if the angular frequency ω and wavevector k form a continuum and are related by a continuous function $\omega(k)$ or $k(\omega)$. An $\omega(k)$ relation is called a *dispersion relation* because it tells how wave velocities vary with frequency or color and tells how color components "disperse" in a general multi-component light pulse. So far, we have mainly considered photons or vacuum optics for which $\omega = kc$. This is the case of constant wave velocity that suffers no dispersion.

The continuum approximation to (4.7.2a) is the following derivative formula.

$$v_{group} = \frac{\omega_1 - \omega_2}{k_1 - k_2} = \frac{\Delta\omega}{\Delta k} \to v_{group} = \frac{d\omega}{dk}, \text{ as: } \Delta k \to 0 \qquad (4.7.6a)$$

For vacuum optics the derivative relation for group velocity always gives speed of light c.

$$v_{group} = \frac{d\omega}{dk} = c, \text{ for: } \omega = kc \qquad (4.7.6b)$$

This is the same as the continuum formula for phase velocity that follows from (4.7.2b).

$$v_{phase} = \frac{\omega}{k} = c \qquad (4.7.7)$$

Without dispersion, velocity V_{group} and V_{phase} are the same as was shown in Fig. 4.2.12.

(c). Counter-versus-co propagating waves

The formula (4.7.6a) for group velocity assumes a continuum of possible ω-values of frequency and k-values of wavevector in order to define a derivative $d\omega/dk$. Quantum mechanics often disallows this because, as we will see in later chapters, these quantities are usually quantized and discrete. Also, a derivative is meaningless for the counter-propagating wave groups since the interfering k-values are of opposite sign so cannot be infinitesimally close. Hence, we must use our discrete algebraic sum and difference formulas (4.1.5f) and (4.1.5g) for V_{group} and V_{phase}. Here a quadratic dispersion $\omega(k) = k^2$ is assumed. (Later, this turns out to be an approximate form for the dispersion of quantum matter waves.)

$$V_{group} = \frac{\omega_2 - \omega_1}{k_2 - k_1} \qquad (4.\ 1.5f) \qquad\qquad V_{phase} = \frac{\omega_2 + \omega_1}{k_2 + k_1} \qquad (4.\ 1.5g)$$

As an example compare a co-propagating pair of $k_1=8$ and $k_2=9$ waves with wave velocities

$$V_{group} = \frac{\omega_9 - \omega_8}{9-8} = \frac{9^2 - 8^2}{9-8} = 17 \qquad (4.7.8a) \qquad\qquad V_{phase} = \frac{\omega_9 + \omega_8}{9+8} = \frac{9^2 + 8^2}{9+8} = 8.53 \qquad (4.7.8b)$$

with a counter-propagating pair of $k_1=-8$ and $k_2=9$ waves with wave velocities

$$V_{group} = \frac{\omega_9 - \omega_8}{9+8} = \frac{9^2 - 8^2}{9+8} = 1 \qquad (4.7.9a) \qquad\qquad V_{phase} = \frac{\omega_9 + \omega_8}{9-8} = \frac{9^2 + 8^2}{9-8} = 145 \qquad (4.7.9b)$$

The resulting waves are rendered into spacetime plots by the following Fig. 4.7.3. These *BohrIt* plots were introduced in Fig. 4.2.11 and Fig. 4.3.3.

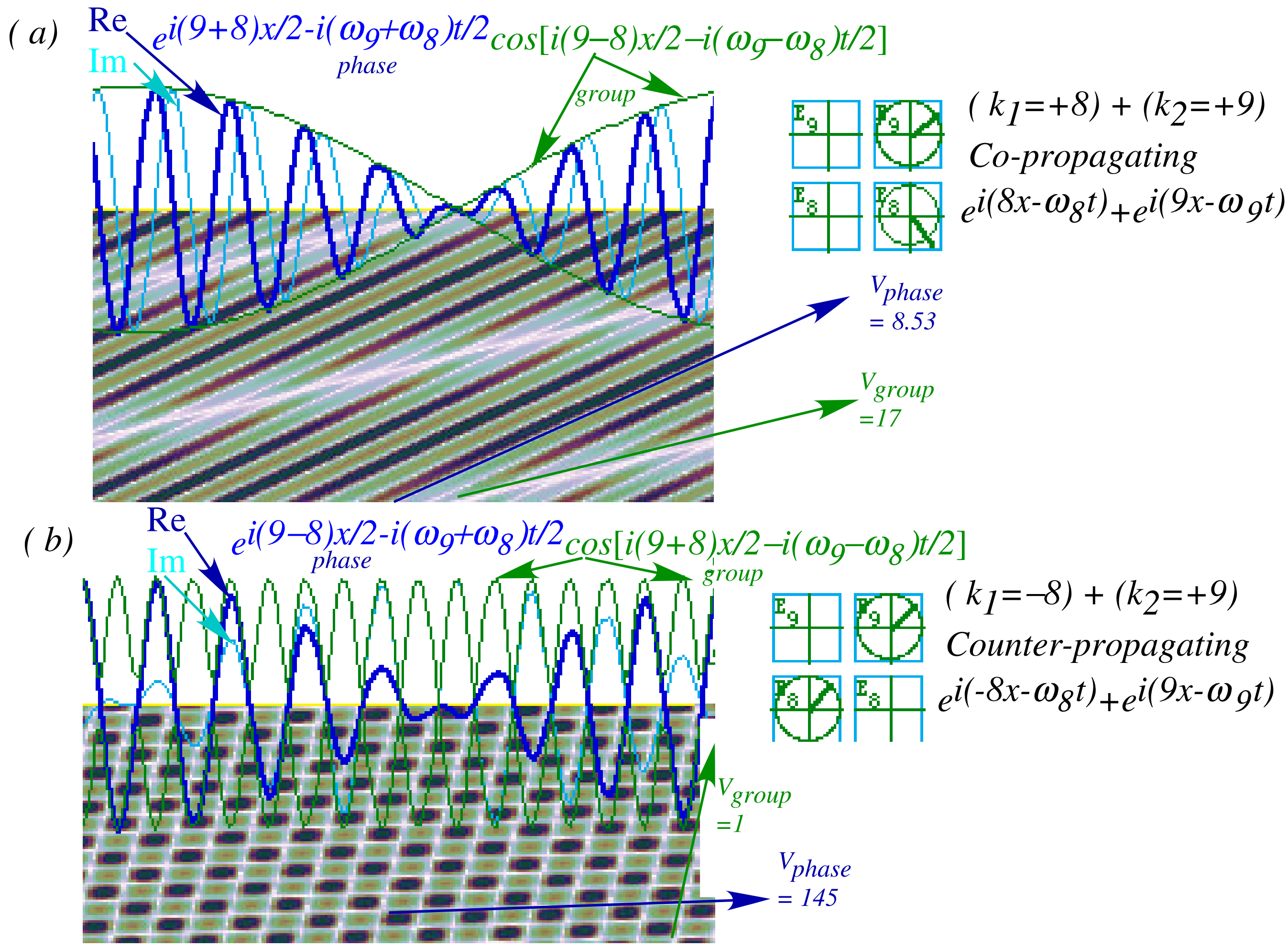

Fig. 4.7.3 Waves for $\omega=k^2$ dispersion (a) Co-propagating and (b) Counter-propagating. (BohrIt plot)

What a difference a ±-sign in k makes! The co-propagating wave in Fig. 4.7.3(a) has a $(k_2-k_1)=1$-half-wave envelope containing $(k_2+k_1)=17$-half waves of phase carrier. For the counter-propagating wave in Fig. 4.7.3 (b) it's vice-versa: a $(k_2-k_1)=17$-half-wave envelope containing a single ($(k_2+k_1)=1$) half wave of phase that looks like more waves because it's constrained by a very kinky envelope.

Furthermore the speeds of the four different wave parts vary greatly between (4.7.8) and (4.7.9). The phase part of the counter-propagating wave in Fig. 4.7.3 (b) zips along at 145 units by (4.7.9b), while the group envelope only creeps by at 1 unit by (4.7.9a). In contrast, the co-propagating group speed 17 is a little less than twice the phase speed 8.53 in Fig. 4.7.3(a) according to (4.7.8a-b).

The real and imaginary parts of the co-propagating phase in Fig. 4.7.3(a) have much the same shape as their counter-propagating counterparts in Fig. 4.7.3(b). But the huge speed 145 of the counter-propagating phase in Fig. 4.7.3(b) makes its imaginary wave pattern march 17 times further ahead of its real part than it does in the co-propagating phase above it in Fig. 4.7.3 (a).

As we will see later, the two wave functions in Fig. 4.7.3 have the same value of energy. Looks and shape can be both deceiving and telling in the quantum wave world!

Problems for Chapter 4

Not casting dispersion

4.2.1. Using 4x4 minor-per-major engineering graph paper with ruler and compass you should be able to easily construct 12-phasor wave diagrams like Fig. 4.2.5-8 with 12 tangent phasors per fundamental (k=1) wavelength L. Use this scheme to render the following wavefunctions. Label&check with complex algebra.

Let ω=ck where c=1 fundamental length L per second.

(a) Fundamental left-to-right moving (k=+1) wave $\psi = e^{i(kx-\omega t)}$ at t=0 and t=(1/4)(2π/ω) or 1/4-period.
(b) Fundamental right-to-left moving (k=-1) wave $\psi = e^{i(kx-\omega t)}$ at t=0 and t=(1/4)(2π/ω) or 1/4-period.
(c) 2nd harmonic left-to-right moving (k=+2) wave $\psi = e^{i(kx-\omega t)}$ at t=0 and t=(1/4)(2π/ω) or 1/4-period.
(d) Half the sum of (b) and (a) at t=0 and t=(1/4)(2π/1) or 1/4-period of fundamental.
(e) Half the sum of (c) and (a) at t=0 and t=(1/4)(2π/1) or 1/4-period of fundamental.
(f) Half the sum of (c) and (b) at t=0 and t=(1/4)(2π/1) or 1/4-period of fundamental.
(g) Half the sum of (a) and a "do-nothing-wave" (k=0) at t=0 and t=(1/4)(2π/1) or 1/4-period of fundamental.

Casting dispersion

4.2.2. Using 4x4 minor-per-major engineering graph paper with ruler and compass you should be able to easily construct 12-phasor wave diagrams like Fig. 4.2.5-8 with 12 tangent phasors per fundamental (k=1) wavelength L. Use this scheme to render the following wavefunctions. Label&check with complex algebra.

Let ω=ck^2 where c=1 fundamental length L per second.

(a) Fundamental left-to-right moving (k=+1) wave $\psi = e^{i(kx-\omega t)}$ at t=0 and t=(1/4)(2π/ω) or 1/4-period.
(b) Fundamental right-to-left moving (k=-1) wave $\psi = e^{i(kx-\omega t)}$ at t=0 and t=(1/4)(2π/ω) or 1/4-period.
(c) 2nd harmonic left-to-right moving (k=+2) wave $\psi = e^{i(kx-\omega t)}$ at t=0 and t=(1/4)(2π/ω) or 1/4-period.
(d) Half the sum of (b) and (a) at t=0 and t=(1/4)(2π/1) or 1/4-period of fundamental.
(e) Half the sum of (c) and (a) at t=0 and t=(1/4)(2π/1) or 1/4-period of fundamental.
(f) Half the sum of (c) and (b) at t=0 and t=(1/4)(2π/1) or 1/4-period of fundamental.

Mastering dispersion

4.2.3. Using engineering graph paper with ruler and compass you should be able to easily construct per-spacetime and spacetime diagrams like Fig. 4.2.11(a-b). Construct vector lattice diagrams for the following wavefunction combinations taken from preceding problems 4.2.1-2. Label&check with algebraic formulas for all relevant wave velocities and how waves moved in problems 4.2.1-2. Note denominator scale D for each.

From Problem 4.2.1 Letting ω=ck where c=1 fundamental length L per second.

(a) Half the sum of (b) and (a).
(b) Half the sum of (c) and (a).
(c) Half the sum of (c) and (b).

From Problem 4.2.2 Letting ω=ck^2 where c=1 fundamental length L per second.

(d) Half the sum of (b) and (a).
(e) Half the sum of (c) and (a).
(f) Half the sum of (c) and (b).

Lorentz's Own-Bra

4.4.1. (a) Derive eigenbras and eigenkets of the Lorentz transformation matrix L_{mn} in (4.3.5e) and discuss the physical interpretation of its eigenvalues and eigenvectors.

(b) Use geometry to construct accurate u = $\pm^3/_5$c and u = $\pm^4/_5$c graph paper using the simplest steps with a rule&compass. For Prob. 4.4.2 it will help to have t range from +5 to +5 sec. , and x between ±3 litesec. Hint: An easy relabeling converts u = +(whatever)-graph paper into u = -(whatever)-graph paper. How?

Spacetime Terrorism

4.4.2 (a) Complete the following happening tables using the Lorentz transformation between ship space-time coordinates (x',ct') and lighthouse coordinates (x,ct) given that the ship is traveling from right to left at a speed of $^3/_5$c and passes the lighthouse at t=0=t'. Calculate and then use a $\pm^3/_5$c graph (preceding exercise) to check the results.

Ship emits light	Explosion #1	Explosion #2	Explosion #3
x = 3 litesec. t = -5 sec.	x = t =	x = -1 litesec. t = -1 sec.	x = t = 1 sec.
x' = t' =	x' = -1 litesec. t' = -3 sec.	x' = t' =	x' = -3 litesec. t' =

(b) Draw the space-time paths of light waves emitted right and left from explosions #1 and #2 on the space-time graph and answer the following questions.

(a) When does light from explosion #1 hit the lighthouse? ________________(Lighthouse time)

(b) When does light from explosion #1 hit the lighthouse? ________________(Ship time)

(c) When does light from explosion #2 hit the lighthouse? ________________(Lighthouse time)

(d) When does light from explosion #2 hit the lighthouse? ________________(Ship time)

(e) Draw the space-time paths of fragments going left and right away from explosions #1 and #2 assuming that each fragment has a speed c/2 or -c/2 relative to the ship.

B.I.G.A.N.N. Investigates

4.4.3 The explosions in problem 4.4.2 lead to an investigation by B.I.G.A.N.N. (Bureau of Intergalactic Aids to Navigation at Night) headed by Rolla H. Ann Hoover (doubly illegitimate granddaughter of J. Edgar Hoover).

(a) When does the first fragment from explosion #1 hit the lighthouse? _______(Lighthouse time)

(b) When does a second fragment from explosion #1 hit the lighthouse? ______(Lighthouse time)

(c) When does a fragment from explosion #1 hit the ship? _________________(Ship time)

(d) When does a fragment from explosion #2 hit the ship? _________________(Ship time)

(e) When does a fragment from explosion #2 hit the Lighthouse? ___________(Lighthouse time)

(f) How fast would the lighthouse say the first fragment was going?_________c (Get sign right.) Does this check with velocity addition formula (4.4.3)?

(g) How fast would the lighthouse say the second fragment was going?______c (Get sign right.) Does this check with velocity addition formula (4.4.3)?

(h) The authorities of BIGANN have spotted a causal (as opposed to acausal) connection between all the explosions. To whom does it point?

Galloping Into the Sunset

4.5.1. The ReΨ zeros of the real part of a general monochromatic light wave

$$\Psi_{gallop} = A_{\Rightarrow}\Psi_{\Rightarrow} + A_{\Leftarrow}\Psi_{\Leftarrow} = A_{\Rightarrow} e^{i(kx-\omega t)} + A_{\Leftarrow} e^{i(-kx-\omega t)}$$

follow a curved "galloping" trajectory such as shown in Fig. 4.5.1.

(a) Derive an equation *x=x(ct)* for one of the curves in Fig. 4.5.1(d) and plot it for that case.

(b) Give a formula for the max and min speeds of the zeros and apply it to Fig. 4.5.1.

(c) Do similar max/min apply to zeros of ImΨ? What about zeros of $|\Psi|$? Are there any?

(d) Discuss limiting cases of (a) to (b) when amplitudes are equal.($A_{\Rightarrow} = A_{\Leftarrow}$)

Hopalong Kepler

4.5.2. The Kepler orbit of an isotropic 2D-oscillator exhibits a kind of galloping motion similar to that of interfering waves. How similar? Compare eccentric anomaly time behavior $\phi(t)$ with wave phase velocity derived in preceding exercise 4.5.1.

Nothing Going Nowhere Fast

4.6.1. The ReΨ zeros of a general counter-propagating dichromatic light wave

$$\Psi_{switch} = A_1\,\Psi_{\Rightarrow} + A_2\,\Psi_{\Leftarrow} = A_1\,e^{i(k_1 x-\omega_1 t)} + A_2 e^{i(-k_2 x-\omega_2 t)}$$

follow a curved "switchback" trajectory such as shown in Fig. 4.6.1(d).

(a) Derive equation*(s)* for one of these curves and plot it for the case in Fig. 4.6.1(d). Hint: Implicit functions are OK. Doppler and Lorentz formulas discussed in section 4.3 may make this a lot easier.

(b) Discuss the zero-speeds at the points near where zeros are created or annihilated in Fig. 4.6.1(d). Apply to your discussion the velocity addition formulas (4.4.3) of Sec. 4.4.

(c) Similar to (b), discuss the maximum and minimum and inflection zero-speeds in Fig. 4.6.1(d).

(c) Discuss limiting cases when amplitudes are equal ($A_{\Rightarrow} = A_{\Leftarrow}$) as it applies to Fig. 4.6.1.

Counterfeit and Cofeit

4.7.1. The ReΨ zeros of an equi-amplitude (A_1=A_2) dichromatic Bohr-matter wave (dispersion: ω=k^2)

$$\Psi_{group\ \mathrm{matter}} = A_1\,e^{i(k_1 x-\omega_1 t)} + A_2 e^{i(k_2 x-\omega_2 t)}$$

follow a grid of spacetime trajectories such as is shown in Fig. 4.7.3(a) for co-propagating (k_1k_2>0) and in Fig. 4.7.3(b) for counter-propagating (k_1k_2<0) cases.

(a) Using the k-values given for each figure (a) and (b) derive the wave lattice (4.2.11) for each case and plot as in Fig. 4.2.11. Indicate “particle paths” as well as wave-zero paths.

(b) The imaginary part ImΨ is hidden more in Fig. 4.7.3(b) than in Fig. 4.7.3(a). Where is it? Derive and/or sketch. Does the counter-propagating ImΨ look at all like its co-propagating cousin?

WaveIt Quiz (You should be able to do this in 10 minutes or less.)
Write down the expo-cosine identity: $(e^{ia} + e^{ib})/2 =$ ____________________
NO CALCULATORS! Many of the answers are in units of *c*. Just write, say, *8c* not *2.4E9* etc.

$\Psi(x,t) =$	Does Ψ have a constant phase velocity?	Does Ψ have a constant group velocity?	Does ReΨ wave speed "gallop" continuously.	Does Ψ wave represent a stationary state?
$3e^{i(2x-2ct)}$ $+2e^{i(4x-4ct)}$	Yes__? or No__? If Yes give value ______________	Yes__? or No__? If Yes give value ______________	Yes__? or No__? If Yes give range of speed:_______ to:_______	Yes__? or No__? If No give beat frequency(ies) :_______ :_______
$2e^{i(2x-2ct)}$ $+2e^{i(-2x-2ct)}$	Yes__? or No__? If Yes give value ______________	Yes__? or No__? If Yes give value ______________	Yes__? or No__? If Yes give range of speed:_______ to:_______	Yes__? or No__? If No give beat frequency(ies) :_______ :_______
$3e^{i(2x-2ct)}$ $+2e^{i(-2x-2ct)}$	Yes__? or No__? If Yes give value ______________	Yes__? or No__? If Yes give value ______________	Yes__? or No__? If Yes give range of speed:_______ to:_______	Yes__? or No__? If No give beat frequency(ies) :_______ :_______
$3e^{i(2x-2ct)}$ $+3e^{i(-4x-4ct)}$	Yes__? or No__? If Yes give value ______________	Yes__? or No__? If Yes give value ______________	Yes__? or No__? If Yes give range of speed:_______ to:_______	Yes__? or No__? If No give beat frequency(ies) :_______ :_______